Spring 5-7-2016

Role of Cell Type and Genetic Alterations in Driving Breast Cancer Pathogenesis

Divya Bhagirath
University of Nebraska Medical Center

ROLE OF CELL TYPE AND GENETIC ALTERATIONS IN DRIVING BREAST CANCER PATHOGENESIS

By

Divya Bhagirath

A DISSERTATION

Presented to the Faculty of the University of Nebraska Graduate College in Partial Fulfillment of the requirements for the Degree of Doctor of Philosophy

Genetics, Cell Biology and Anatomy

Graduate Program

Under the Supervision of Professor Vimla Band

University of Nebraska Medical Center

Omaha, Nebraska

April, 2016

Supervisory Committee:

Hamid Band, M.D., Ph.D. Kay-Uwe Wagner, Ph.D.

Shantaram S. Joshi, Ph.D. Karen Gould, Ph.D.

ACKNOWLEDGMENTS

My heartfelt thank you to my mentor Dr. Vimla Band for her constant support and motivation, while I undertook this thesis project. She has been extremely helpful and encouraging during my stay in her laboratory. She was always available to discuss any problem that I encountered and would give me very useful suggestions to move further with the project. I am greatly thankful to her for encouraging me to develop my own independent thinking and patiently listening and critiquing my ideas, so that I learn the most during my PhD training and develop better as a scientist. I always looked forward to her as a positive source of inspiration and she helped me through various difficult situations. I am highly obliged to have worked under her guidance.

I am extremely thankful to my supervisory committee members Dr. Hamid Band, Dr. Kay-Uwe Wagner, Dr. Shantaram Joshi and Dr. Karen Gould for their valuable suggestions and guidance during my PhD training. I would express my gratitude to Dr. Xiangshan Zhao, whom I have closely worked with during this entire project. He helped me immensely in learning the technical skills required to undertake a project and also taught me to perform mice orthotopic surgeries. I would always cherish the long scientific discussions we had, that in turn allowed me to understand and develop important qualities essential to undertake scientific research. I am sincerely thankful to all the members of Band laboratory for helping through things such as reagents and protocols and giving useful suggestions for my thesis project. Senior postdocs in the laboratory Dr. Riyaz Mir and Dr. Sameer Mirza and graduate students Shashank, Shalis and Nick always shared their experiences and guided me well to learn the best during my training.

Finally, I would like to thank my family for being the most consistent and strongest support of my life and always motivating me to do my best even in worst of situations. It is with their belief and blessings that I have been able to come so far in my life as well as in

my career as a scientist. I also want to thank my fiancée for his constant encouragement during this whole time and for having faith in me. Lastly, I want to thank all my friends here who were there with their support every time I faced a difficult situation and have been like family to me away from home.

DEDICATION

To my family and the Almighty

ROLE OF CELL TYPE AND GENETIC ALTERATIONS IN DRIVING BREAST CANCER PATHOGENESIS

By

Divya Bhagirath, Ph.D.

University of Nebraska Medical Center, 2016

Advisor: Vimla Band, Ph.D.

Breast cancer is the second most leading cause of death among women in the United States. Several environmental and genetic factors contribute to the pathogenesis of the disease. It is classified into different subtypes based on expression of certain markers as well as that of set of genes that define the disease progression and associated mortality. Identification of various subtypes namely: Luminal-like (Luminal-A, Luminal-B), ErbB2 over-expressing, Basal-like and Claudin low types, showed an association of survival outcomes with that of the corresponding gene expression signatures, thus paving a way for therapeutic intervention. It further emphasizes the importance of nature of gene expression changes characteristic of each subtype in regulating the disease outcome. Another important factor that determines disease phenotype is the nature of cell of origin.

As part of my thesis research, I investigated the role of different combination of oncogenes/tumor–suppressor and the nature of cell type in contributing towards phenotypic and pathological differences in development of breast cancer. hTERT immortalized stem/progenitor cell lines K5+/K19- and K5+/K19+ when transformed by combination of triple oncogene/tumor-suppressor -mRas/mp53/wtErbB2 or mRas/mp53/wtEGFR gave rise to heterogeneous primary tumors as well as

spontaneous lung metastasis *in-vivo* upon orthotopic transplantation in mammary glands of immunocompromised NSG mice. Important tumor characteristics such as latency and incidence of primary and metastatic tumors depend on both the nature of cell type and oncogene combination. K5+/K19- over-expressing mRas/mp53/wtEGFR had a significantly late tumor onset than all other tested cell lines. Transformed K5+/K19+ cells overall possess higher anchorage independent growth and metastasis forming ability than K5+/K19- cells. From microarray analysis, we observed that tumors from transformed K5+/K19- cells have a higher EMT gene signature, more so for K5+/K19- over-expressing mRas/mp53/wtErbB2. Tumors from K5+/K19+ cells over-expressing mRas/mp53/wtEGFR express known markers for metastasis in BC, accounting for higher metastasis ability from these tumors. We also observed complete *in-vitro* transformation and tumor formation from either cell lines following over-expression of mRas/mp53/mPI3K oncogene combination. K5+/K19- or K5+/K19+ cells show distinct EMT upon over-expression of mRas/mp53/mPI3K combination and overall K5+/K19- cells have a higher susceptibility to undergo EMT upon transformation as compared to K5+/K19+ cells.

TABLE OF CONTENT **PAGE NUMBER**

LIST OF FIGURES

LIST OF TABLES

ABBREVIATIONS

AFM	Atomic Force Microscopy
BRCA1	Breast Cancer type 1 susceptibility protein
BC	Breast Cancer
CAFs	Cancer Associated Fibroblasts
CD24	Cluster of Differentiation 24
CD44	Cluster of Differentiation 44
CD49f	Cluster of Differentiation 49f
CDH2	N-Cadherin
CK/K	Cytokeratin
COL	Collagen
CSCs	Cancer Stem Cells
Ct	Cycle threshhold
CTCs	Circulating Tumor Cells
CXCL1	C-X-C motif chemokine 1
CXCL12	C-X-C motif chemokine 12
CXCL14	C-X-C motif chemokine 14

DAPI	4'-6-Diamidino-2-phenylindole
DEC	Decorin
DFCI-1	Dana Faber Cancer Institute 1
DKK	Dickkopf WNT signaling pathway inhibitor
DMEM	Dulbecco's Modified Eagle Medium
DNA	Deoxynucleic acid
E6	HPV oncoprotein E6
E7	HPV oncoprotein E6
ECM	Extracellular Matrix protein
EMT	Epithelial to mesenchymal transition
EpCam	Epithelial cell adhesion molecule
ER	Estrogen Receptor
ErbB2	Epidermal Growth factor receptor 2
FACS	Fluorescence-activated cell sorting
FITC	Fluorescein isothiocyanate
GCOS	General Comprehensive Operating System
GFP	Green Fluorescent Protein
GREM1	Gremlin1

GSE	Gene Set Enrichment
GTPase	guanosine triphosphatase
HEPES	4-(2-hydroxyethyl)-1-piperazineethanesulfonic acid
HGF	Hepatocyte growth factor
hMECs	Human mammary epithelial cells
HMGB1	High mobility group box 1
HRP	Horseradish peroxidase
hTERT	Human Telomerase Reverse Transcriptase
IHC	Immunohistochemistry
IL-17A	Interleukin 17A
INK4	INhibitors of CDK4
IPA	Ingenuity Pathway Analysis
IVIS	*In-vivo* imaging system
LGR5	Leucine-rich repeat-containing G-protein coupled receptor 5
LUM	Lumican
MCF-7	Michigan Cancer Foundation-7
MD	Mammographic Density
MEM	Mammary Epithelial Medium

MET	Mesenchymal to Epithelial Transition
MMP1	Matrixmetalloproteinase 1
MMTV	Mouse mammary tumor virus
mp53	mutant p53
mPI3K	mutant PI3K
mRas	mutant Ras
MUC1	Mucin 1
MAP3K1	Mitogen-Activated Protein Kinase Kinase Kinase 1
MEGM	Mammary epithelial growth medium
NSG	NOD-SCID Gamma
NaOH	Sodium Hydroxide
NBF	Neutral Buffered Saline
NEFL	Neurofilament light polypeptide
OLFM4	Olfactomedian 4
p16	cyclin-dependent kinase inhibitor 2A
p63	Tumor protein p63
PA	Polyacrylamide
PE-Cy5	phycoerythrin Cyanine5

PIK3CA	Phosphatidylinositol 3-kinase
pMSCV	Murine Stem Cell Virus
POSTN	Periostin
PR	Progesterone Receptor
PRRX1	Paired Related Homeobox 1
PTEN	Phosphatase and tensin homolog
PTGS2	Prostaglandin-Endoperoxide Synthase 2
PYMT	Polyoma virus-middle T antigen
qPCR	Quantitative Real time Polymerase chain reaction
RB	Retinoblastoma
RERG	RAS-Like, Estrogen-Regulated, Growth Inhibitor
RNA	Ribonucleic acid
RUNX1	Runt-related transcription factor 1
SANPAH	N-Sulfosuccinimidyl-6-(4'-azido-2'-nitrophenylamino) hexanoate
Sc	Santa Cruz
SD	Standard Deviation
SLC6A14	Solute Carrier Family 6
SNAI2	Slug

STEAP2	Six transmembrance epithelial antigen of Prostate 2
SV40	Simian vacuolating virus 40
TCGA	Cancer Genome Atlas
THBS2	Thrombospondin2
TP53	Tumor Protein 53
TWIST1	Twist-related protein 1
UNL	University of Nebraska Lincoln
VIM	Vimentin
wtEGFR	Wild type EGFR
wtErbB2	Wild type ErbB2
YAP	Yes Associated Protein
ZEB1	Zinc Finger E-Box Binding Homeobox 1
ZNF217	Zinc finger protein 217
α-SMA	Alpha Smooth Muscle Actin
2D	Two dimensional
3D	Three dimensional

CHAPTER 1

Introduction

1.1 Heterogeneity in Breast Cancer- "Clonal evolution" versus "Cancer Stem Cell" hypothesis

Tumor heterogeneity refers to variation in the genetic, epigenetic or micro-environmental context of the cells that constitute the tumor. It is mainly divided as inter or intra tumor heterogeneity, where inter-tumor heterogeneity describes the variation in tumors from different patients while an intra-tumor heterogeneity constitutes variation within a tumor (Visvader 2011). Tumors of human mammary gland are highly heterogeneous in nature. Various studies have shown the existence of different sub-populations within primary breast tumors (Dexter et al., 1978; Fidler, 1978; Shipitsin et al., 2007). These variable sub-populations isolated from same primary tumor, when cloned and injected in mice, exhibited different metastatic capacity (Fidler, 1978). These results, therefore suggested that primary tumors harbor heterogeneous cell populations that have distinct growth and invasion abilities and that allow tumors to progress and metastasize (Heppner, 1984; Michor and Polyak 2011).

Many hypotheses have been given to explain these variations within tumors. Two most predominant ones are the- "Clonal Evolution" and "Cancer-Stem cell" hypothesis. According to the clonal evolution model, heterogeneity in tumor develops as a result of accumulation of new mutations in tumor cells that leads to development of various sub-clones (Michor and Polyak 2011). Several breast cancer cell lines exhibit heterogeneity and sub-clones within these cell lines interact with each other to determine the pathogenicity of disease (Dexter et al., 1978; Marusyk et al.). These and findings from various mouse models emphasize the presence of different cell populations that work together under the influence of genetic and microenvironmental forces to determine the progression of disease (Cleary et al.,2014; Koren and Bentires-Alj 2015).

Besides evolution of different clonal populations, another mechanism that is given to account for the heterogeneity is presence of pool of self-renewing and differentiating “Cancer Stem Cells” (CSCs). These CSCs are considered to be the tumor initiating cells, which maintain the tumor growth by self-renewal and give rise to non-tumorigenic differentiated progenies, thus accounting for the generation of heterogeneity within tumors. Patient derived primary tumor specimens were subjected to FACS and analyzed for presence of cells with CD44, CD24 expression. Tumors cells that were $CD44^{high}$, $CD24^{low}$ were able to seed new tumors and propagate and also possessed the ability to produce non-tumorigenic progenies that were $CD44^{low}$, $CD24^{high}$ (Al-Hajj et al., 2003). When differentiated $CD44^{low}$, $CD24^{high}$ cells were transplanted in mice no tumor formation was observed from them. Therefore suggesting that the tumor stem cell behavior was specific to cells with $CD44^{high}$, $CD24^{low}$ phenotype and these cells have been since considered as the CSCs population within tumors. More recently, identification of stem cell markers have allowed isolation of normal stem and cancer stem cell populations and high throughput sequencing analysis of the isolated breast CSCs has provided information about breast cancer heterogeneity (Shipitsin et al., 2007). Furthermore evidence from different transgenic mice model have also shown presence of tumor initiating stem cells within mice tumors (Cho et al., 2008; Zhang et al., 2008). Many breast cancer cell lines have also shown to have CSCs populations (Charafe-Jauffret et al., 2009; Ginestier and Wicha, 2007).

1.2 BC subtypes

Different methods are used to classify BC it into different types. More classical method of tumors classification is based on the expression of growth factor receptors

such as ER, PR and ErbB2. Breast tumors are categorized as 1) ER, PR positive 2) ErbB2 positive 3) ER, PR, ErbB2 negative and the course of therapy is determined by this classification. In order to better understand the phenotypic variations existent in patient tumors, when gene expression analysis of patient derived tumors was done, the gene expression patterns associated with each tumor led to clustering of different tumors in to a particular subtype (Perou et al., 2000; Sorlie et al., 2001). Profiling of breast tumors at molecular level further stratified tumors into various subtypes. These subtypes namely: Luminal like (Luminal-A, Luminal-B), ErbB2 over-expressing, Claudin-low type, normal-like and basal like are each characterized by the expression of certain genetic alterations that are seen among the patients belonging to these subtypes (Prat et al.,2010; Sorlie et al., 2001). Two important findings observed from this study were that - 1) different subtypes had characteristic gene expression changes associated with them and 2) each subtype had gene signatures that closely resembled those of known cell types present in the normal mammary gland i.e. the basal or luminal cells (Perou et al., 2000). Further analysis of gene alterations in relation to clinical outcomes revealed that different subtypes have characteristic survival outcome associated with it, where basal subtype had a worse clinical outcome whereas tumor with luminal specific gene expression had a good overall survival (Sorlie et al., 2001). Given these findings, we therefore sought to study the contributions of both the cell type and/or the oncogene in determining BC pathogenesis.

1.3 Models to study BC pathogenesis

Human mammary gland is organized in to ducts and lobules. Each ductal compartment is a bi-layered structure that consists of an inner layer of luminal epithelial

cells supported underneath by a basal layer of myoepithelial cells. Interspersed in the basal or the sub-basal compartments are the likely stem/progenitors that respond to the chemical stimulus i.e. hormones and differentiate to give rise to luminal and myoepithelial cells. Mammary gland undergoes periodic remodeling to response to different hormones. Upon pregnancy the luminal layer proliferates and differentiates by stimulation from estrogen, prolactin, progesterone to become milk secreting cells and the basal myoepithelial cells under the influence of oxytocin constrict to facilitate passage of milk through the ducts (Wiseman and Werb, 2002).

Breast cancer originates as a result of transforming event occurring in any of these epithelial cell components. Different methods, including isolation of cells from the normal reduction mammoplasty or the primary tumor specimens or generation of tumor specific mice models have been employed to understand the etiology of the disease. Isolation of normal or tumor mammary epithelial cells have been difficult to establish in 2D culture owing to different growth requirements of different lineages. Various growth medium with defined growth factors have since been developed to allow growth of hMECS, as well as breast cancer cells in order to isolate these cells and culture them *in-vitro* to study disease pathogenesis from them (Band, 2003; Band and Sager, 1989). However normal epithelial cells have a limited proliferative capacity and undergo replicative senescence after few weeks in culture. The cells have to undergo immortalization beyond the senescence check point in order to survive in-vitro. Different methods have been employed to immortalize cells in culture. Intact p16/Rb and p53/p21 pathways are required to establish and maintain replicative senescence, thus inactivation of these pathways is necessary for immortalization. Papilloma virus oncogenes E6/E7, SV40 T-antigen can inactivate both p16/Rb and p53/p21 pathways and thus immortalize cells. hTERT, E6, RhoA, ZNF217, mutant p53 can immortalize p16

negative cells (Band, 2003; Dimri et al., 2005). These immortalized mammary cell lines can then serve as models to introduce different oncogenic alterations to study their behavior upon transformation. Cancer is a multistep process that involves genetic changes that allows the cells to become autonomous and proliferate in an uncontrolled manner. Acquisition of new mutations further endows the cells with the capacity to invade and spread to different places in the body. Different mammary transformation models have been derived where different oncogene combinations were expressed to transform the cells. Combination of SV40, hTERT, RAS have been shown to transform normal hMECs and upon injection in nude mice these cells also form metaplastic carcinomas (Elenbaas et al., 2001). Likewise, different cellular oncogenes combinations have been utilized to transform hMECs to study breast cancer pathogenesis (Bhagirath et al., 2015; Ince et al., 2007; Keller et al. 2012; Kendall et al., 2005).

Besides these *in-vitro* methods, various *in-vivo* mouse models also shed light on the etiology of breast tumors. Generation of transgenic or knockout mouse models with a specific genetic alteration including TP53 knockout, transgenic PYMT, MYC, WNT1 targeted specifically to mammary compartment using lineage specific promoters – MMTV, WAP-Cre, K14 or K8 has been another approach to study disease pathogenesis (Koren and Bentires-Alj 2015).

1.4 Factors responsible for BC tumorigenesis

1.4A Role of genetic alterations in BC pathogenesis

More recent comprehensive analysis of large cohort of patient derived breast tumors have led to identification of various subtype specific gene alterations(TCGA 2012, Banerji et al., 2012; Shah et al. 2012). Recurrence of different gene changes such

as mutations in PIK3CA, TP53, MAP3K1, RUNX1 or gene amplification/over-expression of ErbB2, loss of tumor suppressor PTEN, RB and association of these gene changes with different subtypes signifies an important gene alteration and subtype relationship (Banerji et al., 2012; Stephens et al. 2012). PI3KCA gene mutations comprise 45% of luminal-A, 29% luminal-B, 39% of ErbB2 over-expressing and 9% of basal subtype. Likewise TP53 mutations also has a recurrent pattern of occurrence, comprising of 32% of all breast tumors and highest rate of mutation in basal subtype (80%) and ErbB2 subtype (70%) (Sorlie et al., 2001). Off these frequently observed mutations certain genetic changes function as the drivers of disease pathogenesis while others may occur as a result of evolution (Banerji et al., 2012; Stephens et al. 2012). Besides the predominance of somatic mutations in breast tumors, the hereditary breast cancer also constitute about 1-3% of total cases of breast cancer. Hereditary mutations in genes like BRCA1, BRCA2 is another example of genetically driven breast cancer where a single oncogene that has undergone mutations drives the tumor formation and its progression. Further investigation have shown that certain gene mutations correlate with resistance to therapy (Ellis et al. 2012). With advent of new gene sequencing methods and single cell analysis, several recent reports have identified and linked various mutations including those in PIK3CA or TP53 with poor clinical outcome or therapy resistance (Marcotte et al. 2016). Over-expression of oncogene ErbB2 and genes belonging to ErbB2 amplicon comprises of a whole BC subtype defined as ErbB2 over-expressing tumors. Identification of ErbB2 subtype was clinically important, as therapies targeting the receptor made their way to the treatment of tumors that have ErbB2 over-expression or amplification. Likewise tamoxifen treatment has been mainstay of breast cancer therapy to prevent advanced metastatic disease in patients with ER positive primary tumors.

Different oncogenes have been shown to confer transformation ability when over-expressed in hMECs (Bhagirath et al., 2015; Elenbaas et al., 2001; Ince et al., 2007; Keller et al., 2012; Kendall et al., 2005). We over-expressed combinations of oncogene(s)/tumor-suppressor mRas/mp53/mPI3K, mRas/mp53/wtErbB2 or mRas/mp53/wtEGFR in immortalized stem progenitor cells previously developed and characterized in my mentor's laboratory (Zhao et al. 2010) and assessed the contribution of each combination in driving BC pathogenesis. mp53 was included in the combination, owing to the predominance of TP53 mutations in primary breast tumors in patients (Sorlie et al., 2001). Similarly, Ras mutation has also been reported in BC patients and activation of Ras pathway and its effectors is now increasingly reported in patient derived tumors (McLaughlin et al., 2013; Wright et al. 2015). In support of this it has been recently shown that targeting mPI3KCA in different mammary epithelial cell compartment induces formation of distinct tumors, further emphasizing the differential effect of oncogene on cell types (Van Keymeulen et al. 2015).

1.4B Role of cell type in BC pathogenesis

Another likely factor that might contribute to the heterogeneity of breast tumors, are the cellular precursors in which the initiating genetic alterations occur. Normal mammary gland consists of hierarchy of cell populations including the normal adult stem cell, the progenitors and their differentiated progenies mainly the luminal and the myoepithelial cells. According to CSCs hypothesis a single stem cells undergoes transformation and give rise to tumor heterogeneity by its property of differentiation. Besides this another hypothesis has also been suggested to account for cellular heterogeneity in BC. It relies on the basis that cellular precursors at various stage of this

hierarchy have different susceptibilities to form tumors and that the nature of cell determines the subtype of tumors formed as a result (Visvader 2011). The idea gains some strength from the tumor microarray data derived from patients belonging to different subtypes where each subtype shows expression pattern inherently found in the normal cell lineages i.e. luminal or basal cells (Perou et al., 2000).

Different markers have been utilized to identify and define the mammary stem or progenitor cells population within mammary gland. CD49f, CD44, CD24, EpCam are some of the markers that allowed identification of stem cells in mouse mammary glands. $CD49f^{High}$, $EpCAM^{positive}$ cells when isolated and transplanted in mice can fully reconstitute the entire mammary glands of the recipient mice (Shackleton et al., 2006; Stingl et al., 2006). Epithelial cells, are characterized by expression of various keratins. Stem cells in normal mammary gland are known to express several CKs including K5, K4, K14 and K19, and luminal cell express K8,18 (Petersen and Polyak, 2010; Villadsen et al., 2007). The basal subtype of BC is shown to have presence of stem cell gene signatures, including high expression of CKs such as K5, K14, and K17, suggesting stem cell origin of this subtype (Sorlie et al., 2001). These tumors are less differentiated and are associated with worse clinical outcomes. Together these evidences suggest that basal like tumors could be resulting from transformation of a stem cell. In contrast to this, different studies from mouse models have shown that basal subtype can also arise from transformation of a luminal progenitor cell population (Lim et al., 2009; Molyneux et al. 2010).

Given the following associations we wanted to test the hypothesis whether it is the cell type and/or the oncogenic alteration that dictate the progression and onset of different subtypes of breast cancer. We utilized immortalized stem/progenitor cells (described below) that were isogenically derived from same donor, and that represented

different cell types in the hierarchy of mammary epithelial cells. We employed these basal bi-potent progenitor to also test the cancer stem cell and cell of origin hypothesis of BC. We over-expressed different combinations of oncogene(s)/tumor-suppressor (sub-type specific) to study their effect on transforming these cell types and in governing tumor pathogenesis from them. We found that both the nature of cell and transforming oncogene(s) influences the tumor pathogenesis. Tumor characteristics such as onset and incidence of primary or metastatic tumors varied with the oncogene combination that was over-expressed in a particular cell type (Chapter 2). We found that overall the metastatic abilities were dependent on the nature of cell type that gets transformed (Chapter 2, 3). In addition to the nature of cell type, we observed an important role of nature of oncogene on influencing tumor pathogenesis from a defined cell type (Bhagirath et al., 2015). The observations and evidences from this study support the genetic as well as cellular basis for breast tumor heterogeneity.

1.5 Immortalized mammary stem progenitor K5+/K19- and K5+/K19+ cells as models to study BC pathogenesis

In order to study role of oncogene(s)/tumor-suppressor or the nature of cell type in mediating BC pathogenesis, we utilized hTERT immortalized mammary stem/progenitor cell lines designated as K5+/K19- or K5+/K19+. These two different isogenic cell lines that vary on the basis of CK19 from each other, were derived from same normal mammary reduction mammoplasty sample and co-express markers for stem, luminal or basal cell type such as – K8, K18, K5, K14, vimentin, EpCAM, p63 (Zhao et al. 2010). As previously shown, both the cell lines possess the ability to self-renew and differentiate into luminal or myoepithelial cell lines under proper differentiation

conditions. Most of the breast tumors highly express K19 (Bartek et al., 1985). K19+ hMECS are difficult to culture in-vitro (Gudjonsson et al., 2002). Thus these K19+ cell models developed and characterized in my mentors laboratory therefore provided as useful tools to better understand etiology of the disease. Furthermore, expression of K19 is associated with poor prognosis in BC (Kabir et al. 2014). CTCs derived from patients have been also shown to express CK19 (Xenidis et al., 2009). CK19 positive CTCs are indicator of relapsing or metastasized tumors in patients and their presence in patients undergoing chemotherapy indicates re-occurrence of the disease (Giuliano et al., 2014; Janni et al., 2016; Smerage et al. 2014). Together these findings emphasize the clinical importance of K19 expression in BC, and therefore make these cellular models very useful to study BC development.

1.6 Role of mechanical forces in driving pathogenesis

In addition to my study on role of cell types and oncogene combinations in driving BC pathogenesis, I also investigated the effect of matrix derived mechanical stiffness in mediating BC tumorigenesis from breast cancer cell lines, described briefly in Chapter 6.

The microenvironment plays an important role in driving mammary gland tumorigenesis. Human Mammary gland is a complex organ comprising of epithelial and stromal cells that are embedded in matrix of ECM proteins. Epithelial cells are surrounded by a dense matrix of extracellular matrix proteins, in which stromal fibroblast and immune cells are also interspersed. Normal mammary gland undergoes distinct morphological and functional changes in its epithelial and stromal compartment during different stages of its development. These changes are mediated by systemic hormones

and local growth factors that are secreted by the stromal cells (Wiseman and Werb, 2002). In addition to these, the ECM surrounding the ducts/lobules also plays an important role in determining differentiation of epithelial cells and by itself can regulate gene expression changes (Li et al., 1987).

ECM proteins provide the structural framework to the cells and serve as functional ligands to mediate mammary gland changes (Schedin and Keely, 2011; Wiseman and Werb, 2002). It has been shown that the matrix surrounding the epithelium provides mechanical inputs and influences epithelial cell morphogenesis and govern the formation of tubular structures from them (Alcaraz et al., 2008; Wozniak et al., 2003). Thus apart from the growth factor and hormone signaling the ECM mediated mechanical forces also play an important role in maintaining normal tissue homeostasis (Mammoto et al., 2013; Schedin and Keely 2011). Alterations in these normal homeostatic regulations are linked with the disease pathogenesis in an individual. The stromal compartment of mammary glands undergoes significant changes during tumor formation and gradual stiffening of the matrix occurs with progression of disease (Butcher et al., 2009). The cells in the tumor microenvironment regulate proliferation and survival of tumor cells via paracrine controls including the chemokines or growth factors such as CXCL12, CXCL14, HGF (Allinen et al., 2004; Scheel et al. 2011). Matrix stiffness was recently found to be associated with cancer associated fibroblasts (CAFs), where activation of mechano-regulated transcriptional factor Yes-associated protein (YAP) occurs in response to stiffer matrix, which further promotes a feed forward loop that sustains matrix stiffness and subsequent activation of CAFs (Calvo et al. 2013). The stromal compartment of the tumor undergoes gene expression changes with the progression of disease specifically upregulating genes as MMPs that allow tumor cell invasion (Ma et al., 2009). Cancer associated fibroblast (CAFs) have been shown to

influence heterogeneity in tumors and have properties that facilitate invasion of primary tumor cells (Calvo et al. 2013). Stiffer microenvironment as a result of ECM crosslinking has been shown to contribute in breast tumorigenesis (Levental et al., 2009). An increase in matrix stiffness as a result of increase in ECM density has been further shown to promote tumorigenicity and leads to early onset of tumors in the MMTV.PyMT transgenic mice (Provenzano et al., 2008). In addition to this recent in-vitro findings have also shown that the increased matrix stiffness can promote proliferation and invasive behavior of human mammary epithelial cells (hMECS) (Paszek et al., 2005; Provenzano et al., 2009). Together these findings provide a compelling evidence for the important regulatory effect of mechanical stiffness in normal and tumorigenic condition.

CHAPTER 2

Cell type of origin as well as genetic alterations contribute to breast cancer phenotypes

Divya Bhagirath*, Xiangshan Zhao*, William W. West, Fang Qiu, Hamid Band and Vimla Band (*Equal contribution)

Oncotarget. 2015 Apr 20; 6 (11):9018-30.

2.1 INTRODUCTION

BC is the second leading cause of cancer related deaths among women (Siegel et al. 2016). Molecular profiling of patient-derived tumors has revealed different subtypes based on gene expression signatures. The understanding of origin of various subtypes is highly important area of research considering that distinct subgroups result in significantly different outcomes, with the basal-like subtype correlating with the worst outcome, followed by claudin-low, ErbB2 over-expressing, luminal-B, normal-like and luminal-A subtype (Prat et al., 2010; Sorlie et al., 2001). The nature of genetic alterations affecting the cell may therefore play an important role in determining the pathology (i.e. latency, incidence etc.) of resulting tumors. Another important factor is the cell of origin in which the initiating oncogenic event takes place. The characteristic nature of a particular cell may determine its susceptibility towards oncogenic transformation as well as its ability to develop to primary and metastatic tumors.

To understand the importance of cell type in determining tumor phenotype, in previous study investigators isolated two distinct hMECs by culturing normal mammary tissue under different conditions, transformed the cells with an identical set of oncogenes and injected these into mammary glands of immunocompromised mice. The injected cell lines gave rise to distinct tumors depending upon their differentiation states and developed lung metastasis in a cell type dependent manner (Ince et al., 2007). Similarly, another team of investigators showed that the origin of the transformed cell can determine the formation of tumor subtypes (Keller et al. 2012). Both studies support the idea that breast tumor subtypes may represent malignancies of biologically distinct cell types producing distinct disease entities. However, it is still not known whether the intrinsic differences in cell lines (susceptibility to transformation) may regulate the tumor phenotype by itself or

their oncogenic behaviors (transformation ability, tumor onset, incidence and metastatic capability) are also governed by the nature of genetic insults inflicted upon them.

Here, we addressed these questions by subjecting two human mammary epithelial cell lines that exhibit defined differences but are cultured under identical conditions to transformation with defined oncogene combinations. Clonal cell lines corresponding to human mammary stem/progenitor cell types were previously isolated from a single healthy reduction mammoplasty specimen and immortalized using the catalytic subunit of human telomerase (hTERT). These two types of cell lines are designated as $K5^+/K19^-$ or $K5^+/K19^+$ based on cytokeratin expression defining different lineage (Microarray accession no. GSE22580). Both of these cell types exhibit self-renewal and differentiate into both luminal and myoepithelial cells *in vitro* in defined medium (Zhao et al., 2010). Majority of breast cancers are carcinomas and K19 positive (Gudjonsson et al., 2002; Petersen and Polyak 2010). Expression of K19 can be used as prognostic marker for breast cancer (Kabir et al. 2014) and presence of K19+ circulating tumor cells (CTCs) in patients before or after treatment is associated with poor disease free survival (Ignatiadis et al., 2007; Xenidis et al., 2009; Xenidis et al., 2007) . However, K19 positive normal mammary epithelial cells are difficult to isolate and immortalize in culture. Thus, availability of $K5^+/K19^+$ and $K5^+/K19^-$ mammary stem/progenitor cell lines generated in our laboratory provides a unique opportunity to assess their ability to serve as cells of origin for breast tumors and the impact of cell type versus oncogenes in tumor associated characteristics. Transformation of these two cell lines with different oncogene combinations was followed by extensive *in vitro* and *in vivo* analyses to demonstrate that both nature of cell type and genetic alterations contribute to the primary and metastatic behavior of tumors resulting from these cells.

2.2 MATERIALS AND METHODS

Cell lines and retroviral/lentiviral infection

Mutant $p53^{R249S}$ in pLENTI-6 (purchased from Addgene) along with Invitrogen packaging vector (ViraPowerTM Lentiviral Packaging MIX) were transfected into 293FT packaging cells. Lentiviral supernatants were collected after overnight incubation in fresh DMEM media. TSA54 packaging cells were transfected with retroviral constructs, mutant H-Ras ^{Q61L} in pBABE-hygro, wild type ErbB2 or wild type EGFR in pMSCV-puro vector or pMSCV GFP-luciferase vector (kind gift from Dr. Rakesh Singh, UNMC), together with PIK plasmid for packaging, and viral supernatants were collected (as mentioned above for lentiviral). $K5^+/K19^-$ and $K5^+/K19^+$ stem/progenitor cell lines (Zhao et al. 2010) were infected with viral supernatants to generate cell lines with different gene combinations followed by their selection in DFCI-1 medium (Band and Sager, 1989; Band et al., 1990) containing hygromycin (15ul/ml) (for mutant H-Ras), blasticidine (15ul/ml) (for mutant p53), puromycin (0.5ul/ml) (for wild type ErbB2 or EGFR).

Antibodies

The following antibodies were used for western blotting, immunofluorescence, flow-cytometry and IHC: Rabbit anti-human ErbB2 (sc-284), mouse anti-human p53 (DO-1) (sc-126), mouse anti-human α-SMA (sc-32251), mouse anti-human vimentin (sc-6260) were from Santa Cruz Biotechnology. Mouse anti-human Ras (610001), mouse anti-human EGFR (610016), mouse anti-human MUC1 (550486), rat anti-human CD49f (555734), FITC conjugated anti-CD24 (555427), PE-Cy5 conjugated anti- CD49f (551129), PE-conjugated anti-CD44 (555479), FITC conjugated anti-CD227 (MUC1-

559774) and Alexa-488 conjugated E-Cadherin (560061) were from BD Bioscience. Mouse anti-claudin4 (329400) was from Invitrogen. Rabbit anti-human vimentin (clone SP20, RM-9120-S0) was from Thermo Scientific. Rabbit anti-human K5 (PRB-160P) was from Covance.

Anchorage-independence growth assays

40,000 cells suspended in DFCI-1 medium containing 0.3% agarose were seeded in the top layer of each well of 6-well plates containing 0.6% agarose as a bottom layer. Each cell line was plated in triplicates. Colonies (>60 cells) were counted after 3 weeks after crystal violet staining.

***In vitro* tumorsphere formation assays**

40,000 cells were plated per 2 ml in ultra-low attachment 6 well plates (Corning) in MEGM, as described previously by (Dontu et al., 2003). Each cell line had 6 replicates. Cells were fed with fresh medium on alternate days. Tumorspheres were counted under the microscope after 3 weeks of plating.

***In vitro* differentiation assays**

Protocol used for matrigel assay has been described previously (Zhao et al., 2011; Zhao et al. 2012). Briefly, 1 million cells suspended in DFCI-2 (Band and Sager, 1989; Band et al., 1990) medium containing 2% matrigel were plated on P-100 dish coated with 100% reconstituted basement membrane (matrigel from BD Biosciences). After 12 days (alternate day feeding), matrigel was dissolved using dispase enzyme (BD Biosciences)

at 37^{o}C for 1 hr, cells were counted and 1 million cells were stained with FITC conjugated anti-CD227 (MUC1) and PE-Cy5 conjugated anti- CD49f and analyzed by FACS.

Xenograft transplantation assays for primary tumor formation

6-8 weeks old immunodeficient NSG mice (purchased from Jackson laboratories) were injected with 1 million cells (not tagged with GFP-luciferase) in DFCI-1 medium mixed with matrigel in 1:1 proportion (Ince et al., 2007) in the fourth and ninth (contralateral) mammary glands. 4 mice were used for each combination. Tumor formation was assessed by palpation in the area of injection every week until 6 months. After six months, mice with or without tumors were sacrificed by CO_2 inhalation followed by cervical dislocation. Tumors were excised, fixed with 10% neutral buffered formalin and processed to prepare paraffin-embedded tumor blocks that were then sectioned for IHC.

Spontaneous metastasis formation assay

GFP-luciferase tagged tumor cells were injected in mammary glands of NSG mice. 10 mice were used for each combination. Mammary tumors formed after xenotransplantation of GFP-luciferase tagged tumor cells were surgically removed upon reaching 1000mm^3 tumor size. Mice were routinely assessed for luciferase activity (peritoneal injection of 30mg/ml luciferin substrate) by IVIS machine to detect any primary tumor and metastasis formation at different sites. Any subsequent tumors formed were also surgically removed and mice were assessed for metastasis formation for about 8 months.

Immunohistochemistry

Tumor tissues were fixed in 10% NBF and processed into paraffin blocks. 4 μm sections were cut and stained with indicated antibodies. The standard staining procedure was performed using DAKO kit as per the manufacturer's protocol (# K4007) and as described previously (Zhao et al.,2012). For IHC staining, tissue sections were incubated with primary antibodies (anti-K5, anti-MUC1, anti-vimentin, anti-α-SMA or anti-claudin4) in a hydrated chamber, followed by incubation with HRP-tagged secondary IgG against the primary antibodies and subsequently processed for nuclear staining and mounting of tissues. For double-immunofluorescence staining tumor sections were processed similarly and blocked with 10% goat serum for 1 hr. These were then stained with rabbit anti-vimentin, alexa 488 conjugated anti-E-cadherin, mouse anti- α-SMA or mouse anti-claudin4 antibodies. Goat anti-rabbit alexa 594 and goat anti-mouse alexa 488 conjugated secondary antibodies (Invitrogen) were used for staining. The sections were mounted with anti-fade mounting media. Images were taken with fluorescence microscope (Zeiss axioplan 2 imaging microscope).

Statistical Analysis

Statistical analysis was performed to analyze the tumor and metastasis onset and incidence for each transfectant. Time to event outcomes (tumor latency and metastasis latency) were calculated using Kaplan-Meier plots and then compared among all four groups using log-rank tests. If the overall p-value was significant, pairwise comparisons for each pair cell types were made with Sidak's correction. Tumor onset rate at 16-week follow up, lung and liver metastasis rate at 32-week follow up were compared using Fisher's exact tests.

2.3 RESULTS

In vitro oncogenic transformation of $K5^+/K19^-$ or $K5^+/K19^+$cells

We have previously isolated and characterized two types of hTERT-immortalized mammary epithelial stem/progenitor cells that are designated as $K5^+/K19^-$ or $K5^+/K19^+$ based on keratin expression (Microarray accession no. GSE22580, Supp. Table 1)(Zhao et al. 2010). We have reported previously that 100% of cells in these cell lines express designated keratins. These cell lines maintain self-renewal and are able to differentiate into both luminal and myoepithelial lineages upon culturing in defined medium (Zhao et al. 2010). We introduced mRas, mp53, wtErbB2 or wtEGFR in different combinations in both cell types using retroviral/lentiviral infection (Figure 2.1). The choice of mp53, wtEGFR and wtErbB2 as transforming genes was based on their wide use in the literature and their well-known occurrence in breast tumors (Elenbaas et al., 2001; Ince et al., 2007; Keller et al., 2012; Ro et al., 1988; Sainsbury et al., 1987; Slamon et al., 1987). $K5^+/K19^-$ and $K5^+/K19^+$ cells expression of various introduced genes was confirmed using western blotting (Figure 2.2A).

To analyze the transforming ability of exogenously introduced oncogenes and to determine susceptibility of these two cell lines to oncogene induced transformation, we performed *in vitro* soft agar assays and assessed the ability of oncogene-transduced cell lines to proliferate in an anchorage independent manner. As expected, cells expressing vectors alone failed to exhibit anchorage independent growth. In contrast, cells over-expressing wtEGFR or wtErbB2 together with mp53 showed much larger colonies (Figure 2.2C). $K5^+/K19^-$ and $K5^+/K19^+$ cells expressing mRas/mp53 together with either wtErbB2 or wtEGFR showed anchorage independent growth (Figure 2.2B, 2.2C). Notably, total number of colonies in $K5^+/K19^+$ cells, were significantly higher than that of colonies obtained by transformed $K5^+/K19^-$ cells (Figure 2.2B). These results demonstrate that *in-*

vitro transformation ability of a cell type is dependent on intrinsic differences within the cell lines but not the oncogene combination over-expressed by the cells.

Figure 2.1: Generation of $K5^+/K19^-$ and $K5^+/K19^+$ cells with different combination.

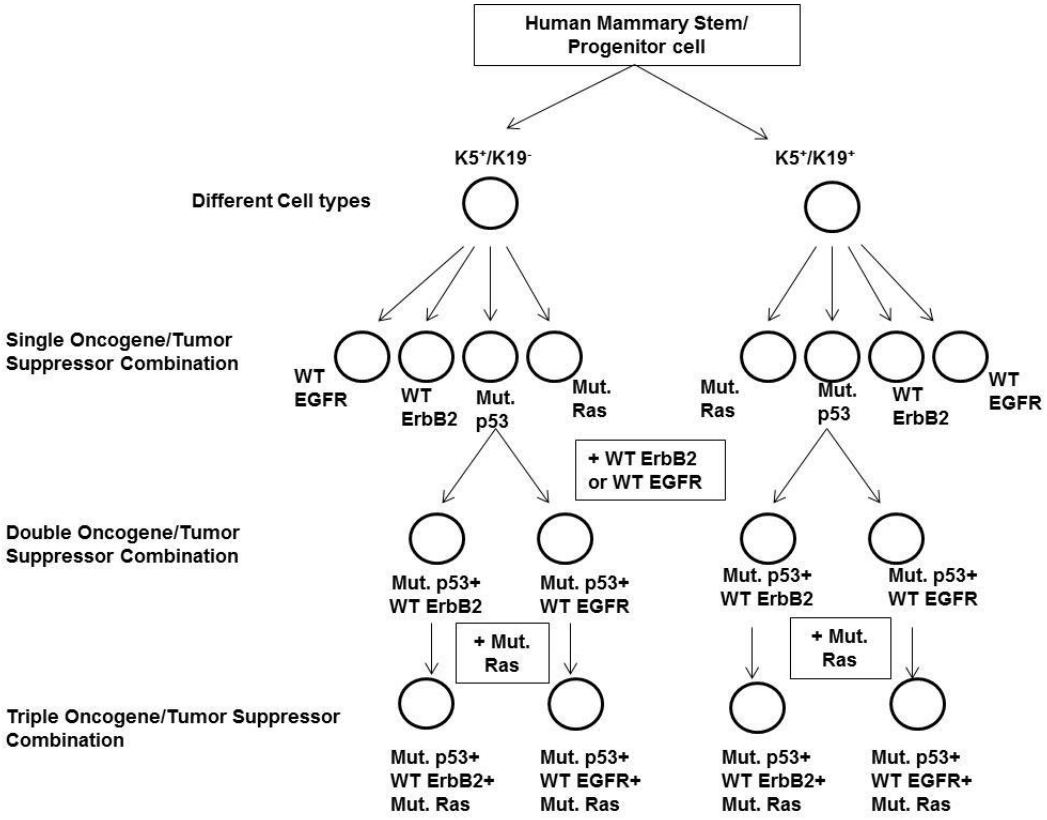

Figure 2.1: Generation of $K5^+/K19^-$ and $K5^+/K19^+$ cells with different combination. Schematic representation of different oncogene combinations (single, double or triple) that were over-expressed in $K5^+/K19^-$ and $K5^+/K19^+$ stem/progenitor cells.

Figure 2.2: Transformation of $K5^{+}/K19^{-}$ or $K5^{+}/K19^{+}$ cells with different gene combinations.

A

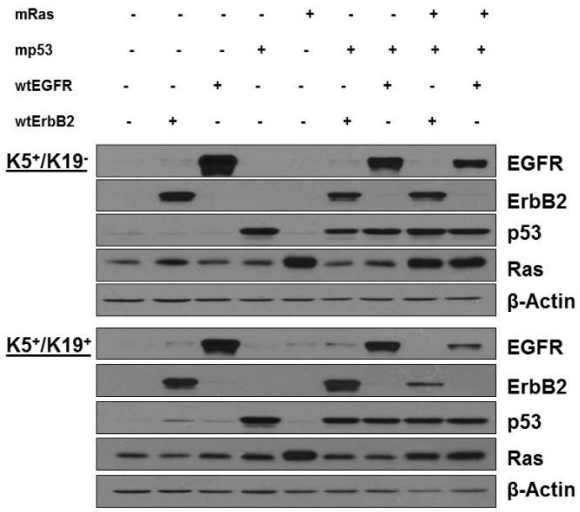

B

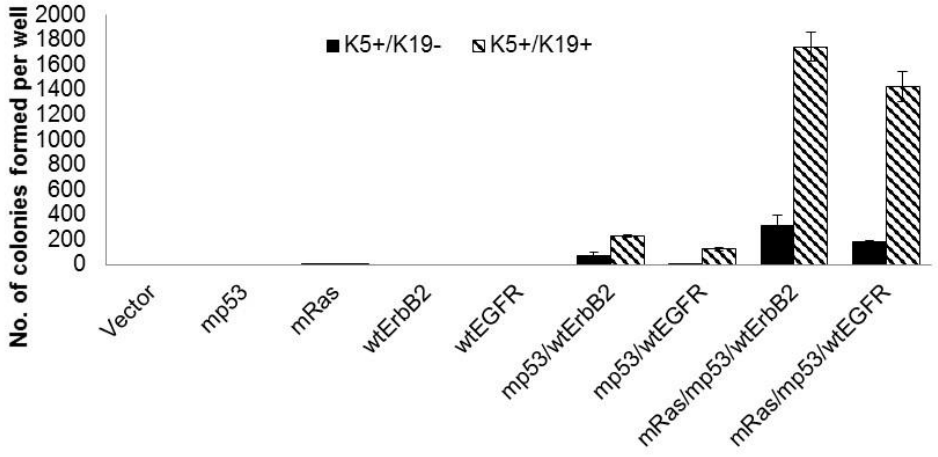

C

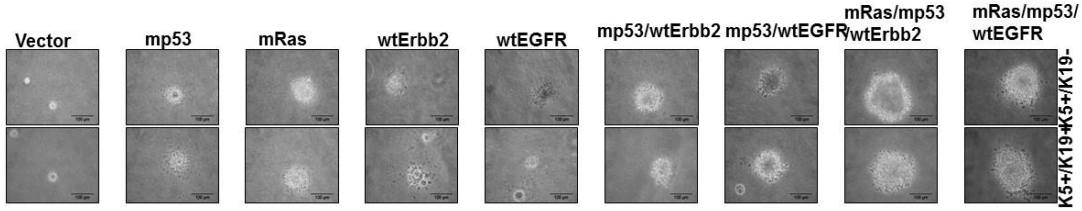

Figure 2.2: Transformation of $K5^+/K19^-$ or $K5^+/K19^+$ cells with different gene combination. A, $K5^+/K19^-$ or $K5^+/K19^+$ cell lines over-expressing mutant p53, mutant Ras, wild type ErbB2 or wild type EGFR in single, double or triple oncogene combinations were analyzed by Western Blotting. β-actin was used as loading control. B, Anchorage independent growth assay of $K5^+/K19^-$ and $K5^+/K19^+$ cells with vector or different gene combinations. Mean ±S.D of a representative experiment done in triplicate is shown. Three independent experiments were done. C, Representative images (magnification 40X) of colonies from $K5^+/K19^-$ and $K5^+/K19^+$ cells with vector or different oncogene combination are shown here.

Transformation of $K5^+/K19^-$ or $K5^+/K19^+$cells leads to enrichment of stem cell population, and reduction in the proportion of differentiated cells

It has been shown that loss of function of the tumor suppressor p53 enhances self-renewal ability of mammary stem cells (Cicalese et al., 2009). Similarly, other studies have shown that EGFR (Brandt et al., 2000; Deugnier et al., 2002), ErbB2 (Nair et al. 2014) or Ras (Cerrito et al., 2004; Jehn et al., 1992) play an important role in mammary stem cell self-renewal. We have previously shown that upon immortalization (pre-neoplastic transformation) with certain oncogenes, the stem/progenitor cell lines lose their ability to differentiate into myoepithelial cells (Zhao et al. 2010). Therefore, in this study we evaluated the impact of over-expression oncogene combinations on stem cell self-renewal and differentiation. We assessed the ability of oncogene over-expressing vs. vector control mammary stem/progenitor cell lines to form tumorspheres in ultra-low attachment plates, a commonly used assay to determine cancer stem cell self-renewal abilities (Charafe-Jauffret et al., 2009; Dontu et al., 2003; Mani et al., 2008; Zhang et al., 2008). Vector expressing cells showed formation of small spheres (<200 μm) and were not counted (Figure 2.3C). However, both cell types overexpressing single or double oncogene combinations showed tumorsphere formation as compared to control cells (Figure 2.3A, 2.3E). Notably, cells expressing the triple combinations of oncogenes exhibited a significant increase in number of tumorsphere (>200 μm in size) formed (Figure 2.3A-D). Both the transformed $K5^+/K19^-$ or $K5^+/K19^+$ cells formed secondary tumorspheres upon re-plating (Figure 2.3B, 2.3C) and the efficiency for tertiary tumorsphere formation was substantially enriched for cells over-expressing oncogene combination mRas/mp53/wtEGFR (Figure 2.3C) demonstrating increased self-renewal capabilities of these transformed cell lines.

Figure 2.3: *In-vitro* self-renewal of $K5^{+}/K19^{-}$ or $K5^{+}/K19^{+}$ cells over-expressing different oncogenes

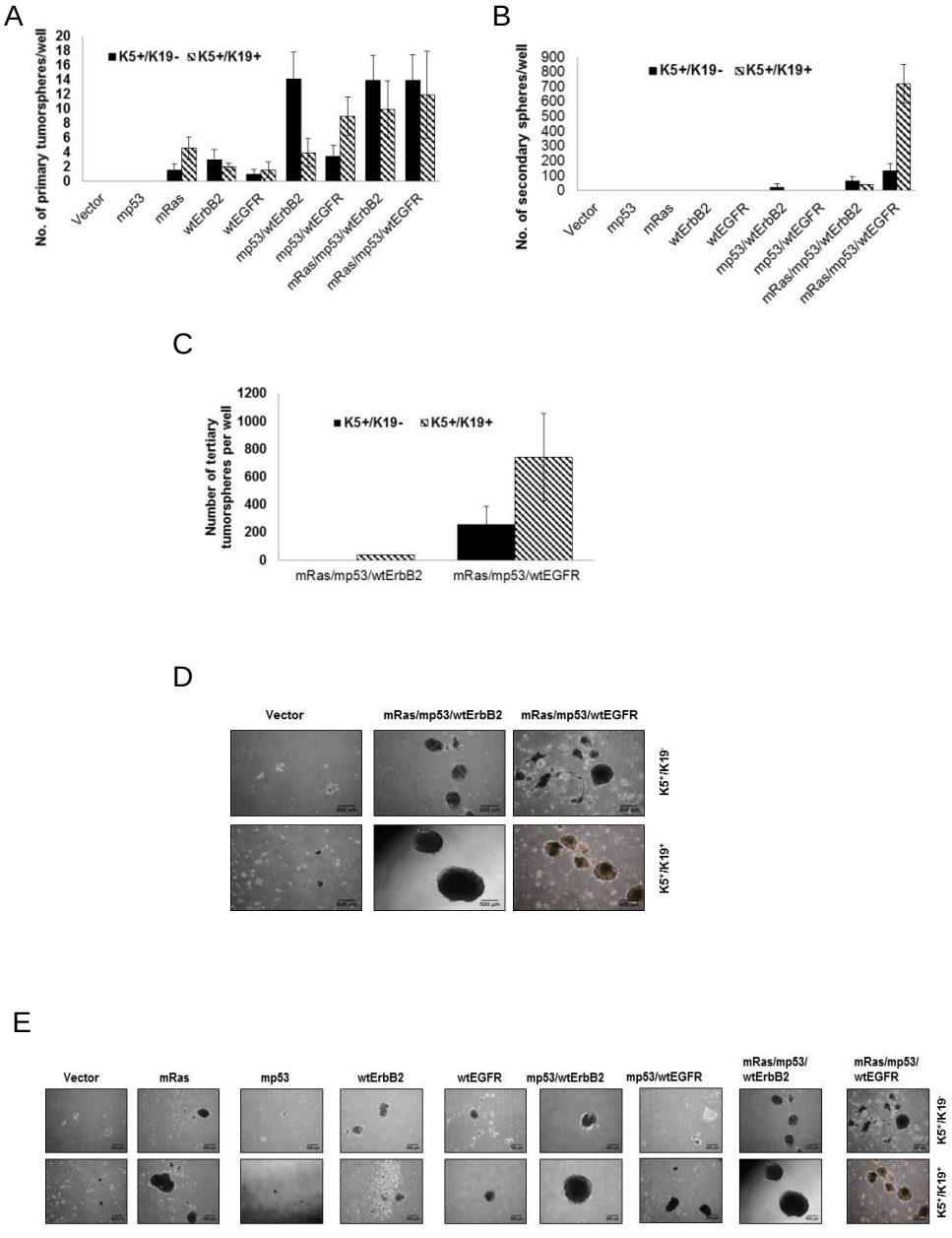

Figure 2.3: *In-vitro* self-renewal of $K5^+/K19^-$ or $K5^+/K19^+$ cells over-expressing different oncogenes. For tumorsphere-formation assay indicated cell lines were cultured in low-attachment plates in MEGM media for 3 weeks. A) Primary tumorshperes were trypsinized and cultured to generate B) secondary or C) tertiary tumorspheres. Spheres ≥200μm were quantified. Mean +/- SD of a representative experiment done in 6 replicates is shown. D), E) Representative images (magnification 4X) of tumorspheres from $K5^+/K19^-$ and $K5^+/K19^+$ cells with vector or different oncogene combinations (single, double or triple) are shown.

Previously, we showed that both $K5^{+}/K19^{-}$ and $K5^{+}/K19^{+}$ cell types express high levels of CD49f and CD44, and variable expression of CD24 where intermediate (inter) and high levels of CD24, reflects more differentiated progenitor cells (Zhao et al.,2010; Zhao et al. 2011). We therefore used a combination of these markers for FACS analysis to assess the relative levels of stem/progenitor cells vs. differentiated cells in various triple transformed derivatives. Notably, we observed a significant decrease in $CD24^{inter}$ and $CD24^{Hi}$ population (Figure 2.4A, 2.4B, 2.5A, 2.5B) in both transformed stem/progenitor cell lines in comparison with the vector-expressing cells, indicating an enrichment of stem cell population in both cell types upon transformation.

As previously shown, $K5^{+}/K19^{-}$ and $K5^{+}/K19^{+}$ mammary stem/progenitor cell lines are bi-potent stem/uncommitted progenitors and are able to differentiate into both luminal and myoepithelial cells under appropriate differentiating conditions (Zhao et al. 2010). Furthermore, when grown in 3D matrigel culture and subjected to differentiating media DFCI-2, the stem/progenitor cells are preferentially induced into luminal differentiation (Zhao et al. 2010). Notably, when we subjected $K5^{+}/K19^{-}$ and $K5^{+}/K19^{+}$ cells expressing triple oncogene combinations to differentiation using *in-vitro* 3D matrigel culture, we observed an increased CD49f+ (marker for stem cell) fraction (97% vs. 86% for $K5^{+}/K19^{-}$ and 96% vs. 92% for $K5^{+}/K19^{+}$) and decrease in MUC1+ (marker for luminal differentiation) fraction (0.4%,0.1% vs. 0.9% for $K5^{+}/K19^{-}$ and 0.5%,0.2% vs. 1.2% for $K5^{+}/K19^{+}$) in transformed lines vs. their controls (Figure 2.6A, 2.6B). These results indicate that oncogene-mediated transformation of mammary stem/progenitor cells reduces their ability to differentiate. Taken together, these results demonstrate an increase in stem cell property of triple oncogene transformed derivatives.

Figure 2.4: Expression of different stem cell markers in $K5^+/K19^-$ or $K5^+/K19^+$ expressing different combinations

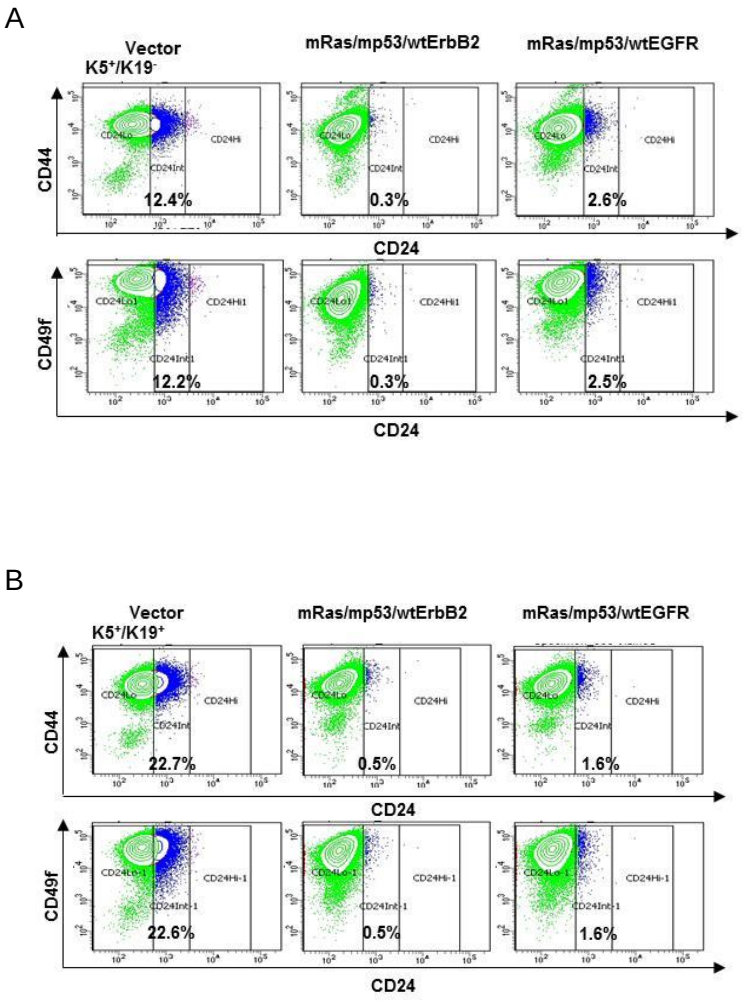

Figure 2.4: Expression of different stem cell markers in $K5^+/K19^-$ or $K5^+/K19^+$ expressing different combinations. Vector or transformed (A) $K5^+/K19^-$ or (B) $K5^+/K19^+$ cells were stained with stem cell markers CD49f, CD44 and CD24 and analyzed by Flow Cytometry. Dot plot analysis of cell population expressing CD44/CD24 (upper panel) and CD49f/CD24 (Lower panel). Decrease in CD24 cell population is seen in middle $CD24^{Int}$ gate.

Figure 2.5: Expression of different stem cell markers in $K5^+/K19^-$ or $K5^+/K19^+$ expressing different combinations.

A

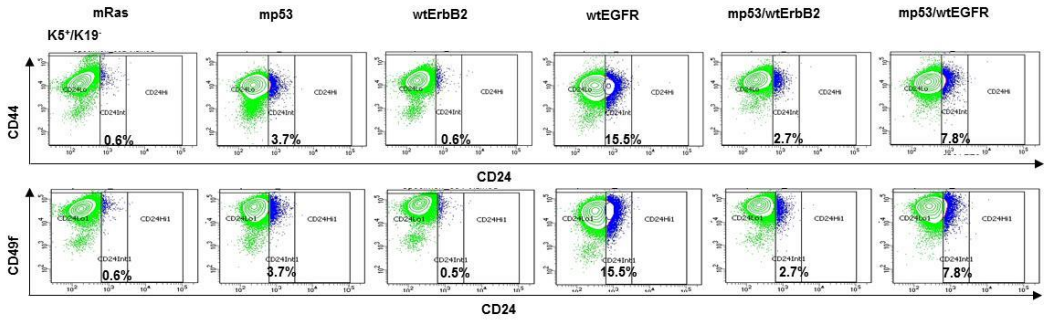

B

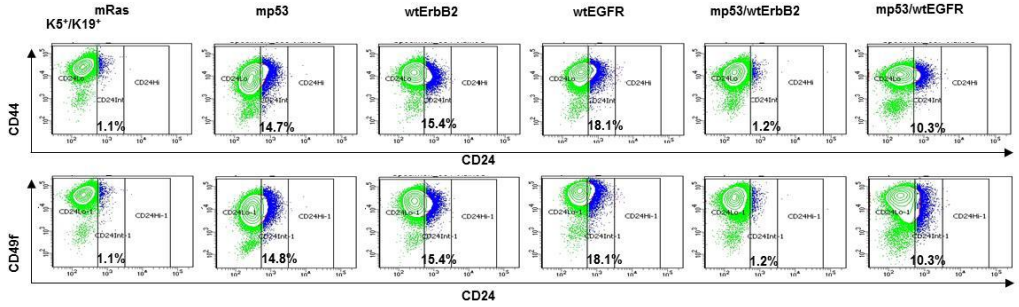

Figure 2.5: Expression of different stem cell markers in $K5^+/K19^-$ or $K5^+/K19^+$ expressing different combinations. A and B. $K5^+/K19^-$ (A) or $K5^+/K19^+$ (B) cells over-expressing single (mp53, mRas, wtErbB2 or wtEGFR) or double (mp53/wtErbB2 or mp53/wtEGFR) were stained with stem cell markers CD49f, CD44 and CD24 and analyzed by Flow Cytometry. Dot plot analysis of cell population expressing CD44/CD24 (upper panel) and CD49f/CD24 (Lower panel). Change in CD24 cell population is seen in middle $CD24^{Int}$ gate.

Figure 2.6: *In-vitro* differentiation ability of transformed K5$^+$/K19$^-$ or K5$^+$/K19$^+$cells.

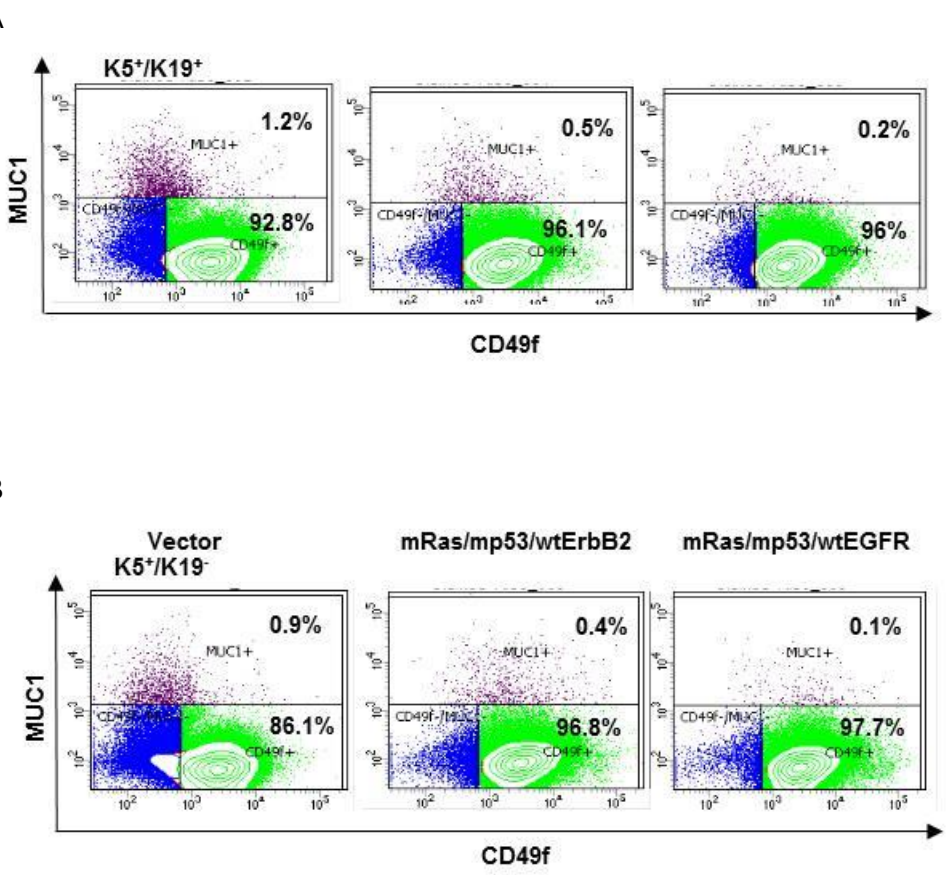

Figure 2.6: *In-vitro* differentiation ability of transformed K5$^+$/K19$^-$ or K5$^+$/K19$^+$ cells A) and B). Control or transformed K5$^+$/K19$^-$(A) or K5$^+$/K19$^+$ (B) cells were grown in DFCI-2 (differentiation) medium in Matrigel. Acini were trypsinized and stained with PE-Cy5 conjugated anti-CD49f and FITC conjugated anti-MUC1 and subjected to FACS analysis.

Oncogene-transformed $K5^+/K19^-$ and $K5^+/K19^+$ cells produce mixed tumors in NSG mice

Given the *in-vitro* capabilities of both cell types to exhibit anchorage independence and enhanced tumorsphere formation when transformed (Figure 2.2B, 2.2C and Fig. 2.3), we assessed their ability to form tumors upon orthotopic implantation in the mammary glands of immunocompromised NSG mice, as a proof of full oncogenic transformation. Triple (mRas/mp53/wtErbB2 or mRas/mp53/wtEGFR) oncogene transformed $K5^+/K19^-$ and $K5^+/K19^+$ cells were injected orthotopically in mice mammary glands. As expected, none of the mice implanted with control vector cells or those with double oncogene combinations produced tumors, while all the triple oncogene transformed $K5^+/K19^-$ and $K5^+/K19^+$ cells gave rise to tumors in mice. Histologically, tumors arising from triple oncogene combinations in $K5^+/K19^-$ and $K5^+/K19^+$ cells appeared distinct from each other. Tumors arising from transformed $K5^+/K19^-$ cells exhibited predominance of spindle-like tumor cell morphology while those arising from transformed $K5^+/K19^+$ cells resembled adenocarcinomas (Figure 2.7). These differences in the tumor phenotype are consistent with previous findings that biological differences in cell types can give rise to distinct histological subtypes of tumors (Ince et al., 2007; Keller et al. 2012). We further observed that all tumors exhibited intra-tumoral heterogeneity as seen by the expression of various markers including MUC1 (for luminal differentiation), K5 (for stem-progenitor/basal), vimentin (for stem-progenitor/basal/myoepithelial), α-SMA (for myoepithelial) and claudin4 (for claudin-low) (Figure 2.8, 2.9). In order to confirm that the claudin-low component within the tumors with mixed phenotype was derived from the transformed human stem/progenitor cells, we performed double immunostaining of these tumors with human specific anti-vimentin together with anti-α-SMA, anti-E-cadherin or anti-claudin4 (Fig. 2.7A-C). $K5^+/K19^-$ cells over-expressing wtErbB2 combination predominantly gave rise to

tumors with high claudin-low (spindle like, α-SMA^{+} ,vimentin^{+}, claudin4^{-}) and less basal (K5^{+}) characteristics, whereas the same cells over-expressing wtEGFR combinations formed tumors with mixed basal, luminal and claudin-low phenotype (Figure 2.7, 2.8, 2.9). Similarly tumors arising from K5^{+}/K19^{+} cells over-expressing wtErbB2 combination showed more luminal and basal characteristics, whereas those derived by wtEGFR combination had both luminal and basal with some claudin-low components (Figure 2.8, 2.9).

Figure 2.7: Transformed $K5^+/K19^-$ or $K5^+/K19^+$ cells give rise to distinct tumors.

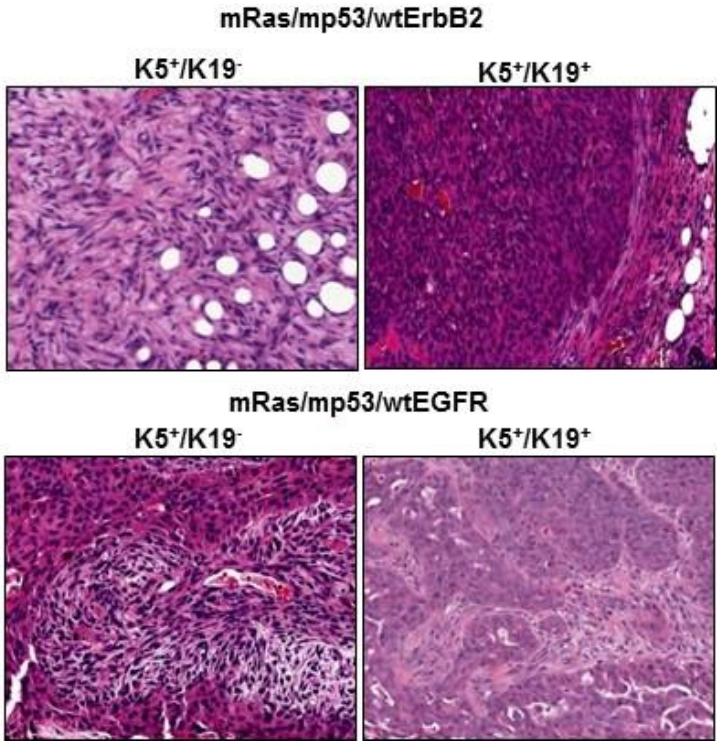

Figure 2.7: Transformed $K5^+/K19^-$ or $K5^+/K19^+$ cells give rise to distinct tumors. A, Representative images of H&E staining of tumor sections (magnification 20X) from $K5^+/K19^-$ and $K5^+/K19^+$ cells over-expressing mRas/mp53/wtErbB2 (upper panel) or mRas/mp53/wtEGFR (Lower panel).

To exclude the possibility of mouse mammary gland contribution, we used human specific vimentin antibody to confirm that the tumors were derived from the injected human cells. Vimentin antibody used here is highly specific for human cells as it neither detects vimentin protein in western blotting using mouse fibroblasts (Figure 2.10) nor does it stains mouse mammary gland (Figure 2.11A, 2.11B). Interestingly, staining of tumor sections from mice injected with $K5^+/K19^+$ cells over-expressing wtEGFR combination showed both infiltrating ductal carcinoma and well-formed ductal structures with varying degrees of hyperplasia. The hyperplastic structures had a well-defined outer α-SMA-positive, vimentin positive (myoepithelial) and inner MUC1 positive (luminal) staining pattern (Fig. 2.11A, 2.11B), indicative of the ability of human $K5^+/K19^+$ cells to differentiate into both myoepithelial and luminal cells *in vivo*. All tumors from transformed $K5^+/K19^-$ and $K5^+/K19^+$ stem/progenitor cells were ER-negative (data not shown) consistent with the ER-negative status of the parental normal stem/progenitor cells (Zhao et al. 2010).

Figure 2.8: Transformed $K5^{+}/K19^{-}$ or $K5^{+}/K19^{+}$ cells give rise to distinct tumors.

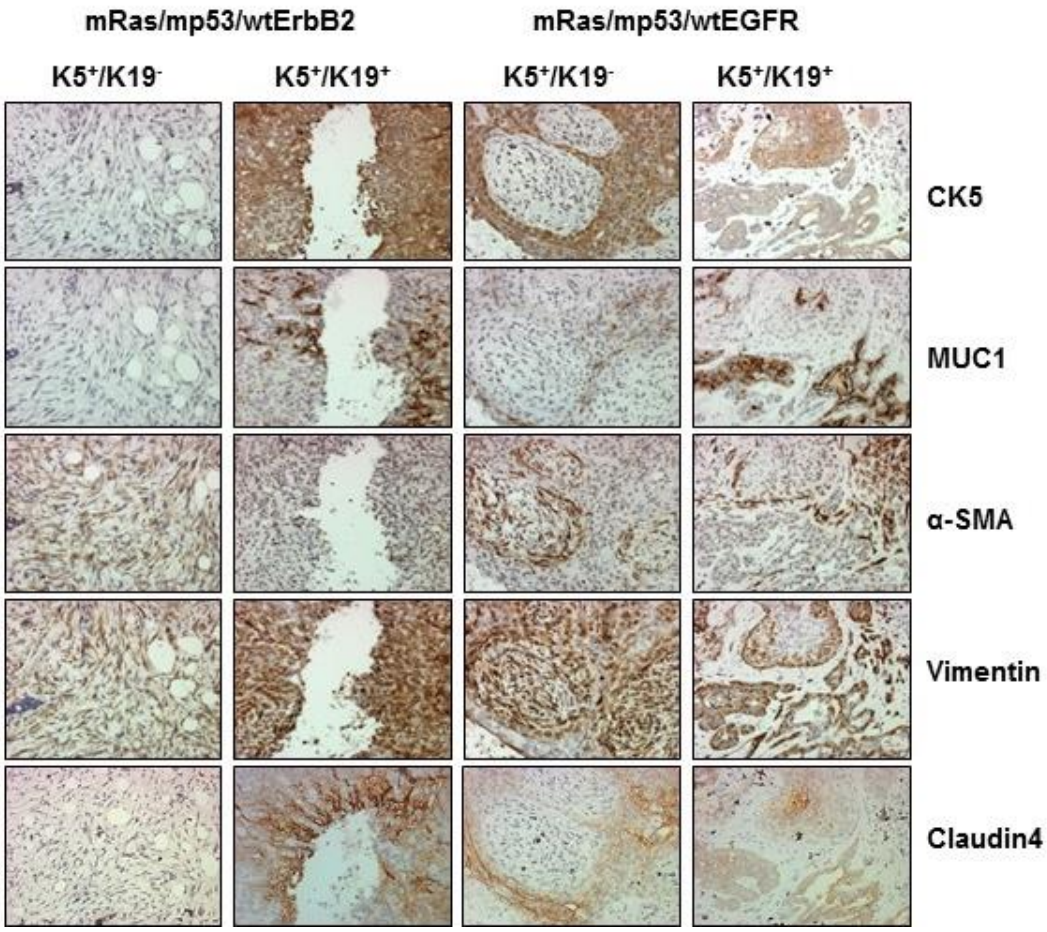

Figure 2.8: Transformed $K5^{+}/K19^{-}$ or $K5^{+}/K19^{+}$ cells give rise to distinct tumors. Images from different tumors at magnification 20X. Immunohistochemical staining of tumor sections with anti-CK5 (Basal/Stem), anti-MUC1 (Luminal), anti-αSMA (Myoepithelial) anti-vimentin (Stem/myoepithelial) and claudin4 (for claudin-low) antibodies.

Figure 2.9: Transformed $K5^+/K19^-$ or $K5^+/K19^+$ cells give rise to distinct tumors.

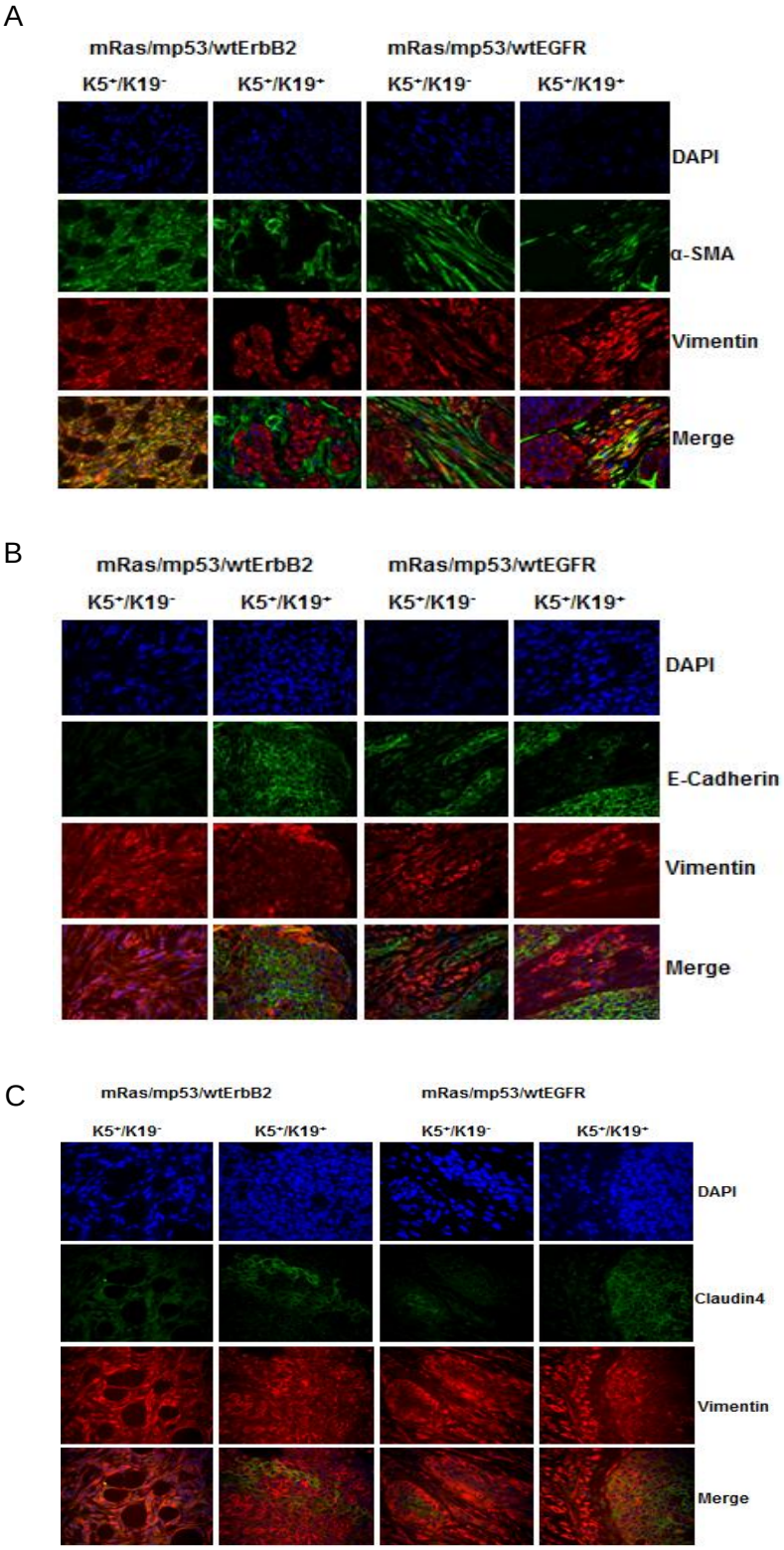

Figure 2.9: Transformed $K5^+/K19^-$ or $K5^+/K19^+$ cells give rise to distinct tumors. Representative image of tumors from $K5^+/K19^-$ or$K5^+/K19^+$ cells double immunostained with A) anti-αSMA (green) and anti-vimentin (red) show presence of claudin-low (SMA^+/$vimentin^+$) areas within different tumors. Same tumor sections double immunostained with B) E-Cadherin (green) and vimentin (red) show presence of luminal like ($E\text{-}Cadherin^+$) areas within different tumors and C) with anti-claudin4 (green) and anti-Vimentin (red) show presence of claudin-low ($claudin4^-$/$Vimentin^+$) areas within different tumors. DAPI (blue) shows nucleus.

Figure 2.10. Human specificity of vimentin antibody.

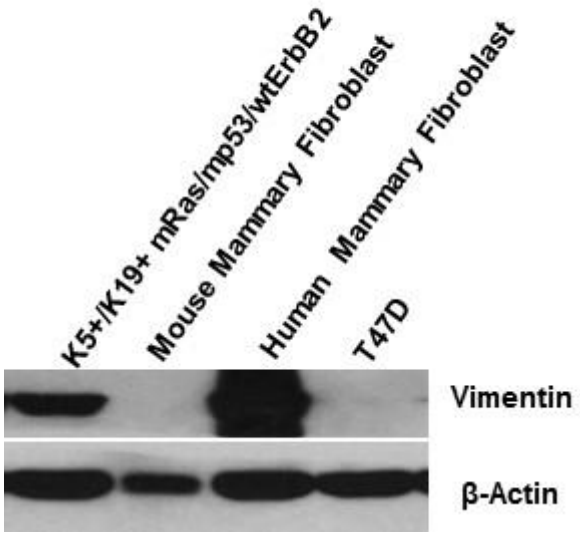

Figure 2.10. Human specificity of vimentin antibody. Western blot. Cell lysates from transformed $K5^{+}/K19^{+}$ cells, mouse and human derived fibroblast cells and breast cancer cell line T47D were probed with human specific vimentin antibody and analyzed by Western Blotting. β-actin was used as loading control.

Figure 2.11: Transformed $K5^+/K19^-$ or $K5^+/K19^+$ cells retain stem cell characteristics *in-vivo*

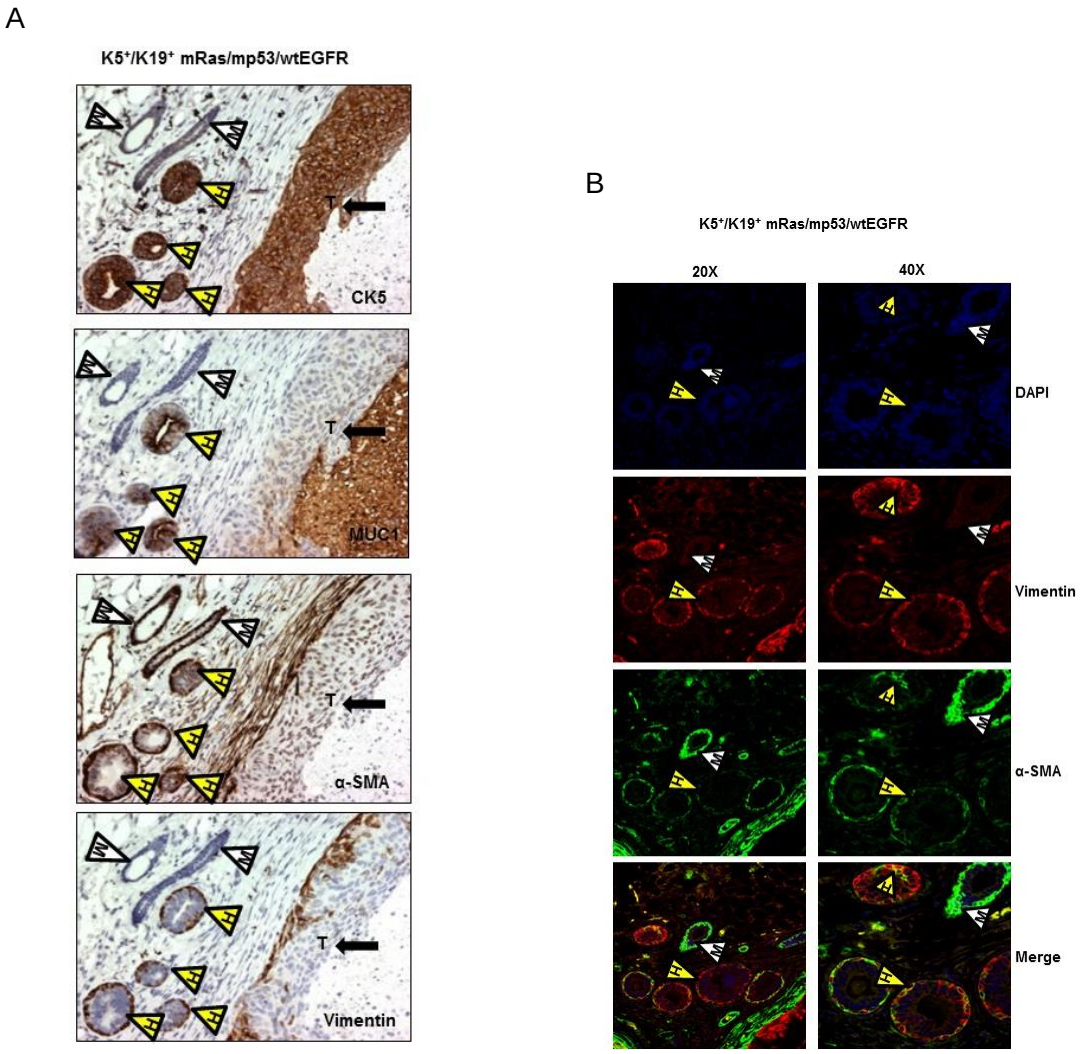

Figure 2.11: Transformed $K5^+/K19^-$ or $K5^+/K19^+$ cells retain stem cell characteristics *in-vivo*. A, Immunostaining with lineage specific markers of tumors and mammary duct like structures with varying degree of hyperplasia originating from $K5^+/K19^+$ cells over-expressing mRas/mp53/wtEGFR. Yellow arrowheads with H indicate human mammary ductal structures, white arrowheads with M indicate mouse mammary ducts and arrow with T shows tumor. B, Immunofluorescence staining of the same tumor section with anti-vimentin (red), anti-αSMA (green) antibodies at magnifications 20X (left panel) and 40X (right panel). White arrowhead indicate mouse ductal structure, yellow arrowheads indicate co-expression in human ductal structures.

Both oncogene and cell type contribute to tumor development and progression in NSG mice

Mice injected with cells over-expressing triple oncogene combinations developed tumors consistently (Table 2.1, 2.2). Notably, tumors arising from mRas/mp53/wtEGFR over-expressing $K5^+/K19^-$ cell line had a statistically significant longer latency and lower tumor incidence than those arising from other cell lines tested (Figure 2.12A, Table 2.4). The average tumor latency was 20 weeks for $K5^+/K19^-$ cell with mRas/mp53/wtEGFR and 11.75 weeks for $K5^+/K19^-$ over-expressing mRas/mp53/wtErbB2 (Figure 2.12A, Table 2.5) . Despite the longer primary tumor latency wtEGFR combination had a higher lung metastasis incidence (Table 2.3, Figure 2.12B, 2.12C, Table 2.6) as compared to wtErbB2 in $K5^+/K19^-$ cell line and unique liver metastasis (Figure 2.12E, Table 2.3, Table 2.7). These results support the conclusion that different oncogenes can drive distinct oncogenic and metastatic potential in same cell type. On the other hand, we observed $K5^+/K19^+$ cell line over-expressing mRas/mp53/wtEGFR had a low primary tumor latency as compared to $K5^+/K19^-$ with same oncogene combination (Figure 2.12A, Table 2.1, 2.2, 2.5) and high tumor incidence (Table 2.8) as compared to all other cell lines tested. More significantly, $K5^+/K19^+$ cell line over-expressing either mRas/mp53/wtErbB2 or mRas/mp53/wtEGFR had statistically significant lower lung metastasis latency (Figure 2.12B, Table 2.9) as compared to $K5^+/K19^-$ with mRas/mp53/wtErbB2, higher lung metastasis incidence (Table 2.3, 2.6) and bigger metastatic tumors (Figure 2.12D) as compared to $K5^+/K19^-$ cells over-expressing either of the oncogene combinations, indicating that the nature of cell type also affects the tumor and metastasis formation.

Table 2.1 Tumor latency for $K5^+/K19^-$ and $K5^+/K19^+$ stem/progenitor cells with different combination.

Cell Line	Tumor Onset (Time first tumor appeared)	No. of mice that formed tumors (by 24 weeks)
$K5^+/K19^-$ mRas/mp53/wtErbB2	12 weeks	4/4
$K5^+/K19^+$ mRas/mp53/wtErbB2	9 weeks	4/4
$K5^+/K19^-$ mRas/mp53/wtEGFR	24 weeks	2/4
$K5^+/K19^+$ mRas/mp53/wtEGFR	12 weeks	4/4

Table 2.2 Tumor latency for $K5^{+}/K19^{-}$ and $K5^{+}/K19^{+}$ stem/progenitor cells with different combination.

Cell Line	Tumor Onset (Time first tumor appeared)	No. of mice that formed tumors (by 16 weeks)	No. of mice that formed tumors (by 16 weeks)
$K5^{+}/K19^{-}$ mRas/mp53/wtErbB2	7 weeks	10/10	10/10
$K5^{+}/K19^{+}$ mRas/mp53/wtErbB2	9 weeks	8/10	10/10
$K5^{+}/K19^{-}$ mRas/mp53/wtEGFR	16 weeks	2/7	7/7
$K5^{+}/K19^{+}$ mRas/mp53/wtEGFR	7 weeks	10/10	10/10

Figure 2.12: In-vivo tumor and metastasis formation from transformed $K5^{+}/K19^{-}$ or $K5^{+}/K19^{+}$ cells.

A

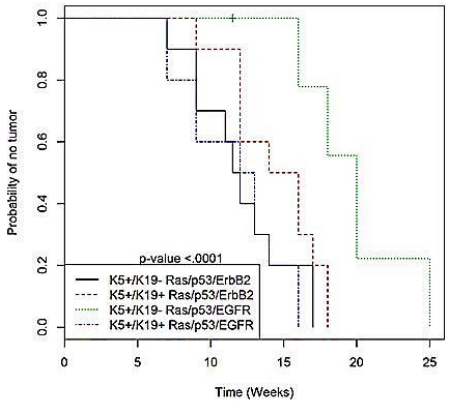

B

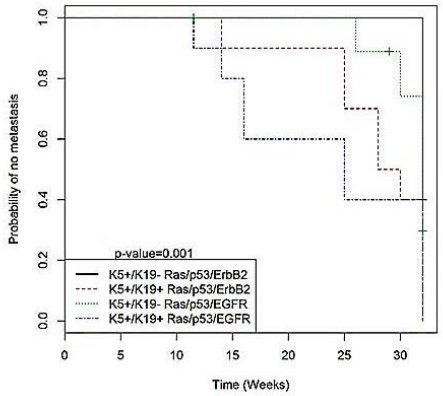

C

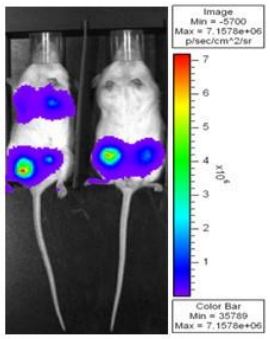

D

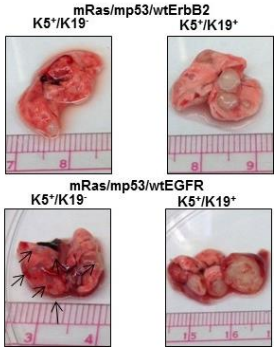

E

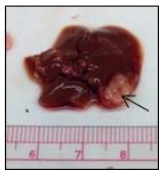

Figure 2.12: In-vivo tumor and metastasis formation from transformed $K5^+/K19^-$ or $K5^+/K19^+$ cells. A, Kaplan-Meier plot for probability of no tumor in mice injected with $K5^+/K19^-$ and $K5^+/K19^+$ cells over-expressing mRas/mp53/wtErbB2 or mRas/mp53/wtEGFR from the second experiment. B, Kaplan-Meier plot for probability of no metastasis in above mentioned mice. C, Representative image of mice with or without lung metastasis as shown by IVIS luciferase imaging. D, Representative image of lung metastatic lesions formed by different cell types with either mRas/mp53/wtErbB2 (upper panel) or mRas/mp53/wtEGFR (Lower panel). E, Representative image of liver metastasis as seen in mice injected with $K5^+/K19^-$ cells over-expressing mRas/mp53/wtEGFR.

Table 2.3 Metastasis observed with $K5^{+}/K19^{-}$ and $K5^{+}/K19^{+}$ stem/progenitor cells with different combination.

Cell Line	Metastasis first appeared in mice	No. of mice that formed lung metastasis by 32 weeks	No. of mice that formed liver metastasis by 32 weeks
$K5^{+}/K19^{-}$ mRas/mp53/wtErbB2	31^{st} week	6/10	0/10
$K5^{+}/K19^{+}$ mRas/mp53/wtErbB2	25^{th} week	10/10	0/10
$K5^{+}/K19^{-}$ mRas/mp53/wtEGFR	26^{th} week	5/7	2/7
$K5^{+}/K19^{+}$ mRas/mp53/wtEGFR	11^{th} week	10/10	0/10

Table 2.4 Log-rank test for time (in weeks) taken to form tumors in mice (n=10 each).

Cell lines	Median survival time to first tumor (weeks)	Log-rank test overall P-value	Pairwise comparsion with Sidak's correction			
			$K5^+/K19^-$ mRas/mp53/ wtErbB2	$K5^+/K19^+$ mRas/mp53 /wtErbB2	$K5^+/K19^-$ mRas/mp53/ wtEGFR	$K5^+/K19^+$ mRas/mp53/ wtEGFR
$K5^+/K19^-$ mRas/mp53/ wtErbB2	11.75	<.0001	--	0.85	0.0002	0.99
$K5^+/K19^+$ mRas/mp53/ wtErbB2	15			--	0.04	0.77
$K5^+/K19^-$ mRas/mp53/ wtEGFR	20				--	<.0001
$K5^+/K19^+$ mRas/mp53/ wtEGFR	12.5					--

$K5^+/K19^-$ mRas/mp53/wtEGFR group had longer tumor latency compared with $K5^+/K19^-$ mRas/mp53/wtErbB2, $K5^+/K19^+$mRas/mp53/wtErbB2, and $K5^+/K19^+$ mRas/mp53/wtEGFR. Sidak adjusted p-value: 0.0002, 0.04, and <.0001 respectively

Table 2.5. Lung metastasis rate at 32-week follow up

Variables		No metastasis n (%)	Lung metastasis n (%)	p-value
Cell line	$K5^+/K19^-$ mRas/mp53/wtErbB2	4 (40)	6 (60)	0.03
	$K5^+/K19^+$ mRas/mp53/wtErbB2	0 (0)	10 (100)	
	$K5^+/K19^-$ mRas/mp53/wtEGFR	2 (28.6)	5 (71.4)	
	$K5^+/K19^+$ mRas/mp53/wtEGFR	0 (0)	10 (100)	

There was indication of a difference among four groups with regard to lung metastasis rate at 32-week follow up (p=0.03).The $K5^+/K19^-$ mRas/mp53/wtErbB2 group had lowest lung metastasis rate and $K5^+/K19^+$ mRas/mp53/wtErbB2 and $K5^+/K19^+$ mRas/mp53/wtEGFR group had the highest lung metastasis rate among four groups.

Table 2.6. Liver metastasis rate at 32-week follow up

Variables		No metastasis n (%)	Liver metastasis n (%)	p-value
Cell line	$K5^+/K19^-$ mRas/mp53/wtErbB2	10 (100)	0 (0)	0.03
	$K5^+/K19^+$ mRas/mp53/wtErbB2	10 (100)	0 (0)	
	$K5^+/K19^-$ mRas/mp53/wtEGFR	5 (71.4)	2 (28.6)	
	$K5^+/K19^+$ mRas/mp53/wtEGFR	10 (100)	0 (0)	

There was indication of a difference among four groups with regard to liver metastasis rate at 32-week follow up (p=0.03). The $K5^+/K19^-$ mRas/mp53/wtEGFR group had highest liver metastasis rate among four groups

Table 2.7. Tumor incidence rate at 16-week follow up.

Variables		No tumor n (%)	Tumor by 16 week n (%)	p-value
Cell line	$K5^+/K19^-$ mRas/mp53/wtErbB2	2(20)	8 (80)	0.01
	$K5^+/K19^+$ mRas/mp53/wtErbB2	3 (30)	7 (70)	
	$K5^+/K19^-$ mRas/mp53/wtEGFR	5 (71.4)	2 (28.6)	
	$K5^+/K19^+$ mRas/mp53/wtEGFR	0 (0)	10 (100)	

There was indication of a difference among four groups with regard to tumor onset rate at 16-week follow up (p=0.01).The $K5^+/K19^-$ mRas/mp53/wtEGFR group had lowest tumor rate and $K5^+/K19^+$ mRas/mp53/wtEGFR group had the highest tumor rate among four groups

Table 2.8. Log-rank test for time (in weeks) taken to form metastasis in mice

Cell lines	Median survival time to first metastasis (weeks)	Log-rank test over all P-value	Pairwise comparsion with Sidak's correction			
			$K5^+/K19^-$ mRas/mp53/ wtErbB2	$K5^+/K19^+$ mRas/mp53/ wtErbB2	$K5^+/K19^-$ mRas/mp53/ wtEGFR	$K5^+/K19^+$ mRas/mp53/ wtEGFR
$K5^+/K19^-$ mRas/mp53/ wtErbB2	32	0.001	--	0.02	0.87	0.004
$K5^+/K19^+$ mRas/mp53/ wtErbB2	29			--	0.23	0.99
$K5^+/K19^-$ mRas/mp53/ wtEGFR	32				--	0.08
$K5^+/K19^+$ mRas/mp53/ wtEGFR	25					--

$K5^+/K19^-$ mRas/mp53/wtErbB2 group took longer time to develop the first metastasis compared with $K5^+/K19^+$ mRas/mp53/wtErbB2 (median survival time in weeks: 32 vs. 29, Sidak adjusted p-value: 0.02), and $K5^+/K19^+$ mRas/mp53/wtEGFR (median survival time in weeks: 32 vs. 25, Sidak adjusted p-value: 0.004)

2.4 DISCUSSION

Diversity in breast tumors is multifactorial. Classification of tumors in to various subtypes emphasizes the important role of genetic mutation/overexpression in characterizing a tumor (Perou et al., 2000; Sorlie et al., 2001). Besides, the type of cell in which a particular genetic event occurs is another important factor that may determine the phenotype of tumors (Ince et al., 2007; Keller et al. 2012). While it is likely that tumor heterogeneity is of multifactorial origin, there is now wider acceptance of the idea that breast cancers exhibit a stem cell hierarchy (Al-Hajj et al., 2003; Liu et al., 2010; Reya et al., 2001).Thus, one aspect of cellular diversity in tumors is thought to reflect the relative contributions to tumor mass of cells representing various points in the stem cell program. However, experimental support for the relative importance of cell types from which tumors arise versus the oncogenic events themselves has been difficult as suitable cellular models have not been available. Here, we have transformed immortal human mammary stem/progenitor cell lines with breast cancer-relevant cellular oncogenes to address these issues. Our analyses show that both the cell of origin as well as makeup of oncogenic events are important factors that shape the phenotype, oncogenicity as well as the metastatic behavior of a particular tumor.

We utilized two unique, well characterized normal human mammary stem/progenitor cell lines originating from a single donor that exhibit stable differences in keratin 19 expression as well as other genes (Microarray accession no. GSE22580, Supp. Table 1) and are, designated as $K5^{+}/K19^{-}$ and $K5^{+}/K19^{+}$. These cells can be propagated in culture as they have been rendered immortal with hTERT (Zhao et al. 2010). The cells remain in an undifferentiated state when grown in DFCI-1 medium but can be predictably induced to differentiate into myoepithelial and luminal lineages when cultured in differentiating media, thereby demonstrating their bi-potent nature (Zhao et al. 2010).

Although majority of breast cancers are K19+ the mechanistic insights of this observation has not been addressed much in the literature. A correlative study suggested K19+ breast cancers exhibit poor prognosis (Kabir et al. 2014). Further studies have demonstrated, K19+ CTCs in breast cancer patients are associated with poor disease-free survival (Ignatiadis et al., 2007; Xenidis et al., 2009). Additionally, treatment with trastuzumab can eliminate chemotherapy resistant K19 positive CTCs and can lead to reduction in disease recurrence and increased disease-free survival, suggesting K19 positive CTCs are associated with poor disease outcome (Georgoulias et al. 2012) . Another study demonstrated presence of CTCs with K19+ expression during tamoxifen treatment is associated with increased risk of disease relapse (Xenidis et al., 2007). Taken together, these studies underscore the importance of studying K19+ transformed breast cell lines.

Selection of transforming genes was based on a combination of relevance to human breast cancer and experimental ease. Choice of mp53, wtErbB2 or wtEGFR reflects a plethora of evidence that demonstrates a prevalent role of these in the pathogenesis of human breast cancers (Ro et al., 1988; Sainsbury et al., 1987; Slamon et al., 1987). For example EGFR is overexpressed in basal subtype (Livasy et al., 2006), ErbB2 is overexpressed in ErbB2+ subtype (Slamon et al., 1987) while p53 is known to be frequently mutated in most breast cancer subtypes. While selection of mutant Ras oncogene was based on evidence from a number of investigators, that mutant active Ras functions as a potent collaborator in full transformation of human mammary epithelial cells in *in vitro*, as well as in mouse mammary orthotopic tumorigenesis models (Elenbaas et al., 2001; Ince et al., 2007; Keller et al., 2012; Kendall et al., 2005). Notably, although the frequency of Ras mutations is low in breast cancer (about 5% of total breast cancer cases), activation of Ras pathway is frequently seen in breast tumors and in several breast cancer cell lines (Janes et al., 1994; von Lintig et al., 2000). In addition to overexpression of

upstream receptor tyrosine kinases EGFR and ErbB2 that are well known to activate Ras pathway as part of the oncogenic signaling program (Janes et al., 1994; von Lintig et al., 2000), recent evidence has identified other oncogenic events that can activate the Ras pathway in breast cancer, including recurrent mutations in MAP3K1 (Banerji et al.,2012; Stephens et al. 2012) and mutations of RASAL2, a RasGAP gene that functions as negative regulator of Ras (McLaughlin et al. 2013).

When we overexpressed defined combination of three oncogenes we observed an efficient anchorage independent growth in soft agar assays (Figure 2.2B, 2.2C). Consistent with the *in-vitro* transformation (assessed by their ability to be anchorage independent) cells with triple oncogene combinations gave rise to tumors when orthotopically-implanted into mammary glands of immunocompromised mice. Significant differences in the onset of primary tumors and lung metastasis was observed when comparing different cell lines and different oncogene combination (Table 2.1-2.9). $K5^+/K19^+$ cells had a higher susceptibility towards transformation (Figure 2.2B) and had an early onset of primary tumors as well as lung metastasis as compared to $K5^+/K19^-$ (Table 2.1, 2.2, 2.3, 2.5, 2.9 Figure 2.12) suggesting that overall these $K19^+$ stem/progenitors are more prone to transformation. This may be the likely reason why more than 90% of human breast tumors are K19 positive (Gudjonsson et al., 2002; Petersen and Polyak 2010). This indicates that the cell type in which tumor initiates plays an important role in development and progression of tumor. In addition we found that, presence of EGFR instead of ErbB2 in the triple oncogene combination potentially drives an early lung metastasis and give unique liver metastasis from same cellular precursor i.e $K5^+/K19^-$ (Table 2.3, 2.7) suggesting the significant effect of an oncogene on pathogenicity of tumor. Most of the basal like breast tumors express or over-express EGFR and have a high propensity for metastasis. There are clinical reports that have shown an up-regulated

EGFR expression in both primary and metastatic tumors (Hicks et al., 2006; Hohensee et al. 2013). However the exact mechanism by which EGFR function in promoting metastasis is not very well understood. Besides the tumor latency and metastasis progression we also observed cell type dependent effect on primary tumor histology (Figure 2.7, 2.8). Together these data support the idea that both oncogenes and cell type in which oncogenesis was initiated contribute to key tumor traits, such as latency and incidence.

The mammary stem/progenitor cell lines utilized here are endowed with self-renewal and bipotent differentiation capabilities (Zhao et al. 2010), allowing us to assess the impact of oncogenic transformation on their ability to self-renew and give rise to differentiated progeny. We present evidence that introduction of oncogenes into these stem/progenitor cell lines enhances their self-renewal capability as assayed using tumorsphere assays (Figures 2.3) and reduces their differentiation potential (Figure 2.7). It is likely that these traits are important in the tumorigenic phenotype as we observe these only upon oncogene overexpression. This is consistent with previous findings using *in vivo* mammary tumorigenesis models that tumor cells with loss of p53 function or overexpression of ErbB2 exhibit increased self-renewal (Cicalese et al., 2009), and that activated Ras or over-expression of EGFR inhibit normal mammary gland differentiation (Brandt et al., 2000; Cerrito et al., 2004).

Tumors in mice implanted with oncogene-transformed $K5^+/K19^+$ or $K5^+/K19^-$ cell lines exhibited substantial cellular heterogeneity with respect to the components of luminal, basal and/or claudin-low like cells, which were assessed by the expression of luminal and myoepithelial cell specific markers. Oncogene-transformed derivatives of $K5^+/K19^+$ cells predominantly give luminal adenocarcinoma phenotype, whereas tumors arising from transformed $K5^+/K19^-$ cell type produced more metaplastic carcinomas (Figure 2.7). Thus, our results clearly show that differences in cell of origin can

substantially influence the tumor phenotype, consistent with previous reports where primary human mammary epithelial cells propagated in different culture conditions were used for transformation (Ince et al., 2007).

In conclusion, using a unique set of stem/progenitor hMECs, we demonstrate that both the cell type in which oncogenic events are initiated and the nature of oncogenic events contribute to breast cancer histology, onset and incidence of primary and metastatic tumor. These unique cellular models should be highly useful to further explore the mechanisms that contribute to cellular heterogeneity in breast cancer as well as other important traits linked to cancer stem cells such as therapy resistance and poor survival.

CHAPTER 3

Gene expression analysis of the primary and metastatic tumors formed by transformed K5+/K19- or K5+/K19+ cells

Divya Bhagirath, Xiangshan Zhao, Hamid Band, Vimla Band

(To be submitted)

3.1 INTRODUCTION

Tumor progression is a multi-factorial process. The extent of disease progression may vary from one patient to another. Several cell intrinsic and extrinsic factors contribute to the dissemination of primary tumor cells and their colonization at the metastatic sites (Thiery et al., 2009). Subtype classification of breast tumors has allowed for categorization of different tumors in to those with good or poor prognosis. The prediction for patient survival is mainly based on the gene signatures of the tumors as well as the mutational status of important oncogenes/tumor–suppressor such as p53, PTEN, PI3K within the tumor (TCGA 2012, Sorlie et al., 2001) . Basal subtype of breast cancer that is associated with the worst survival outcomes, have gene signatures associated with higher cell proliferation (Banerji et al., 2012; Perou et al., 2000; Sorlie et al., 2001). On the other hand, tumors belonging to luminal subtype express genes for luminal differentiation and overall have a good survival (Perou et al., 2000; Sorlie et al., 2001) . Furthermore, gene expression analyses of patient derived primary tumors also possess a strong predictive value in evaluating disease progression and distant metastasis (Minn et al., 2005; van 't Veer et al., 2002) . Presence of disseminated or circulating tumors cells (CTCs) in patient's blood circulation, serve as early predictor for metastatic disease (Giuliano et al. 2014) and are strong prognostic indicator of disease free-survival and drug therapy response (Bidard et al., 2010; Janni et al., 2016; Smerage et al. 2014). CTCs have been shown to express CK19 mRNA and serve as an independent predictor for disease free survival and their presence in patients undergoing chemotherapy suggests likelihood of a relapsing disease or metastasis (Georgoulias et al.,2007; Ignatiadis et al., 2007; Xenidis et al., 2009) . This association emphasizes an important characteristic of disseminated tumor cells, therefore understanding the pathogenesis of disease from K19+ cellular precursor becomes important.

As previously described in Chapter 2 (Bhagirath et al. 2015), we developed primary and metastatic tumors models from K5+/K19- or K5+/K19+ stem/progenitor cells transformed by either mRas/mp53/wtErbB2 or mRas/mp53/wtEGFR. We observed that both the nature of cell type i.e. either K5+/K19- or K5+/K19+ cells and the introduced oncogene combination affected the phenotype, latency and incidence of primary and metastatic tumors in mice. Particularly, transformed K5+/K19+ cells overall have a higher anchorage independent growth and metastasis incidence as compared to transformed K5+/K19- cells (Table 2, 3 chapter 2). Given the prognostic relevance of K19 expression in metastatic disease progression and its expression in CTCs, it will be important to study the factors associated with K19+ tumor models that we have generated and compare them with their corresponding K19- derivatives. In the present chapter, we describe gene expression changes that are associated with the different tumors and identify gene alterations that most likely predict poor survival outcomes.

In conclusion, we observed that the tumors from transformed K5+/K19- cells had an up-regulated EMT gene signature, particularly in those from K5+/K19- mRas/mp53/wtErbB2 combination. Transformed K5+/K19+ with oncogene combination mRas/mp53/wtEGFR have gene changes associated with breast cancer metastasis, that explain the early onset and higher frequency of lung metastasis as observed previously for this combination.

3.2 MATERIALS AND METHODS

RNA extraction and Affymetrix Chip-Based Microarray Analyses

Liquid nitrogen snap frozen tumor tissues were homogenized to powder using mortar and pestle. Total RNA was isolated from tumors using the TRIzol reagent (Invitrogen). A total of 200 ng of total RNA from primary or metastatic tumors was reverse transcribed and cRNA generated per manufacturer's instructions using the Affymetrix 3′ IVT Express labeling kit (Affymetrix). Resultant cRNA probes were hybridized to the Affymetrix human U133 Plus 2 genome array per manufacture's suggestions and the chips were scanned using a GeneChip 3,000 6G scanner through UNMC DNA Microarray Core Facility. The resultant datasets were scaled using GCOS software, evaluated with respect to quality assurance parameters to include background, hybridization kinetics, and reverse transcription efficiency. Affymetrix comparison analysis software was used to determine fold-change differences between samples.

Antibodies

The following antibodies were used for immunofluorescence and immunohistochemistry (IHC): mouse anti-human α- SMA (sc-32251), mouse anti-human vimentin (sc-6260) were from Santa Cruz Biotechnology. Mouse anti-human MUC1 (550486) and mouse Alexa-488 conjugated E-Cadherin (560061) were from BD Bioscience. Rabbit anti-human vimentin (clone SP20, RM-9120-S0) was from Thermo Scientific.

Immunohistochemistry

Metastatic lung tumors were fixed in 10% Neutral Buffered Formalin (NBF) and processed into paraffin blocks. 4 µm sections were cut and stained with indicated antibodies. The standard staining procedure was performed using DAKO kit as per the manufacturer's protocol (# K4007) and as described in (Zhao et al. 2010). For IHC staining, tissue sections were incubated with primary anti-MUC1antibody in a hydrated chamber, followed by incubation with HRP-tagged secondary IgG against the primary antibodies and DAB solution and subsequently processed for nuclear staining with hematoxylin and mounting of tissues. For double-immunofluorescence staining tumor sections were processed similarly and blocked with 10% goat serum for 1 hr. These were then stained with rabbit anti-vimentin, alexa 488 conjugated anti-E-cadherin or mouse anti- α-SMA antibodies. Goat anti-rabbit alexa 594 and goat anti-mouse alexa 488 conjugated secondary antibodies (Invitrogen) were used for staining. The sections were mounted with anti-fade mounting media. Images were taken with fluorescence microscope (Zeiss axioplan 2 imaging microscope).

Ingenuity Pathway analysis

Top 50 differentially up or downregulated genes from different combination were added to IPA dataset and analyzed for networks, canonical pathways, disease and molecular functions associated with each combination. Analysis was done as previously described (Kramer et al. 2013)

Quantitative Real-time PCR

1 µg of total RNA was used for reverse transcriptase reaction using SuperScript™ II reverse transcriptase (Invitrogen). Real-time PCR quantification was performed in triplicate using SYBR Green PCR master mix (Applied Biosystems) and the primers listed in Table 3.1. Expression levels were normalized against β-actin RNA levels, and the results were calculated by the ΔΔCt method (Livak and Schmittgen, 2001).

Table 3.1: Primers used for Real Time-qPCR

Oligo Name	Sequence 5' to 3'
SLC2A3 –F	GCCACGGAGAGCAGCAACAA
SLC2A3 –R	GGGGAAGTTTTGGTCTTAGGTGG
POSTN –F	TATCTCAGGCAGCTGGAGGT
POSTN –R	GGAGTGGACTTGTACCAGCC
PTGS2 –F	CGCTCCGAGTCACCAGGAA
PTGS2 –R	CCTCAGTCCGGGCTTGGA
GREM1 –F	TCAACCGCTTTGGCAGGC
GREM1 –R	AACCAAGCGACCCAGGATC
STEAP4 –F	GGCAAATTGCTGGCAGGGTT
STEAP4 –R	CAGCATAAAGCGTTTGCGGTAC
RERG –F	CCCGCCGCACTGACAGTAT
RERG –R	GATGGCACCTTGGGACCC
OLFM4 –F	GCGCCTCTCCCTCAGTTATG
OLFM4 –R	CCCAGTGATCTTCCAAAATCACC
SLC6A14 –F	AGACACTGCTGGTCAGGAAG
SLC6A14 –R	AGTGGCAGCACTTCCTCAAA
ACTB –F	GCGAGAAGATGACCCAGATC
ACTB -R	CGTCACCGGAGTCCATCAC

3.3 RESULTS

Differential gene expression changes in xenograft tumors formed by transformed K5+/K19- or K5+/K19+ cell lines

In order to study the molecular basis for differences in tumor characteristic, we performed microarray analysis of the primary tumor from all 4 groups (K5+/K19- mp53/mRas/wtErbB2, K5+/K19+ mp53/mRas/wtErbB2, K5+/K19- mp53/mRas/wtEGFR and K5+/K19+ mp53/mRas/wtEGFR) and lung metastatic tumor derived from K5+/K19+ mp53/mRas/wtEGFR. Metastatic tumors from K5+/K19+ mp53/mRas/wtEGFR had a significantly shorter latency and higher incidence and were therefore chosen for the analysis (Table 3, 4 chapter 2). These tumors were generated from the xenograft assay as described previously in Chapter 2. To delineate the respective contributions of cell type or oncogene in determining tumor pathogenesis, we assessed the gene expression changes in different combinations (Figure 3.1).

Differentially expressed genes were assessed by deriving fold change in expression from the microarray data. Table 3.2-3.6 shows top 10 genes that were up- or down- regulated in different combinations (Figure 3.1). Neurofilament light polypeptide NEFL was found to be highly expressed in tumors formed by K5+/K19- over-expressing mp53/mRas/wtErbB2. Different studies have shown that NEFL gene hypermethylation or loss of NEFL mRNA is linked to disease progression in BC (Calmon et al.,2015; Li et al. 2012). Interestingly, gene expression of S100 proteins- S100A7, S100A8, S100A9, S100AP were also observed to be decreased in these tumors (Table 3.2, 3.3). S100 proteins are most commonly deregulated protein in different cancers including breast, prostate, lung, pancreatic or colorectal cancers and are involved in process of growth and metastasis in tumors (Bresnick et al. 2015). Low expression of these genes and

over-expression of NEFL in K5+/K19- mp53/mRas/wtErbB2 tumors, provide some explanation for the overall lower incidence of metastasis in these tumors (Table 3, Chapter 2). Additionally, K5+/K19- mRas/mp53/wtErbB2 tumors had an up-regulated expression of collagen mRNA including COL15A and COL3A as compared to tumors from transformed K5+/K19+ (Table 3.2) or K5+/K19- mRas/mp53/wtEGFR cells (Table 3.3). Increased collagen expression has been previously shown to be associated with EMT like behavior of the tumor cell (Wei et al. 2015). PRRX1, an important mediator of EMT and metastasis (Ocana et al. 2012) in tumor cell was also found to be highly expressed in this combination as compared to tumors from K5+/K19- mRas/mp53/wtEGFR (Table 3.2), further correlated the up-regulated EMT status of K5+/K19- mRas/mp53/wtErbB2 tumors. Basal cyto-keratin K6 was also found to be differentially downregulated in these EMT like K5+/K19- mRas/mp53/wtErbB2 tumors as compared to K5+/K19- mRas/mp53/wtEGFR or tumors from transformed K5+/19+ cells with either combination.

Extracellular matrix proteins- LUM and DEC were observed to be highly expressed in K5+/K19- mRas/mp53/wtEGFR tumors (Table 3.4). LGR5 marker of intestinal stem cells was found to be highly expressed in K5+/K19+ mRas/mp53/wtErbB2 tumors (Table 3.5). When we compared primary with the metastatic tumor from K5+/K19+ mRas/mp53/wtEGFR combination, we found that amino acid transporter protein SLC6A14 was highly up regulated (Table 3.6). Additionally, markers associated with EMT and metastasis in tumors from breast cancer patients including- POSTN, GREM1, PTGS2 (Grigoriadis et al., 2006; Malanchi et al.,2012; Minn et al., 2005) were upregulated in primary tumors from K5+/K19+ mRas/mp53/wtEGFR combination (Table 3.6). We confirmed the expression of most highly expressed genes in metastatic tumors - SLC6A14, OLFM4, STEAP2 and RERG

in three different mice derived paired primary and metastatic tumors and found SLC6A14 to be consistently high in metastasis as compared to primary tumors, suggesting an important role of this protein at metastatic sites (Figure 3.2). Similarly, we also tested the expression of genes differentially expressed in primary tumors- GREM1, POSTN, PTGS2 and SLC2A3. Out of these, POSTN and PTGS2 were found to be consistently increased in two independent mice primary tumors (Figure. 3.3).

Figure 3.1: Different combination tested for gene expression analysis of primary or metastatic tumors

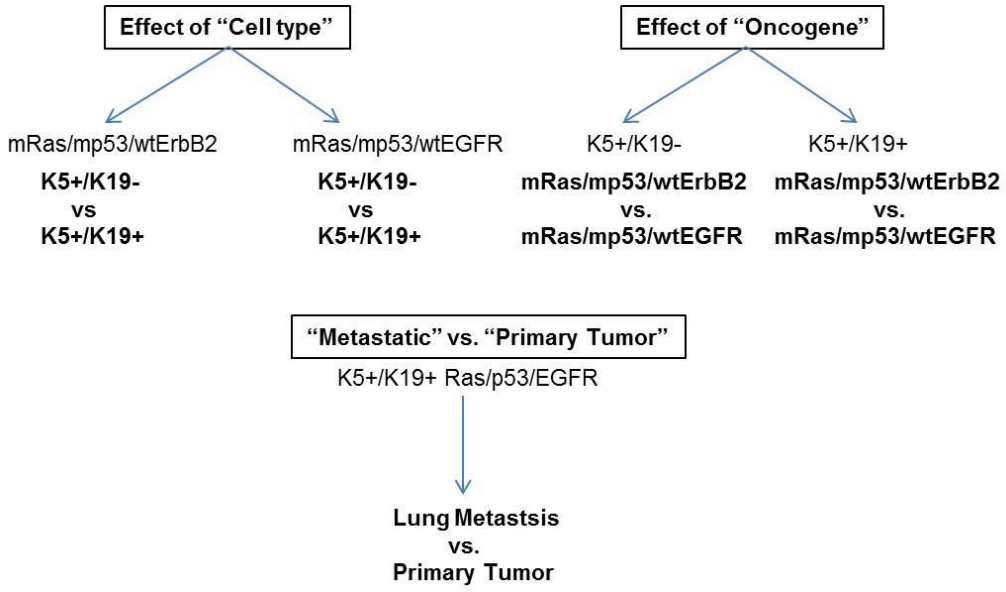

Figure 3.1: Different combination tested for gene expression analysis of primary or metastatic tumors. Microarray derived gene expression changes in primary tumors from K5+/K19- mp53/mRas/wtErbB2, K5+/K19+ mp53/mRas/wtErbB2, K5+/K19- mp53/mRas/wtEGFR or K5+/K19+ mp53/mRas/wtEGFR and metastatic tumor from K5+/K19+ mp53/mRas/wtEGFR combination were compared with each other in different combinations to test the effect of "Cell type" or "Oncogene" in driving tumor pathogenesis.

Table 3.2: Differentially expessed genes in K5+/K19- mp53/mRas/wtErbB2 tumors as compared to K5+/K19+ mp53/mRas/wtErbB2 (Cell type effect)

Gene symbol	Gene title	Fold Change (K5+/K19-mRas.mp53.wtErbb2)/(K5+/K19+mRas.mp53.wtErbb2)
NEFL	neurofilament, light polypeptide	**247.366**
COL15A1	collagen, type XV, alpha 1	**137.896**
VCAM1	vascular cell adhesion molecule 1	**111.287**
LPPR4	lipid phosphate phosphatase-related protein type 4	**107.623**
PRRX1	paired related homeobox 1	**90.051**
FHL1	four and a half LIM domains 1	**88.136**
OLFML3	olfactomedin-like 3	**79.713**
ACTG2	actin, gamma 2, smooth muscle, enteric	**79.439**
MYADM	myeloid-associated differentiation marker	**77.675**
COL3A1	collagen, type III, alpha 1	**69.210**
PROM1	prominin 1	**-247.905**
S100A8	S100 calcium binding protein A8	**-211.802**
LGR5	leucine-rich repeat containing G protein-coupled receptor 5	**-187.943**
S100A7	S100 calcium binding protein A7	**-184.915**
SCGB2A2	secretoglobin, family 2A, member 2	**-153.985**
S100A9	S100 calcium binding protein A9	**-150.514**
EHF	ets homologous factor	**-134.252**
MMP10	matrix metallopeptidase 10 (stromelysin 2)	**-103.018**
KRT6A	keratin 6A	**-98.634**
KRT19	keratin 19	**-98.516**

Table 3.3: Differentially expessed genes in K5+/K19- mp53/mRas/wtErbB2 tumors as compared to K5+/K19- mp53/mRas/wtEGFR (Oncogene effect)

Gene symbol	Gene title	Fold Change K5+/K19-(mRas.mp53.wtErbb2)/(mRas.mp53.wtEGFR)
NEFL	neurofilament, light polypeptide	**108.658**
VCAM1	vascular cell adhesion molecule 1	**66.323**
SLIT2	slit homolog 2 (Drosophila)	**28.804**
COL15A1	collagen, type XV, alpha 1	**27.732**
LOC104968398		**27.332**
ACTG2	actin, gamma 2, smooth muscle, enteric	**24.938**
ST6GAL2	ST6 beta-galactosamide alpha-2,6-sialyltranferase 2	**24.616**
FBN1	fibrillin 1	**24.322**
PEG10	paternally expressed 10	**24.102**
LAMA1	laminin, alpha 1	**24.001**
S100A7	S100 calcium binding protein A7	**-273.373**
SPRR1B	small proline-rich protein 1B	**-191.388**
S100A8	S100 calcium binding protein A8	**-183.385**
PI3	peptidase inhibitor 3, skin-derived	**-126.167**
KRT6A	keratin 6A	**-107.066**
S100A9	S100 calcium binding protein A9	**-102.249**
SPRR2B	small proline-rich protein 2B	**-95.703**
SPRR3	small proline-rich protein 3	**-73.368**
CD24	CD24 molecule	**-66.631**
S100P	S100 calcium binding protein P	**-60.842**

Table 3.4: Differentially expessed genes in K5+/K19- mp53/mRas/wtEGFR tumors as compared to K5+/K19+ mp53/mRas/wtEGFR (Cell type effect)

Gene symbol	Gene title	Fold Change (K5+/K19-mRas.mp53.wtEGFR)/(K5+/K19+mRas.mp53.wtEGFR)
LUM	Lumican	**409.927**
SPRR3	small proline-rich protein 3	**64.225**
NTM	neurotrimin-like /// neurotrimin	**57.507**
SPRR2B	small proline-rich protein 2B	**56.095**
PCDH18	protocadherin 18	**37.676**
DCN	Decorin	**35.693**
THBS2	thrombospondin 2	**35.133**
ADAMTS2	ADAM metallopeptidase with thrombospondin type 1 motif, 2	**31.002**
SPRR1B	small proline-rich protein 1B	**28.156**
COL10A1	collagen, type X, alpha 1	**27.387**
KRT19	keratin 19	**-430.293**
MGST1	microsomal glutathione S-transferase 1	**-93.397**
VCAM1	vascular cell adhesion molecule 1	**-83.347**
DIRAS3	DIRAS family, GTP-binding RAS-like 3	**-80.626**
GPC6	glypican 6	**-68.512**
SCGB2A2	secretoglobin, family 2A, member 2	**-52.091**
CHI3L1	chitinase 3-like 1 (cartilage glycoprotein-39)	**-51.010**
CA2	carbonic anhydrase II	**-41.594**
EPCAM	epithelial cell adhesion molecule	**-36.212**
RAP1A	RAP1A, member of RAS oncogene family	**-33.871**

Table 3.5: Differentially expessed genes in K5+/K19+ mp53/mRas/wtErbB2 tumors as compared to K5+/K19+ mp53/mRas/wtEGFR (Oncogene effect)

Gene symbol	Gene title	Fold Change K5+/K19+ (mRas.mp53.wtErbb2)/(mRas.mp53.wtEGFR)
LGR5	leucine-rich repeat containing G protein-coupled receptor 5	**118.092**
NTRK2	neurotrophic tyrosine kinase, receptor, type 2	**41.837**
TENM2	teneurin transmembrane protein 2	**36.523**
BBOX1	butyrobetaine (gamma), 2-oxoglutarate dioxygenase (gamma-butyrobetaine hydroxylase) 1	**32.313**
SNCAIP*	synuclein, alpha interacting protein	**31.928**
ARHGAP29*	Rho GTPase activating protein 29	**26.436**
ITGA9	integrin, alpha 9	**18.071**
NTM	neurotrimin-like /// neurotrimin	**18.030**
PTPRZ1	protein tyrosine phosphatase, receptor-type, Z polypeptide 1	**17.775**
CFHR1	complement factor H /// complement factor H-related 1	**17.276**
VCAM1	vascular cell adhesion molecule 1	**-139.860**
SPP1	secreted phosphoprotein 1	**-127.649**
LPPR4	lipid phosphate phosphatase-related protein type 4	**-116.741**
DIRAS3	DIRAS family, GTP-binding RAS-like 3	**-82.244**
ACTG2	actin, gamma 2, smooth muscle, enteric	**-69.759**
MYADM	myeloid-associated differentiation marker	**-57.650**
C15orf48	chromosome 15 open reading frame 48	**-46.816**
RAP1A	RAP1A, member of RAS oncogene family	**-42.562**
TCN1	transcobalamin I (vitamin B12 binding protein, R binder family)	**-42.384**
RORB	RAR-related orphan receptor B	**-32.776**

Table 3.6: Differentially expessed genes in metastatic tumors as compared to primary tumors from K5+/K19+ mp53/mRas/wtEGFR combination

Gene symbol	Gene title	Fold Change K5+/K19+(metastasis)/(primary)
SLC6A14	solute carrier family 6 (amino acid transporter), member 14	**150.927**
OLFM4	olfactomedin 4	**128.009**
STEAP4	STEAP family member 4	**51.565**
LCN2	lipocalin 2	**48.042**
GABRP	gamma-aminobutyric acid (GABA) A receptor, pi	**43.699**
CCL28	chemokine (C-C motif) ligand 28	**34.648**
CEACAM5	carcinoembryonic antigen-related cell adhesion molecule 5	**31.977**
PDZK1IP1	PDZK1 interacting protein 1	**31.049**
LTF	Lactotransferrin	**28.693**
RERG	RAS-like, estrogen-regulated, growth inhibitor	**28.008**
IL1B	interleukin 1, beta	**-34.296**
C11orf96	chromosome 11 open reading frame 96	**-31.839**
IL6	interleukin 6 (interferon, beta 2)	**-18.537**
GREM1	gremlin 1, DAN family BMP antagonist	**-16.447**
HS3ST3A1	heparan sulfate (glucosamine) 3-O-sulfotransferase 3A1	**-14.375**
HEPH	Hephaestin	**-13.514**
PTGS2	prostaglandin-endoperoxide synthase 2 (prostaglandin G/H synthase and cyclooxygenase)	**-13.386**
POSTN	periostin, osteoblast specific factor	**-11.509**
CH25H	cholesterol 25-hydroxylase	**-11.366**
SLC2A3	solute carrier family 2 (facilitated glucose transporter), member 3	**-10.784**

Figure 3.2: mRNA expression analysis for genes up-regulated in metastatic tumors from K5+/K19+ mp53/mRas/wtEGFR combination

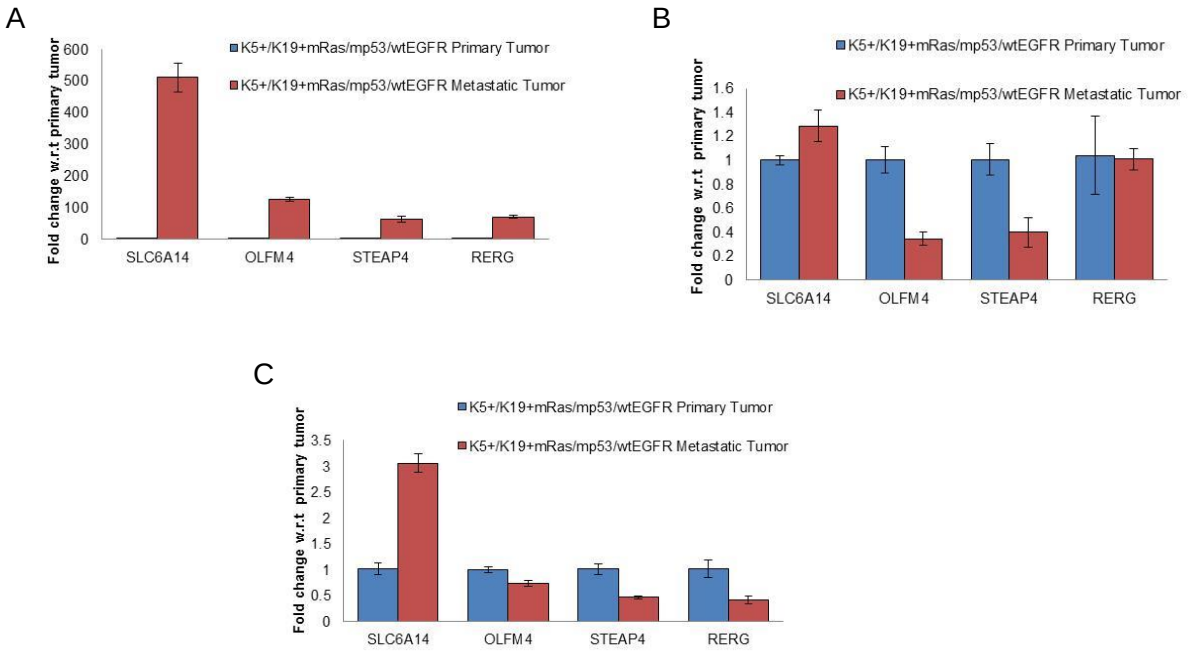

Figure 3.2: mRNA expression analysis for genes up-regulated in metastatic tumors from K5+/K19+ mp53/mRas/wtEGFR combination. mRNA extracted from 3 independent mice paired primary and metastatic tumors (A, B and C) was analyzed by real time PCR for expression of SLC6A14, OLFM4, STEAP4 and RERG. Each sample was run in triplicates.

Figure 3.3: mRNA expression analysis for genes up-regulated in primary tumors from K5+/K19+ mp53/mRas/wtEGFR combination

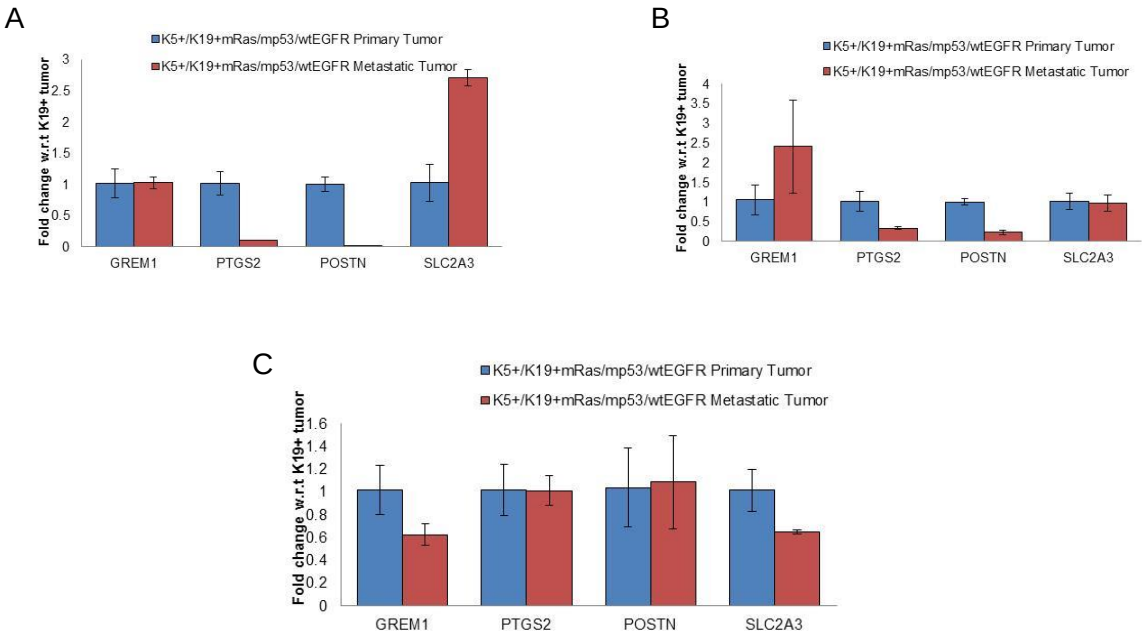

Figure 3.3: mRNA expression analysis for genes up-regulated in primary tumors from K5+/K19+ mp53/mRas/wtEGFR combination. mRNA extracted from 3 independent mice paired primary and metastatic tumors (A, B and C) was analyzed by real time PCR for expression of GREM1, PTGS2, POSTN and SLC2A3. Each sample was run in triplicates.

Analysis of EMT and metastasis gene signature in tumors from transformed K5+/K19- or K5+/K19+

In order to better understand the differences in incidence and latency for primary and metastatic tumors from different groups i.e. K5+/K19- mp53/mRas/wtErbB2, K5+/K19+ mp53/mRas/wtErbB2, K5+/K19- mp53/mRas/wtEGFR or K5+/K19+ mp53/mRas/wtEGFR, we analyzed the mRNA expression of various EMT and metastasis related genes in these tumors (Minn et al., 2005; Soundararajan et al. 2015). Fold change in expression was derived by comparing different primary or metastatic tumors with each other as shown in Table 3.7. We observed, that tumors formed by transformed K5+/K19- cell type overall had a higher expression of EMT related genes including- ZEB1, ZEB2, SNAI2, PRRX1, TWIST1, VIM and loss of CDH1 or E-Cadherin (Table 3.7) as compared to those from transformed K5+K19+ tumors. These results are in concordance with and confirm the EMT phenotype observed for tumors from transformed K5+/K19- as previously shown in chapter 2 (Figure 2.6 and 2.7). Interestingly, tumors from K5+/K19- over-expressing oncogene combination expressing mp53/mRas/wtErbB2 had a higher EMT gene signatures as compared to those from K5+/K19- over-expressing mRas/mp53/wtEGFR. Correspondingly, the lung metastatic tumor derived from K5+K19+ mRas/mp53/wtEGFR had an up-regulated epithelial gene expression including CDH1 and down regulated EMT gene signatures such as CDH2, SNAI2, TWIST1, TWIST2, ZEB1 or ZEB2 (Table 3.7). Immunostaining of the lung metastatic tumor also showed a high expression of luminal marker MUC1 (Figure 3.4A) and α-SMA^{neg}/vimentin^{low} or E-Cadherin^{positive}/ vimentin^{low} phenotype (Figure 3.4B, 3.4C), confirming their epithelial phenotype.

Metastasis signature genes- CXCL1, MMP1, PTGS2, that are previously shown to be up-regulated in primary tumors in patients having metastasis were included for the

analysis (Minn et al., 2005). We observed an up-regulated expression of metastasis genes PTGS2 and MMP-1 in the primary tumors from K5 + K19+ mRas/mp53/wtEGFR combination as compared to its corresponding metastatic tumor (Table 3.7). As previously observed, primary tumor from K5+K19+ mRas/mp53/wtEGFR combination had high expression of PTGS2 (Table 3.6) as compared all other primary tumors (Table 3.7), therefore suggesting possible role of PTGS2 in mediating higher metastasis from these tumors.

Table 3.7: Analysis of EMT and metastasis gene signature in tumors from transformed K5+/K19- or K5+/K19+ cells

Gene	K5+/19- mRas/mp53/wtErbB2 vs. K5+/K19+ mRas/mp53/wtErbB2	K5+/19- mRas/mp53/wtErbB2 vs. K5+/K19- mRas/mp53/wtEGFR	K5+/19- mRas/mp53/wtEGFR vs. K5+/K19+ mRas/mp53/wtEGFR	K5+/19+ mRas/mp53/wtErbB2 vs. K5+/K19+ mRas/mp53/wtEGFR	K5+/K19+ mRas/mp53/wtEGFR Metatasis vs. Primary
PRRX1	90	2.7	1.42	0.11	0.142
ZEB1	30.49	0.88	26.9	0.77	0.575
ZEB2	4.8	1.85	0.49	0.18	0.155
FOXC1	0.108	0.3	0.46	1.31	1.31
VIM	1.75	1.86	0.64	0.68	0.53
CDH1	0.011	0.074	0.3	1.9	1.85
CDH2	1.25	105.8	0.28	1	0.22
TWIST1	4.94	4.94	1	1	0.258
TWIST2	3.56	2.23	1.2	0.8	0.43
SNAI2	1.89	1.89	1	1	0.39
S100A4	1.74	1	0.4	0.281	1.1
NFIL3	1.41	2.6	0.45	0.84	0.505
CKS2	0.96	2.7	0.329	0.94	0.89
CTNNB1	0.63	2.3	0.42	1.58	0.99
DDR1	0.34	0.85	0.58	1.45	0.98
FN1	1	1.39	0.7	0.9	0.52
COI1A	6.8	1.26	1.11	0.2	0.233
CXCL1	0.9	2.69	0.53	1.56	0.96
MMP1	0.3	0.219	2.68	1.8	0.18
PTGS2	1	1.49	0.153	0.22	0.12
SPARC	4	1.55	1.44	0.55	0.28
KYNU	0.01	0.9	0.15	13	3.1

Figure 3.4: Epithelial phenotype of lung metastatic tumor from K5+/K19+ mp53/mRas/wtEGFR combination.

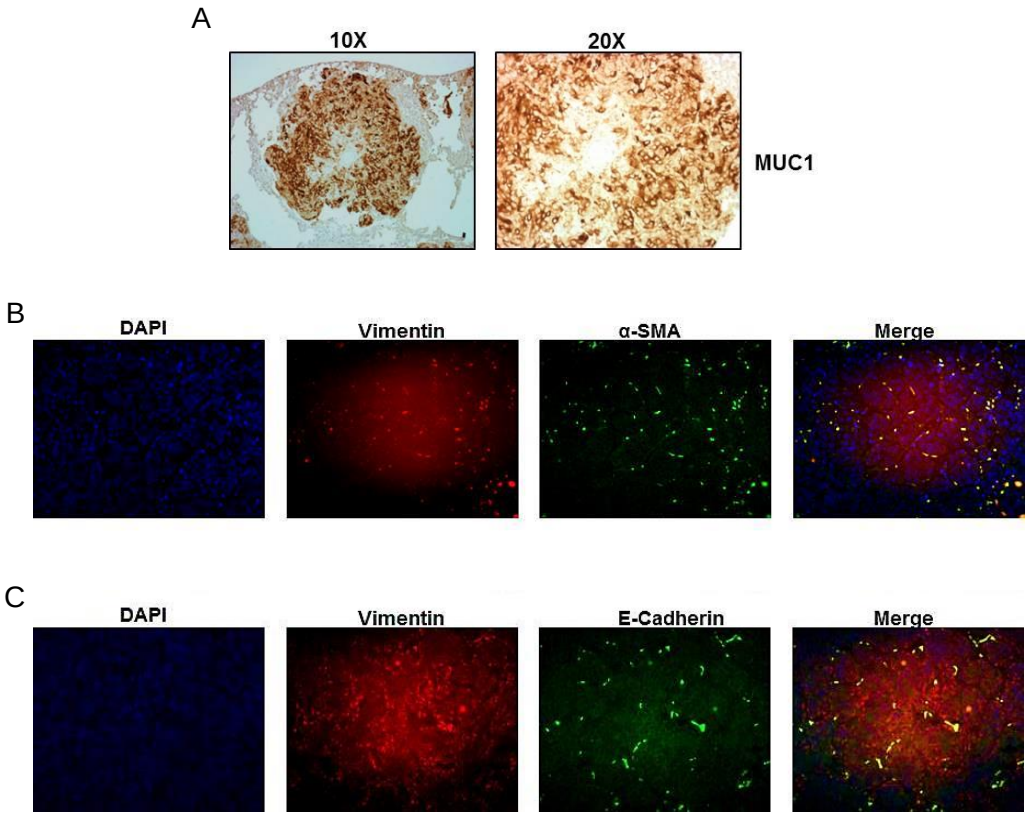

Figure 3.4: Epithelial phenotype of lung metastatic tumor from K5+/K19+ mp53/mRas/wtEGFR combination. Immunohistochemical staining of lung tumor sections from K5+/K19+ mp53/mRas/wtEGFR. A) Representative image of tumor section stained with anti-MUC1 antibody. Representative image (magnification 20X)of tumors double immunostained with B) anti-αSMA (green) and anti-vimentin (red) show presence of (α-SMA^{negative}/vimentin^{low}) area within metastatic tumor. C) Same tumor sections double immunostained with E-Cadherin (green) and vimentin (red) show presence of luminal like (E-Cadherin^{positive}) areas within the tumors. DAPI (blue) shows nucleus.

Shared and unique networks and canonical pathways in tumors formed from transformed K5+/K19- or K5+/K19+

In order to identify networks and canonical pathways that were altered in these tumors, we performed bioinformatic analysis using IPA (Kramer et al. 2013), on the genes that were differentially expressed in various combinations (Table 3.2-3.6). From IPA, we identified cancer (range of molecules involved: 61-77), organismal injury and abnormalities (61-77) and reproductive system disease (42-58), as the topmost disease and biological functions associated with each combination. Cellular movement (26-46), cell-to-cell signaling and interaction (18-43), cell death and survival (29-46) were the top molecular and cellular function identified in various combinations. Besides these, each combination had a unique function associated with them (Table 3.8) that may be resulting from the differential effect of either the cell type or the oncogene in different groups. Top regulator effect network as analyzed by IPA, show association of - “chemotaxis of neutrophils” with tumors from K5+/K19- over-expressing mp53/mRas/wtErbB2 or “activation of neutrophils” with tumors from K5+/K19+ over-expressing mp53/mRas/wtErbB2 (Table 3.9). Activation of osteoclast and remodeling of bone was the top regulator effect network observed, when primary tumor from K5+/K19+ mp53/mRas/wtEGFR was compared with its respective metastatic tumor (Table 3.9).

Atherosclerosis signaling, hepatic fibrosis/hepatic stellate cell activation, agranulocyte adhesion and diapedesis, role of IL-17A in psoriasis, cell cycle: G2/M DNA damage checkpoint regulation and HMGB1 signaling were the most common top canonical pathways associated with each combination. Tumors from K5+/K19- over-expressing mp53/mRas/wtErbB2 oncogene combination show inhibition of matrix metalloproteinase (MMPs) and glutathione redox reaction as the associated canonical pathway when compared with tumors from K5+/K19+ over-expressing

mp53/mRas/wtErbB2 (Table 3.10), suggesting a likely cell type effect. Tumors from K5+/K19- over-expressing mp53/mRas/wtEGFR show altered DNA damage induced 14-3-3 signaling and those from K5+/K19+ over-expressing mp53/mRas/wtEGFR show differential regulation of cytokine production and role of osteoclast, osteoblast and chondrocytes in rheumatoid arthritis as the associated canonical pathway (Table 3.10).

Cellular movement, hematological system development and function, immune cell trafficking, dermatological diseases and conditions, cancer and organismal injury and abnormalities were the topmost associated networks associated with tumors from different combination (Figure 3.5-3.10). The networks associated with tumor from K5+/K19- over-expressing mp53/mRas/wtErbB2 oncogene combination were characterized by increase in expression of collagens including COL1A1, COL3A1 and COL15A1 and low expression of MMPs, S100 proteins -S100A8, S100A9, S100P and cyto-keratins 6 and 15 (Figure 3.5, 3.6 and 3.7). Comparative analysis of tumors from K5+/K19- or K5+/K19+ over-expressing mp53/mRas/wtEGFR, showed hair and skin development and function as the top associated network, that it was characterized by an upregulated expression of extracellular matrix proteins- COL, LUM, DEC, EMT marker-ZEB1 and Wnt pathway (Wnt 5A ↑, Wnt inhibitor DKK ↓) (Figure 3.8) . Cellular movement, skeletal and muscular system development and function, cell-to-cell signaling and interaction was the top most associated network in tumor from K5+/K19+ over-expressing mp53/mRas/wtErbB2 (Figure 3.9), while comparison of primary and metastatic tumors from K5+/K19+ over-expressing mp53/mRas/wtEGFR showed connective tissue disorders and developmental disorder as top associated network (Figure 3.10).

Table 3.8: Top molecular and cellular functions uniquely associated with each combination.

Tumors	Molecular and cellular functions	p-value	Molecules
K5+/K19- mRas/mp53/wtErbB2 vs K5+/K19+ mRas/mp53/wtErbB2	Cellular Assembly and Organization Cellular Function and Maintenance	3.61E-03 - 1.17E-05 3.61E-03 - 1.17E-05	21 15
K5+/K19- mRas/mp53/wtErbB2 vs K5+/K19- mRas/mp53/wtEGFR	 Cell Cycle Cellular Compromise	 6.04E-03 – E-1.43E-05 6.04E-03 – E-1.98E-05	 10 9
K5+/K19- mRas/mp53/wtEGFR vs K5+/K19+ mRas/mp53/wtEGFR	 Cellular Development Cellular Growth and Proliferation	 5.61E-03 – 9.03E-11 5.61E-03 – 9.03E-11	 39 40
K5+/K19+ mRas/mp53/wtErbB2 vs K5+/K19+ mRas/mp53/wtEGFR	 Cellular Development Cellular Growth and Proliferation	 2.05E-04 – 1.08E-08 1.90E-04 – 2.05E-08	 44 44
K5+/K19+ mRas/mp53/wtEGFR(primary tumor) vs K5+/K19+ mRas/mp53/wtEGFR(metastatic tumor)	Cell Cycle Molecular Transport Small Molecule Biochemistry	1.44E-04 - 1.25E-09 1.92E-04 - 2.36E-09 2.00E-04 - 2.36E-09	15 29 26

Table 3.9: Top regulator effect networks associated with each combination.

Tumors	Top Regulator Effect Networks	Consistency score
K5+/K19- mRas/mp53/wtErbB2 vs K5+/K19+ mRas/mp53/wtErbB2	EHF,estrogen receptor,IL17C,IL22,MGEA5,MKL1,MKL2 (+2 more) ----antimicrobial response,chemotaxis of neutrophils (+2 more)	15.765
	TNF ------mammary tumor	-7.216
K5+/K19- mRas/mp53/wtErbB2 vs K5+/K19- mRas/mp53/wtEGFR	GATA3,IL17C,MKL1,MKL2,SRF --------chemotaxis of neutrophils	9.0
K5+/K19- mRas/mp53/wtEGFR vs K5+/K19+ mRas/mp53/wtEGFR	-	
K5+/K19+ mRas/mp53/wtErbB2 vs K5+/K19+ mRas/mp53/wtEGFR	AGT,Akt,AKT1,ANGPT2,Ap1,CXCL12,ERK1/2,F2,IFI16 (+10 more) ----activation of neutrophils (+7 more)	90.067
	AGT,Akt,AKT1,ANGPT2,Ap1,AVP,Cg,CXCL12,ERK1/2, F2 (+13 more) -------activation of neutrophils (+10 more)	74.914
	Ap1,CXCL12,NR3C1,SMARCA4,TREM1 -----activation of neutrophils (+7 more)	14.422
K5+/K19+ mRas/mp53/wtEGFR(primary tumor) vs K5+/K19+ mRas/mp53/wtEGFR(metastatic tumor)	AGT,ERK1/2,F2,FGF2,IgG,IL3,Jnk,KITLG,NR3C1,PDGF BB (+2 more) -------activation of osteoclasts,attachment of cells (+7 more)	57.125
	AGT,AKT1,EDN1,ERK1/2,F2,IgG,IL3,Jnk,KITLG,NR3C 1 (+3 more) -------activation of osteoclasts,attachment of cells (+7 more)	41.754
	TGFB1 --------remodeling of bone	3.536

Table 3.10: Top canonical pathways uniquely associated with each combination.

Tumors	Canonical Pathway	p-value
K5+/K19- mRas/mp53/wtErbB2 vs K5+/K19+ mRas/mp53/wtErbB2	1. Inhibition of Matrix Metalloproteases (7.7%, 3/39)	3.75E-04
	2. Glutathione Redox Reactions I (10.5%, 2/19)	2.11E-03
K5+/K19- mRas/mp53/wtErbB2 vs K5+/K19- mRas/mp53/wtEGFR	1. Granulocyte Adhesion and Diapedesis (1.7 % 3/177)	1.65E-02
K5+/K19- mRas/mp53/wtEGFR vs K5+/K19+ mRas/mp53/wtEGFR	1. Aryl Hydrocarbon Receptor Signaling (2.9%, 4/140)	9.06E-04
	2. Mitotic Roles of Polo-Like Kinase 4.5 %, 3/66	1.10E-03
	3. DNA damage-induced 14-3-3 Signaling (10.5 % , 2/19)	1.53E-03
K5+/K19+ mRas/mp53/wtErbB2 vs K5+/K19+ mRas/mp53/wtEGFR	1. Leukocyte Extravasation Signaling (3.5 % 7/198)	1.23E-05
K5+/K19+ mRas/mp53/wtEGFR(primary tumor) vs K5+/K19+ mRas/mp53/wtEGFR(metastatic tumor)	1. Differential Regulation of Cytokine Production in Intestinal Epithelial Cells by IL-17A and IL-17F(13.0 % 3/23)	7.89E-05
	2. Role of Osteoblasts, Osteoclasts and Chondrocytes in Rheumatoid Arthritis (2.7 % 6/219)	1.51E-04
	3. Role of IL-17F in Allergic Inflammatory Airway Diseases (6.8 % 3/44)	5.58E-04

Figure 3.5: Top associated network (I) for K5+/K19- mRas/mp53/wtErbB2 versus K5+/K19+ mRas/mp53/wtErbB2 combination.

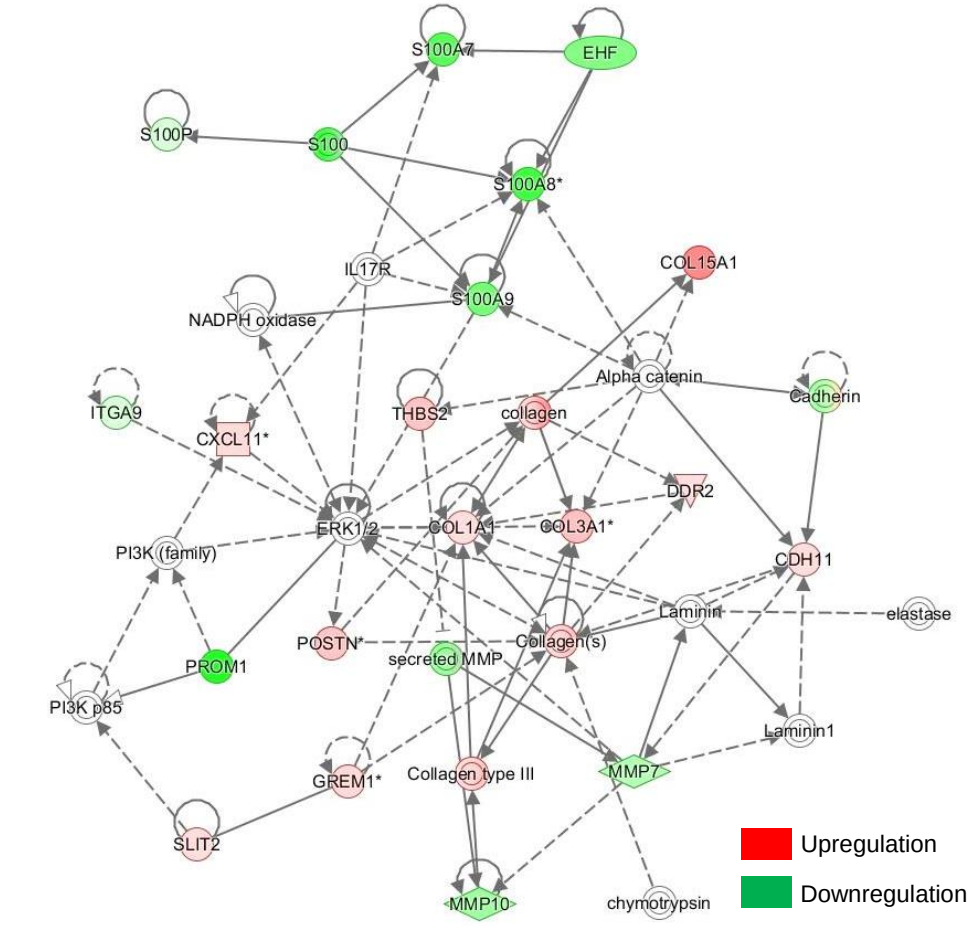

Figure 3.5: Top associated network (I) for K5+/K19- mRas/mp53/wtErbB2 versus K5+/K19+ mRas/mp53/wtErbB2 combination. Cellular Movement, Hematological System Development and Function, Immune Cell Trafficking were the associated network functions.

Figure 3.6: Top associated network (II) for K5+/K19- mRas/mp53/wtErbB2 versus K5+/K19+ mRas/mp53/wtErbB2 combination.

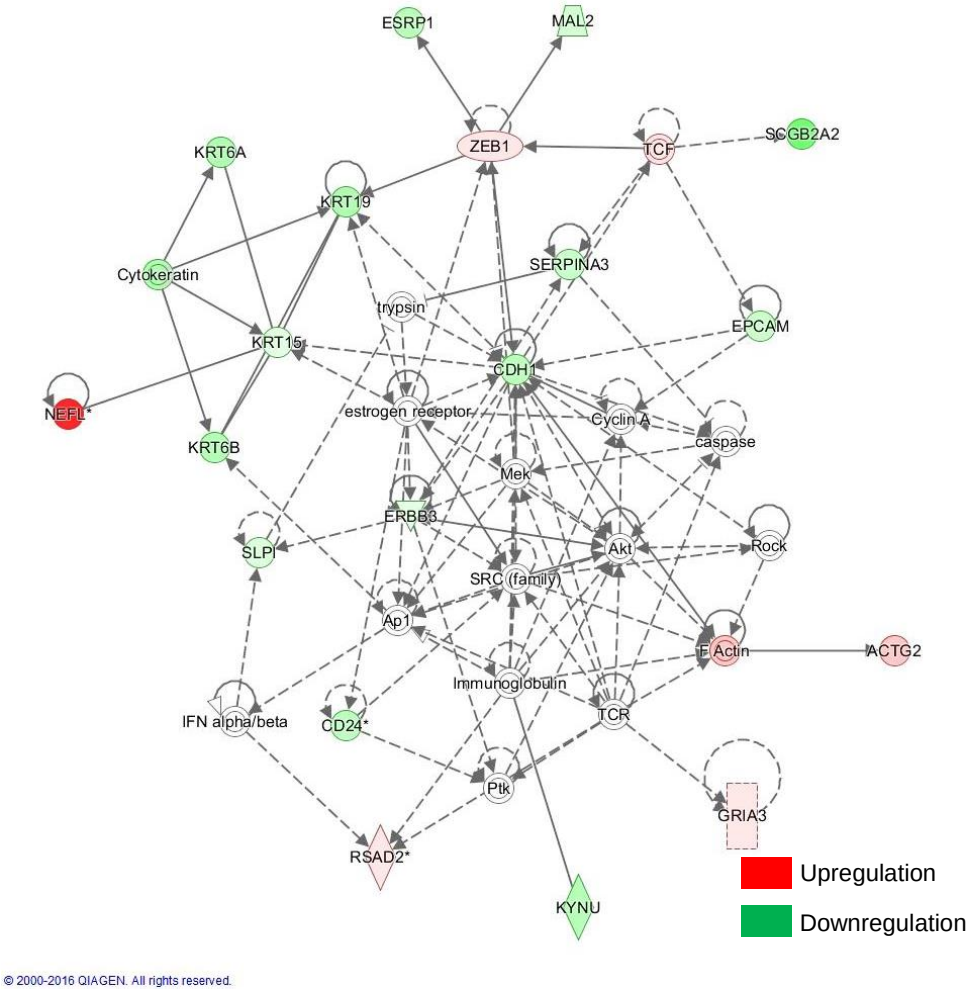

Figure 3.6: Top associated network (II) for K5+/K19- mRas/mp53/wtErbB2 versus K5+/K19+ mRas/mp53/wtErbB2 combination. Dermatological Diseases and Conditions, Cancer, Organismal Injury and Abnormalities were the associated network functions.

Figure 3.7: Top associated network for K5+/K19- mRas/mp53/wtErbB2 versus K5+/K19- mRas/mp53/wtEGFR combination.

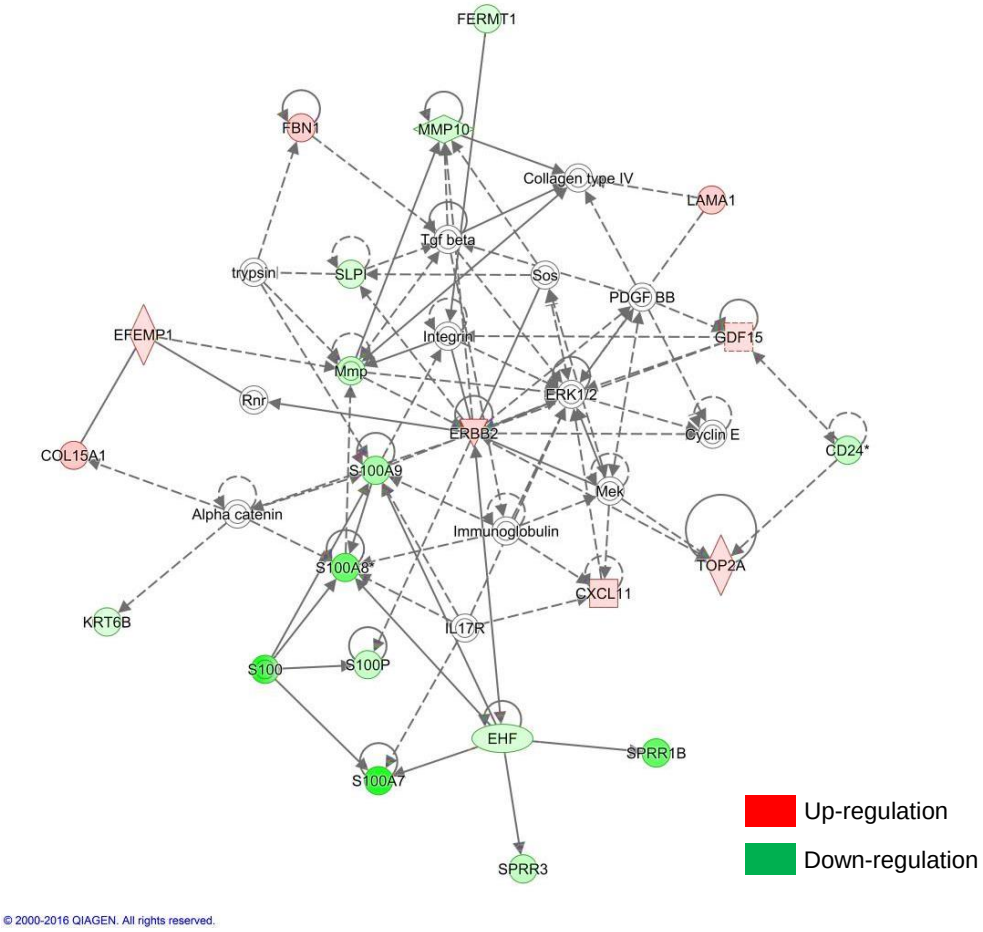

Figure 3.7: Top associated network for K5+/K19- mRas/mp53/wtErbB2 versus K5+/K19- mRas/mp53/wtEGFR combination. Dermatological Diseases and Conditions, Cancer, Organismal Injury and Abnormalities were the associated network functions.

Figure 3.8: Top associated network for K5+/K19- mRas/mp53/wtEGFR versus K5+/K19+ mRas/mp53/wtEGFR combination.

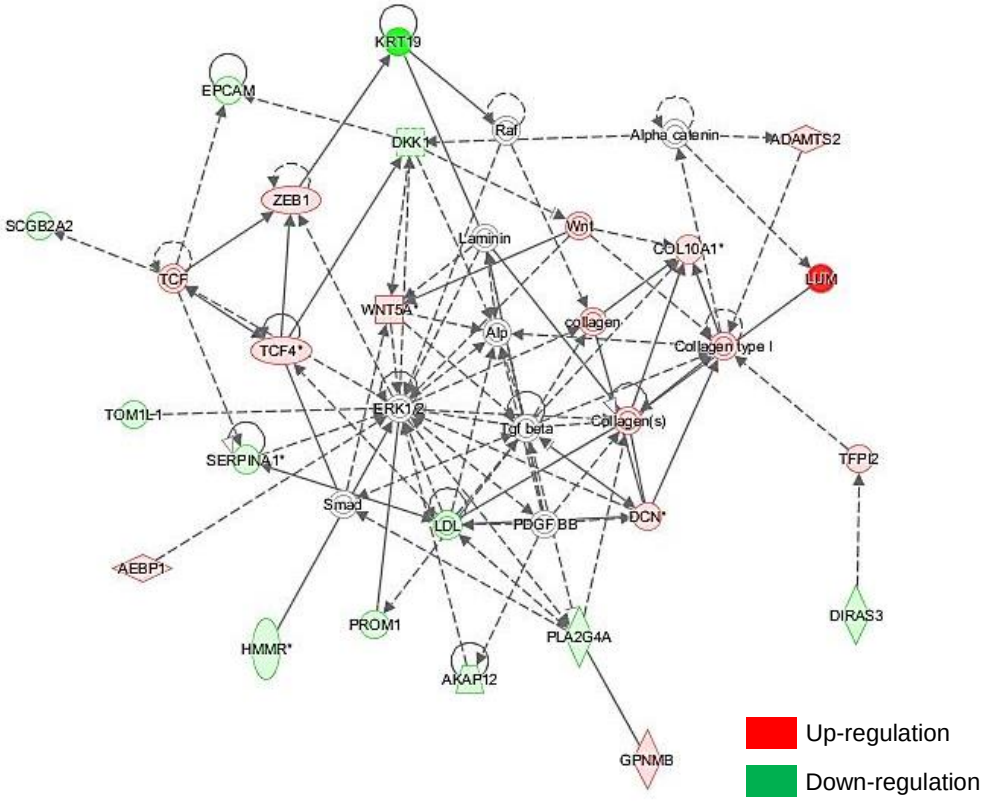

Figure 3.8: Top associated network for K5+/K19- mRas/mp53/wtEGFR versus K5+/K19+ mRas/mp53/wtEGFR combination. Dermatological Diseases and Conditions, Hair and Skin Development and Function, Cancer were the associated network functions.

Figure 3.9: Top associated network for K5+/K19+ mRas/mp53/wtErbB2 versus K5+/K19+ mRas/mp53/wtEGFR combination.

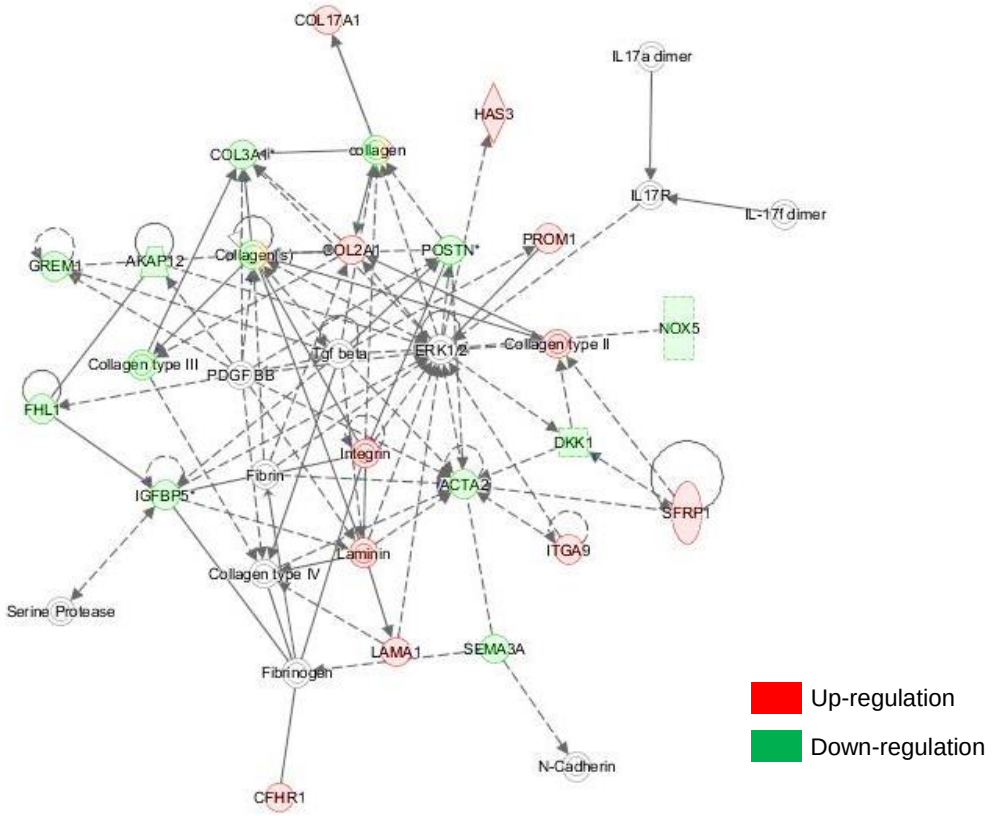

Figure 3.9: Top associated network for K5+/K19+ mRas/mp53/wtErbB2 versus K5+/K19+ mRas/mp53/wtEGFR combination. Cellular Movement, Skeletal and Muscular System Development and Function, Cell-To-Cell Signaling and Interaction were the associated network functions.

Figure 3.10: Top associated network for metastatic versus primary tumors from K5+/K19+ mRas/mp53/wtEGFR combination.

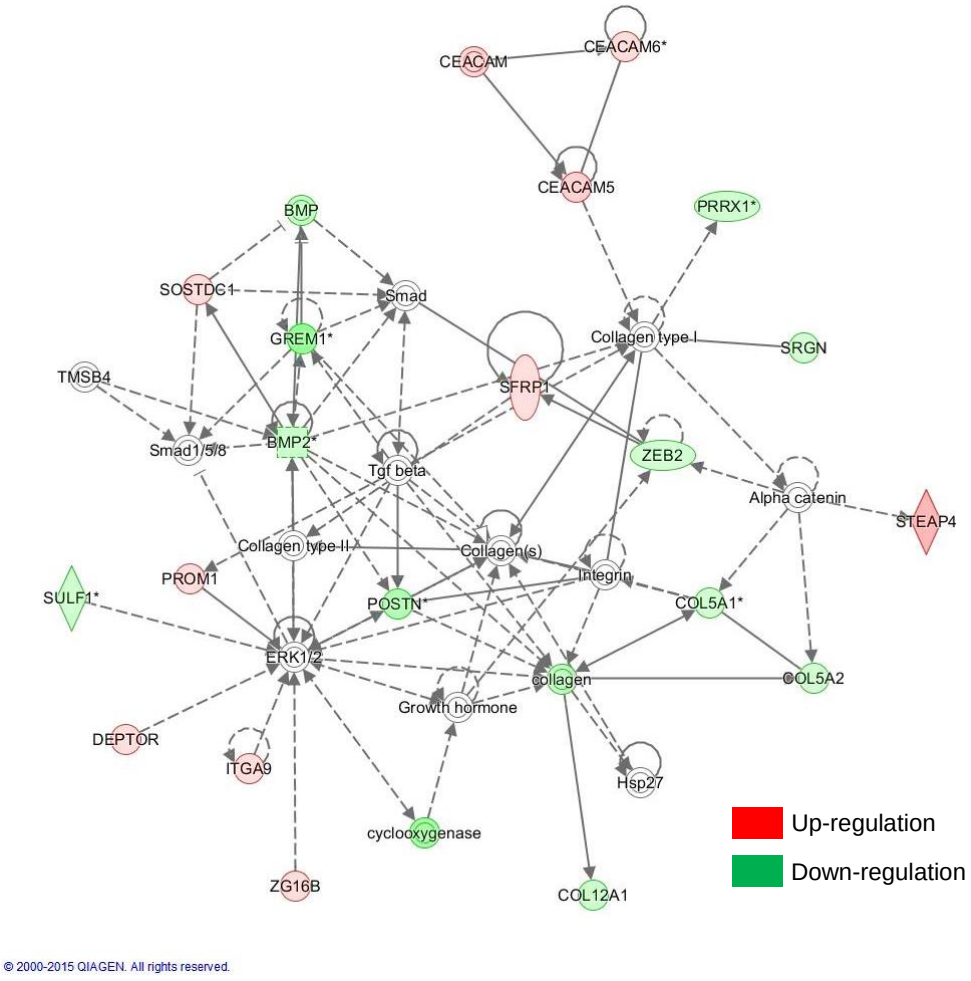

Figure 3.10: Top associated network for metastatic versus primary tumors from K5+/K19+ mRas/mp53/wtEGFR combination. Connective Tissue Disorders, Dermatological Diseases and Conditions, Developmental Disorder were the associated network functions.

3.4 DISCUSSION

The process of breast cancer progression is governed by various gene expression changes occurring within the cells of primary tumor as well as by alterations in the tumor microenvironment. Tumor cells undergo genetic and epigenetic modifications in order to acquire properties that allow extravasation from the primary tumor site, survival in the circulation and finally colonization at the secondary metastatic site. In order to do so, cells undergo the process of EMT and MET so as to metastasize to different locations in the body (Del Pozo Martin et al.,2015; Thiery et al., 2009). Patients with invasive breast cancer have metastatic tumors mostly in bones, lungs and brain. Gene expression profiling studies have identified gene signatures that predict the progression of disease and metastasis in patients (Minn et al., 2005; van 't Veer et al., 2002). However, the pathways that govern the pathogenesis of disease and its eventual progression to various secondary locations are still under investigation. Here, we used our transformed K5+/K19- or K5+/K19+ cells derived tumor models (described in chapter 2), to study the gene changes occurring during the process of disease progression. We found that tumors from K5+/K19- cells over-expressing mRas/mp53/wtErbB2 combination, despite of having a shorter primary tumor latency had a higher latency and lower incidence for metastasis (Table2.1, 2.2-Chapter 2). We also observed that tumors from transformed K5+/K19+ cells overall had a higher metastasis efficiency than those transformed K5+/K19- cells. Most breast tumors have a high K19 expression (Bartek et al., 1985). Notably, the CTCs in patients with a relapsing or metastasis disease are CK19 positive (Giuliano et al., 2014; Xenidis et al., 2009). In this chapter, we analyzed the mRNA expression changes within different tumors (Figure 3.1) in order to identify the factors that might govern disease pathogenesis within different combinations. We observed that tumors formed by transformed K5+/K19- cellular precursors, mostly had

an upregulated EMT gene expression in comparison to those from tumors transformed K5+/K19- cells (Table 3.1, Table 3.6). Specifically, tumors from K5+/K19- cells over-expressing mRas/mp53/wtErbB2 were characterized by increased expression of collagens including COL15A and COL3A, transcription factors – ZEB1, ZEB2, SNAI2 TWIST1, PRRX1 and decreased basal keratin expression than K5+/K19- cells over-expressing mRas/mp53/wtEGFR (Table 3.2, 3.3, 3.7), suggesting likely effect of oncogene ErbB2 in inducing more EMT characteristics in comparison to EGFR. Although, the tumor from K5+/K19- mRas/mp53/wtErbB2 combination had an up regulated EMT gene signature, they do not show a good correlation with metastasis formation efficiency *in-vivo* (Table 3, chapter 2). Contrary to the known literature, that higher EMT in tumor would indicate a higher metastasis we found that overall tumors with basal like expression in addition to EMT markers (K5+/K19+ mRas/mp53/wtEGFR combination) had a higher metastasis forming efficiency. Our results are in concordance with the recent report that shows that basal stem cell signature in addition to EMT is associated with higher metastasis burden (Lawson et al. 2015). Another study done by Soundarajan *et al*, also showed that high expression EMT gene signatures (PRRX1, TWIST1, SNAI2, VIM) induced during embryonic development, does not correlates significantly with metastatic or recurrent disease (Soundararajan et al. 2015), suggesting that mere upregulation EMT genes may not be the only determinant of tumor dissemination and metastasis in breast cancer. Inhibition of matrix metalloproteinase (MMPs) pathway (as analyzed by IPA) in tumors from K5+/K19- over-expressing mp53/mRas/wtErbB2 oncogene combination also provide likely explanation for the lower metastasis formation from this combination (Table 3.10).

Homeobox factor 1 (PRRX1), a transcription factor that induces EMT, was highly elevated in tumors from transformed K5+/K19- (Table 3.7). PRRX1 is shown to play an

important role in EMT and metastasis, and loss of PRRX1 is required by cancer cells to colonize at secondary locations (Ocana et al. 2012). In accordance with these results, we found a similar correlation between high PRRX1 in primary tumor and lowering of its expression in metastatic tumors in K5+/K19+ mRas/mp53/wtEGFR combination (Table 3.7). Upon analysis of mRNA expression, we found that expression of PRRX1 was lower in the parental K5+/K19- or K5+/K19+ untransformed cells (Zhao et al. 2010). However, we found an induction of PRRX1 expression upon transformation of these cells by mRas/mp53/wtErbB2 or mRas/mp53/wtEGFR oncogene combination, more so for K5+/K19- over-expressing mRas/mp53/wtErbB2. These results, therefore suggest that K5+/K19- cells have a higher susceptibility to undergo EMT by upregulating PRRX1 expression upon transformation.

Furthermore, we found that tumor from mRas/mp53/wtEGFR transformed K5+/K19+ cells, overall had a lower upregulation of EMT gene signature in comparison to those from transformed K5+/K19- cells, but they expressed more metastasis related gene signatures (Table 3.7). Upregulated expression of PTGS2, MMP1, CXCL1 has been shown to be associated with breast tumorigenicity and lung mutagenicity (Minn et al., 2005). We found that PTGS2 was highly expressed in primary tumors from K5+/K19+ mRas/mp53/wtEGFR combination, signifying that our data is in accordance with known literature. Bioinformatic analysis using IPA also validate the nature of these tumor models as we observed, cancer and reproductive system disease as the top disease associated with each combination.

Lastly, we found amino acid transporter SLC6A14, as the most highly expressed gene in metastatic tumors in comparison to primary tumor from K5+/K19+ mRas/mp53/wtEGFR combination, emphasizing its importance in metastatic disease (Table 3.6). SLC6A14, is important for tumor development and knockout mouse fail to

form spontaneous tumors (Babu et al. 2015). Analysis of three independent paired primary and metastatic tumors from different mice consistently showed an up regulated SLC6A14 expression (Figure 3.2). It therefore suggests, that amino acid metabolism may be an important process required for colonization at new locations and it can serve as probable therapeutic target to cure metastatic diseases (Karunakaran et al.,2011; McCracken and Edinger).

Our results although based on microarray data from single tumor from each combination, showed a good association with the expression of known markers for metastatic disease and explain the differences in relative primary tumor and metastasis latency and incidence which we reported earlier. Furthermore, we also validated these results in tumors derived from different mice (Figure 3.2, 3.3). In addition, we also identified certain genes that are characteristic of metastatic tumors and could be potential therapeutic targets to cure high grade tumors. In conclusion, we found that tumors from transformed K5+/19- or K5+/19+ cells overall have different susceptibility for metastasis formation due to differential gene expression associated with each primary tumor and which in turn also governs the tumor characteristics and EMT. Further exploration of pathways associated with the genes identified in the current analysis would provide an important insight into the process of primary tumor dissemination and metastasis in human patients as well as provide important therapeutic target to tackle advanced stages of the disease.

CHAPTER 4

Differential EMT induction in K5+/K19- and K5+/K19+ stem/progenitors upon oncogenic transformation with mRas/mp53/mPI3K

Divya Bhagirath, Xiangshan Zhao, William W. West, Hamid Band, Vimla Band

(In preparation)

4.1 INTRODUCTION

Breast cancer is a heterogeneous disease and is classified into different subtypes, namely- Luminal-like, ErbB2 over-expressing, Basal-like and Claudin-low (Perou et al., 2000; Prat et al., 2010; Sorlie et al., 2001). Different subtypes have characteristic gene expression changes, that involve over-expression, hyper or hypo DNA methylation or mutations in key oncogenes or tumor suppressor (TCGA 2012, Banerji et al., 2012; Sorlie et al., 2001; Stephens et al. 2012). The nature of cell type that gets transformed is an important determinant for development of different breast tumor types (Bhagirath et al., 2015 ; Ince et al., 2007; Johnson et al.,2014; Keller et al., 2012; Melchor et al. 2014). More recently, we and others have shown that the transforming oncogenes also play an important role in determining the pathogenesis and progression of disease (Bhagirath et al., 2015; Melchor et al. 2014). As described previously in Chapter 2, we investigated the role of oncogene combinations mRas/mp53/wtErbB2 or mRas/mp53/wtEGFR in determining breast tumor type from mammary stem/progenitor cell lines designated as K5+/K19- and K5+/K19+, by over-expressing these oncogene combinations. Prevalence of these oncogenes (ErbB2, EGFR) in different BC subtypes (luminal-like, ErbB2 over-expressing or basal-like) and their association with poor survival outcome in patients suggest that these oncogenes may play an important role in BC pathogenesis. Indeed, we found an important relationship between the oncogene that is over-expressed, with the cell type in which it is present and their combinatorial effect in governing the tumor phenotype as well as primary tumor and metastasis latencies. K5+/K19- cells over-expressing ErbB2 in combination with mRas and mp53 generated primary tumors with shorter latency in comparison to K5+/K19- cells over-expressing mRas/mp5/wtEGFR. Although, the latency for primary tumor formation was much higher for K5+/K19- over-expressing mRas/mp5/wtEGFR, these cells had a similar

latency for developing lung metastasis as that of K5+/K19- cells with mRas/mp5/wtErbB2. Another important observation was that, the nature of cell type also determined the metastasis latency and incidence. K5+/K19+ cells overall had a higher rate of developing metastasis than K5+/K19- transformed cells, suggesting an increased susceptibility of K5+/K19+ precursors for metastasis. Given, these differential effects of oncogenes and cell type on pathogenesis of breast tumors, in the current study we investigated the effect of over-expression of oncogene combination mRas/mp53 along with mutant PI3K on K5+/K19- and K5+/K19+ cells. PI3K is the most commonly mutated oncogene in luminal like breast tumors (TCGA 2012). It has been previously shown that combination of Ras and PI3K can efficiently transform hMECS in vitro (Oda et al., 2008; Wang et al. 2013) and more recently it has been demonstrated that induction of PI3K mutation in different cell lineages affects the tumor phenotype (Van Keymeulen et al. 2015).

We observed that over-expression of oncogene combination mRas/mp53/mPI3K drives complete EMT in K5+/K19- cells whereas a mixed epithelial and EMT phenotype in K5+/K19+ cells. The tumors formed *in-vivo* by same oncogene combination gave rise to metaplastic carcinomas from transformed K5+/K19- and mixture of metaplastic and adenocarcinomas from transformed K5+/K19+, with an overall higher EMT characteristics in both the tumors. This study and our previous findings strongly suggest an increased susceptibility of K5+/K19- precursors to undergo EMT upon transformation than K5+/K19+ cell types.

4.2 MATERIALS AND METHODS

Cell lines and retroviral/lentiviral infection

Mutant p53R249S in pLENTI-6 (purchased from Addgene) along with Invitrogen packaging vector (ViraPowerTM Lentiviral Packaging MIX) were transfected into 293FT packaging cells. Lentiviral supernatants were collected after overnight incubation in fresh DMEM media. TSA54 packaging cells were transfected with retroviral constructs, mutant H-Ras Q61L in pBABE-hygro, mPI3KH1047 in pMSCV-puro vector, together with PIK plasmid for packaging, and viral supernatants were collected (as mentioned above for lentiviral). K5+/K5+/K19- and K5+/K19+ stem/progenitor cell lines (Zhao et al. 2010) were infected with viral supernatants to generate cell lines with different gene combinations followed by their selection in DFCI-1 medium (Band and Sager, 1989; Band et al., 1990) containing hygromycin (15ul/ml) (for mutant H-Ras), blasticidine (15ul/ml) (for mutant p53), puromycin (0.5ul/ml) (for mPI3K).

Antibodies

The following antibodies were used for western blotting, immunofluorescence, flow-cytometry and IHC: mouse anti-human p53 (DO-1) (sc-126), mouse anti-human α-smooth muscle actin (SMA) (sc-32251), mouse anti-human vimentin (sc-6260) were from Santa Cruz Biotechnology. Mouse anti-human Ras (610001), mouse anti-human MUC1 (550486), rat anti-human CD49f (555734), FITC conjugated anti-CD24 (555427), PE-conjugated anti-CD44 (555479) and Alexa-488 conjugated E-Cadherin (560061) were from BD Bioscience. Rabbit anti-human vimentin (clone SP20, RM-9120-S0) was from Thermo Scientific. Rabbit anti-human K5 (PRB-160P) was from Covance.

Anchorage-independence growth assay

40,000 cells suspended in DFCI-1 medium containing 0.3% agarose were seeded in the top layer of each well of 6-well plates containing 0.6% agarose as a bottom layer. Each cell line was plated in triplicates. Colonies (>60 cells) were counted after 3 weeks after crystal violet staining.

Flow cytometry analysis

1 million cells were incubated with FITC conjugated anti-CD24 and PE-conjugated anti-CD44 at 4^{o}C for 45 min. Following incubation, the cells were washed three times with washing buffer (phosphate buffer saline with 0.2% fetal bovine serum) and were subjected to fluorescence-activated cell sorter (FACS) analysis.

Migration and invasion assay

20,000 cells were plated in trans-well chambers (BD-for migration, BD-for invasion) and incubated at 37^{o}C for 13Hrs. or 23Hrs. Migration or invasion of plated cells was stopped at respective time periods. Cells on upper chamber were cleaned using cotton swab, while the cells on the bottom of the chamber were fixed with HEMA fixative (#122-911A), followed by staining with HEMA solution I (#122-911B) and HEMA solution II (#122-911C) for 5min. each. Stained cells were counted under the inverted microscope.

In vitro matrigel polarity assay

Protocol used for matrigel assay has been described previously (Zhao et al., 2011; Zhao et al. 2012). Briefly, 1000 cells suspended in DFCI-1 medium containing 2% matrigel were plated on glass coverslips with 100% reconstituted basement membrane (matrigel from BD Biosciences in 24 well plate. After 12 days (alternate day feeding) cells were stained with FITC conjugated anti-CD227 (MUC1) and PE-Cy5 conjugated anti- CD49f and analyzed under Zeiss 510 confocal microscope (UNMC facility).

Xenograft transplantation assays for primary tumor formation

6-8 weeks old immunodeficient NOD-SCID gamma (NSG) mice (purchased from Jackson laboratories) were orthotopically injected with 1 million cells (not tagged with GFP-luciferase) in DFCI-1 medium mixed with matrigel in 1:1 proportion (Ince et al., 2007) in the fourth and ninth (contralateral) mammary glands. 4 mice were used for each combination. Tumor formation was assessed by palpation in the area of injection every week until 6 months. After six months, mice with or without tumors were sacrificed by CO2 inhalation followed by cervical dislocation. Tumors were excised, fixed with 10% neutral buffered formalin and processed to prepare paraffin-embedded tumor blocks that were then sectioned for IHC.

Immunohistochemistry

Tumor tissues were fixed in 10% Neutral buffered Formalin (NBF) and processed into paraffin blocks. 4 µm sections were cut and stained with indicated antibodies. The standard staining procedure was performed using DAKO kit as per the manufacturer's

protocol (# K4007) and as described (Zhao et al. 2012). For IHC staining, tissue sections were incubated with primary antibodies (anti-K5, anti-MUC1, anti-vimentin or anti-α-SMA) in a hydrated chamber, followed by incubation with HRP-tagged secondary IgG against the primary antibodies and DAB solution and subsequently processed for nuclear staining with hematoxylin and mounting of tissues. For double-immunofluorescence staining tumor sections were processed similarly and blocked with 10% goat serum for 1 hr. These were then stained with rabbit anti-vimentin, alexa 488 conjugated anti-E-cadherin or mouse anti- α-SMA antibodies. Goat anti-rabbit alexa 594 and goat anti-mouse alexa 488 conjugated secondary antibodies (Invitrogen) were used for staining. The sections were mounted with anti-fade mounting media. Images were taken with fluorescence microscope (Zeiss axioplan 2 imaging microscope).

Isolation and culture of primary tumor derived cells

Xenograft tumors were excised from NSG mice and minced with sterilized scalpel in clean P-60 petri dishes. Minced tumors were cultured in either alpha-MEM or DFCI1 medium for 1-2 weeks, following which the cells were trypsinized. Isolated cells were then subjected to antibiotic (blasticidine, hygromycin and puromycin) selection to isolate human cells.

4.3 RESULTS

Over-expression of mRas/mp53/mPI3K leads to oncogenic transformation of K5+/K19- and K5+/K19+ cells

Oncogene combination mRas/mp53/mPI3K was ectopically over-expressed in K5+/K19- and K5+/K19+ cell lines and stable cells lines were generated using antibiotic selection. Protein expression of over-expressed genes was analyzed by western blotting (Figure 4.1A). To test if over-expression of mRas/mp53/mPI3K transforms the two cell types we performed *in-vitro* anchorage independence assay. Both, K5+/K19- and K5+/K19+ cells upon over-expression of mRas/mp53/mPI3K give rise to colonies in 0.3% agar (Figure 4.1B), signifying a complete *in-vitro* transformation. This assay is still ongoing for enumeration of colonies from mRas/mp53/mPI3K transformed K5+/K19- or K5+/K19+ cells.

Figure 4.1: *In-vitro* transformation of K5+/K19- and K5+/K19+ cells by mRas/mp53/mPI3K

A.

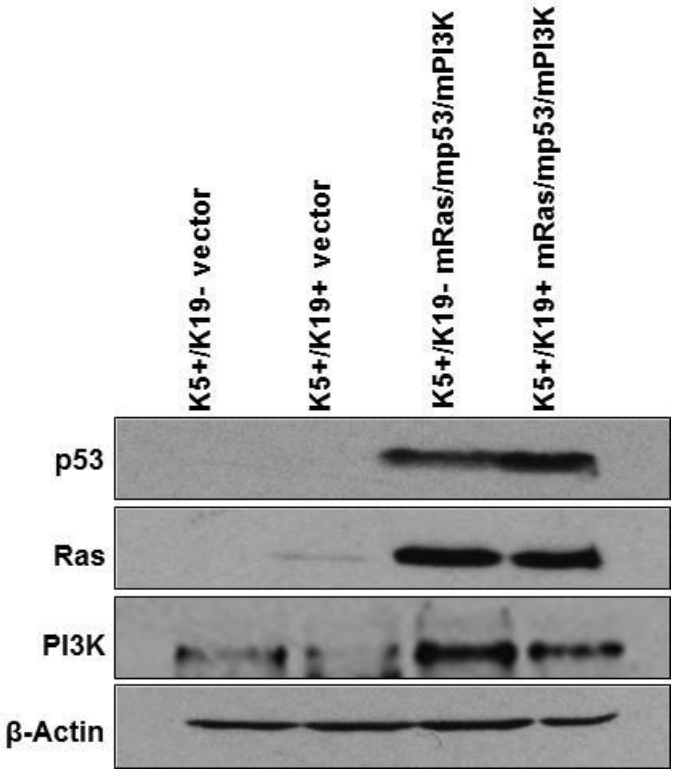

B.

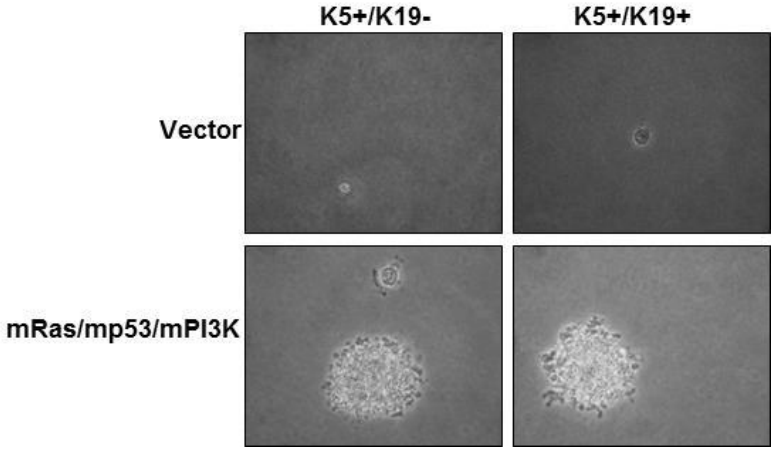

Figure 4.1: *In-vitro* transformation of K5+/K19- and K5+/K19+ cells by mRas/mp53/mPI3K. A). $K5^{+}/K19^{-}$ or $K5^{+}/K19^{+}$ cell lines over-expressing vector or mRas/mp53/mPI3K oncogene combination were analyzed by Western Blotting. β-Actin was used as loading control. B). Representative images (magnification 40X) of colonies from $K5^{+}/K19^{-}$ and $K5^{+}/K19^{+}$ cells with vector or mRas/mp53/mPI3K oncogene combination assessed by anchorage independent growth assay.

Oncogenic transformation with mRas/mp53/mPI3K oncogene combination leads to complete and partial EMT in K5+/K19- and K5+/K19+ cells respectively.

We further observed that in addition to *in-vitro* transformation, over-expression of mRas/mp53/mPI3K led to generation of complete EMT in K5+/K19- cells and mixed EMT and epithelial morphology in K5+/K19+ cells *in-vitro* in culture. To further confirm this differential effect on K19- and K19+ cellular precursors, we over-expressed mRas/mp53/mPI3K in different clones derived from K5+/K19- and K5+/K19+ cells. Both the clones displayed differences in morphology as expected (Figure 4.2A). This is in contrast with the previously observed transformations with oncogene combinations mRas/mp53/wtErbB2 or mRas/mp53/wtEGFR, where complete EMT was only observed *in-vivo* in tumors from K5+/K19- with ErbB2 combination. The transformed K5+/K19- cells with mRas/mp53/wtErbB2 or mRas/mp53/wtEGFR however had an epithelial morphology *in-vitro*. Thus, suggesting that PI3K is more potent EMT inducer than ErbB2 or EGFR and it is drives K5+/K19- cellular precursors to complete phenotypic EMT *in-vitro*. Figure 4.2A shows phenotypic differences in morphology of K19- clone 62 and K19+ clone 21. We also assessed expression of different EMT markers (E-Cadherin, vimentin) in mRas/mp53/mPI3K transformed K5+/K19- and K5+/K19+ cell lines. As expected transformed cells showed a decrease in E-Cadherin and increase in vimentin expression (Figure 4.2B)

We assessed expression of cell surface markers CD44 and CD24 in mRas/mp53/mPI3K transformed K5+/K19- and K5+/K19+ cells, to identify $CD44^{high}/CD24^{low}$ cell population within these cells. $CD44^{high}/CD24^{low}$ is a marker for tumor-initiating cells (Al-Hajj et al., 2003) and its expression is associated with EMT like Claudin-low tumors (Prat et al. 2010). We observed that K5+/K19- transformed cells that had undergone complete EMT *in-vitro* showed a significant shift towards

$CD44^{high}/CD24^{low}$ phenotype as compared to transformed K5+/K19+ cells (Figure 4.3). These results are in accordance with the respective EMT morphologies observed for the two transformed cell lines and K5+/K19- transformed cells as expected shows higher $CD44^{high}/CD24^{low}$ population as compared to mixed EMT and epithelial K5+/K19+ transformed cells.

We then determined the functional effects of mRas/mp53/mPI3K over-expression in K5+/K19- and K5+/K19+ cells. For that, we first assessed the migration and invasion abilities of the transformed cell lines *in-vitro*. We observed that both the mRas/mp53/mPI3K transformed K5+/K19- and K5+/K19+ cells had an increased migration and invasion ability as compared to vector cells (Figure 4.4A, 4.4B). PI3K oncogene has been associated with increased EMT like characteristics and is expected to increase the migratory and invasive capacity of cells. Thus, over-expression of mRas/mp53/mPI3K in K5+/K19- or K5+/K19+ affects cellular pathways of both the cell types towards increased motility and invasion. However, we did not observed any difference in the invasion or migration abilities between transformed K5+/K19- or K5+/K19+, despite the differences in extent of EMT in the two cell lines.

Next, we assessed the ability of mRas/mp53/mPI3K transformed K5+/K19- or K5+/K19+ cells to form polarized acinar structure in matrigel. We observed that EMT like transformed K5+/K19- cells lose their ability to form polarized acini and give rise to branched invasive structures with a low CD49f staining (Figure 4.5A). K5+/K19+ cells however, still maintain their ability to form acini upon transformation and form branched structure and rounded acini in matrigel (Figure 4.5B) as opposed to transformed K5+/K19- cells, suggesting a differential effect of mRas/mp53/mPI3K oncogene combination on K5+/K19- and K5+/K19+ cells.

Figure 4.2: Differential EMT in mRas/mp53/mPI3K transformed K5+/K19- and K5+/K19+ cell lines.

A

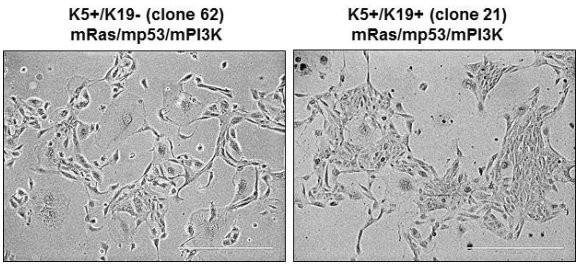

B

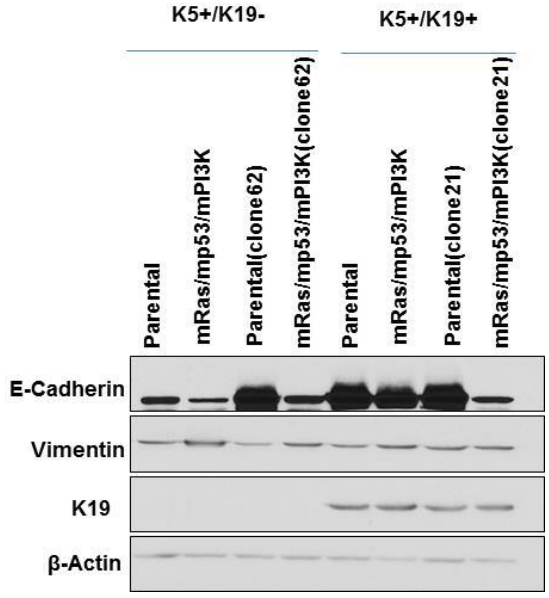

Figure 4.2: Differential EMT in mRas/mp53/mPI3K transformed K5+/K19- and K5+/K19+ cell lines. Phase contrast images showing differences in EMT phenotype in transformed $K5^{+}/K19^{-}$ (clone 62) or $K5^{+}/K19^{+}$ (clone 21) cells (magnification 10X). B) Parental or transformed $K5^{+}/K19^{-}$ or $K5^{+}/K19^{+}$ cells were analyzed by western blotting for expression of EMT markers- E-Cadherin or Vimentin. β-actin was used as loading control.

Figure 4.3: Expression of $CD44^{high}/CD24^{low}$ population in mRas/mp53/mPI3K transformed K5+/K19- and K5+/K19+ cells

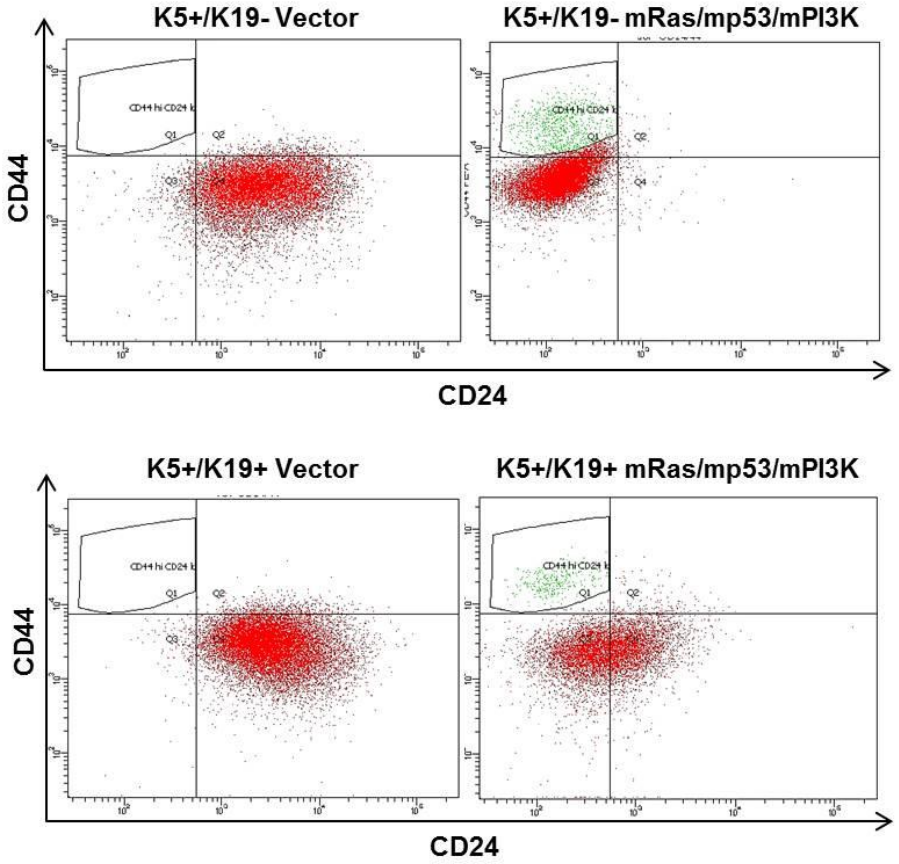

Figure 4.3: Expression of $CD44^{high}/CD24^{low}$ population in mRas/mp53/mPI3K transformed K5+/K19- and K5+/K19+ cells. Vector or transformed $K5^{+}/K19^{-}$ or $K5^{+}/K19^{+}$ cells were stained with stem cell markers CD44 and CD24 and analyzed by flow Cytometry. Dot plot analysis of cell population expressing $CD44^{high}/CD24^{low}$ (gated-upper left).

Figure 4.4: Migration and invasion abilities of mRas/mp53/mPI3K transformed K5+/K19- and K5+/K19+ cells

A

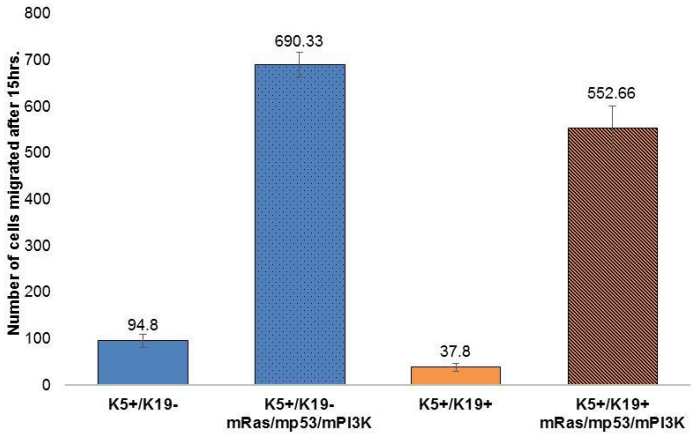

B

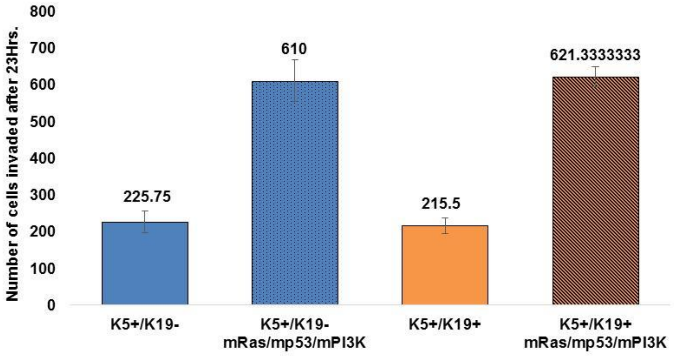

Figure 4.4: Migration and invasion abilities of mRas/mp53/mPI3K transformed K5+/K19- and K5+/K19+ cells. Vector or transformed $K5^{+}/K19^{-}$ or $K5^{+}/K19^{+}$ cells were plated in trans-well chambers. Migration or invasion of cells was stopped at 13 Hr. and 23Hrs. respectively. Cells were stained and counted to assess migration (A) and invasion (B) after respective time periods.

Figure 4.5: *In-vitro* matrigel polarity assay for mRas/mp53/mPI3K transformed K5+/K19- and K5+/K19+ cells.

A.

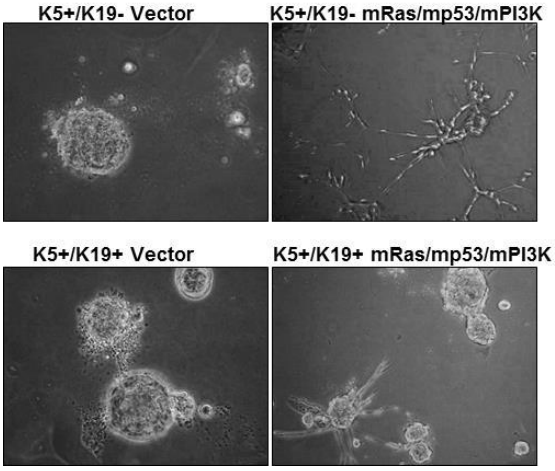

B.

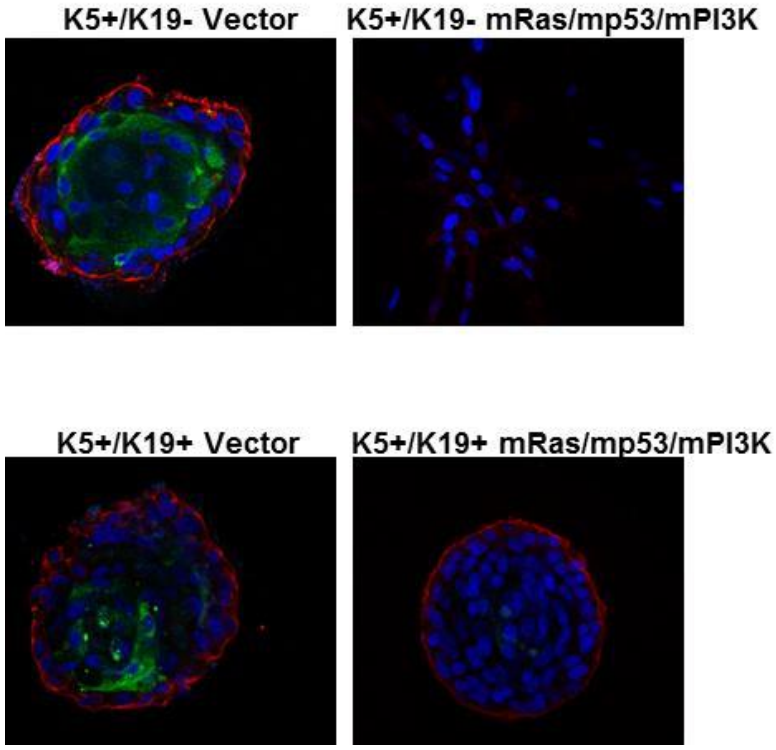

Figure 4.5: In-vitro matrigel polarity assay for mRas/mp53/mPI3K transformed K5+/K19- and K5+/K19+ cells. (A) Representative phase contrast images of branched structure and acini formed by vector transformed $K5^+/K19^-$ or $K5^+/K19^+$ cells. (B) Vector or transformed $K5^+/K19^-$ or $K5^+/K19^+$ cells were grown in DFCI-1 (differentiation) medium in Matrigel. Acini or branched structures were stained with PE-Cy5 conjugated anti-CD49f (red) and FITC conjugated anti-MUC1 (green).

Transformed K5+/K19- and K5+/K19+ cells give rise to spindle like metaplastic carcinomas and adenocarcinomas *in-vivo*

To confirm if the transformation observed *in-vitro* as a result of mRas/mp53/mPI3K over-expression in K5+/K19- and K5+/K19+ cells is complete, we assessed the tumor formation ability of the tranformed cell lines. Vector or mRas/mp53/mPI3K over-expressing K5+/K19- and K5+/K19+ were injected orthotopicaly in mammary glands of NSG mice. The vector cells as expected did not show any tumor formation, while both the transformed cells gave rise to mammary tumors in mice. mRas/mp53/mPI3K transformed K5+/K19- EMT like cells were most potent in forming tumors and all the 4 mice formed primary tumors within 4 weeks of injection. While mRas/mp53/mPI3K transformed K5+/K19+ had a latency period slightly higher than transformed K5+/K19- cells and injected mice formed tumors by 6^{th} week of injection. Thereby, suggesting that EMT phenotypes may play an important role in forming early primary tumors.

While the tumors formed by transformed K5+/K19- cells had a spindle like morphology and resembled metaplastic carcinomas of breast, those from transformed K5+/K19+ resembled adenocarcinomas with spindle like metaplastic carcinoma componenent (Figure 4.6A). We assessed the phenotypes of tumors by evaluating the expression of different makers for EMT, epithelial or stem-like cells such as MUC1 or E-Cadherin for epithelial, α-sma or vimentin for EMT and K5 or vimentin for stem or basal-like cells. Immunohistochemical analysis of tumors from transformed K5+/K19- showed a concordance in terms of expression of EMT markers, with the morphological EMT that was observed *in-vitro* (Figure 4.6B, 4.7A, 4.7B). Transformed K5+/K19+ as expected had a mixed expression for EMT and epithelial markers (Figure 4.6B, 4.7A, 4.7B), consistent with their morphology *in-vitro*. Overall, we observed increased EMT like

phenotype in tumors from mRas/mp53/mPI3K transformed K5+/K19- and K5+/K19+ cells, more so for transformed K5+/K19- cells.

We then tested if the tumor cells isolated from primary tumors also maintain their EMT like morphology *in-vitro* upon culture. We observed, that tumor derived cells maintain the EMT or epithelial morphology as was observed in the injected parental cells (Figure 4.8), suggesting that oncogene combination mRas/mp53/mPI3K confers EMT like phenotype in K5+/K19- cells that is maintained by the cells. Morever, these EMT like cells derived from tumors formed by tranformed K5+/K19- cells had a drastically lower Pan-CK expression owing to the EMT induced as a result of mRas/mp53/mPI3K over-expression. However, K5+/K19+ cells still retained expression of keratins after over-expression, suggesting that K5+/K19- cells overall have a higher susceptibilty to undergo EMT as compared to K5+/K19+ cells (Figure 4.9A, 4.9B).

Figure 4.6: mRas/mp53/mPI3K transformed $K5^{+}/K19^{-}$ or $K5^{+}/K19^{+}$ cells give rise tumors with distinct EMT characteristics

A.

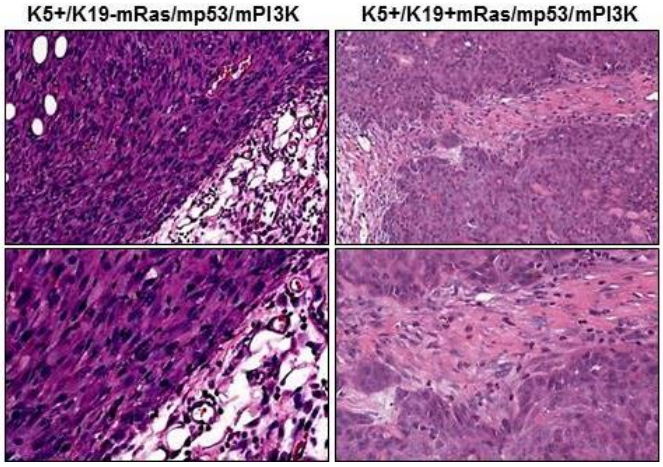

B.

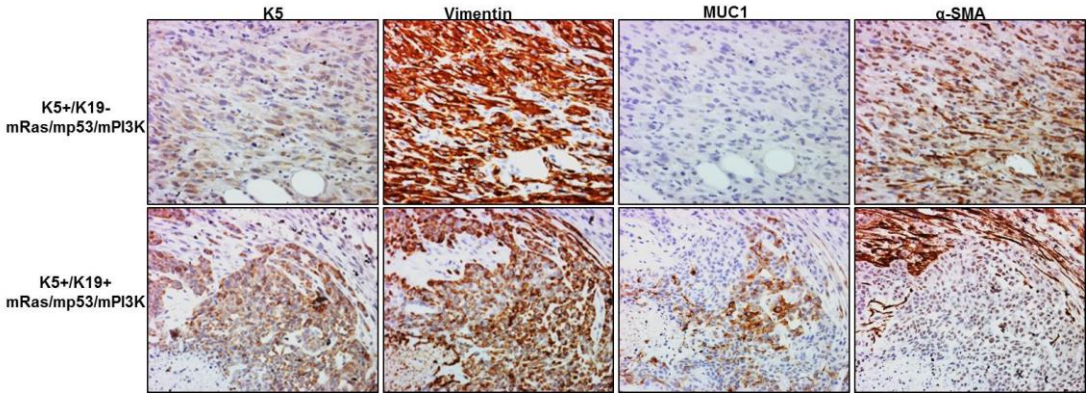

Figure 4.6: mRas/mp53/mPI3K transformed $K5^+/K19^-$ or $K5^+/K19^+$ cells give rise tumors with distinct EMT characteristics. A) Representative images of H&E staining of tumor sections (magnification 20X upper panel, 40X lower panel) from $K5^+/K19^-$ or $K5^+/K19^+$ cells over-expressing mRas/mp53/mPI3K. B) Images from different tumors at magnification 20X. Immunohistochemical staining of tumor sections from transformed $K5^+/K19^-$ or $K5^+/K19^+$ cells, with anti-CK5 (Basal/Stem), anti-vimentin (Basal/EMT), anti-MUC1 (Luminal) and anti-α-SMA (EMT) antibodies.

Figure 4.7: mRas/mp53/mPI3K transformed $K5^{+}/K19^{-}$ or $K5^{+}/K19^{+}$ cells give rise tumors with distinct EMT characteristics

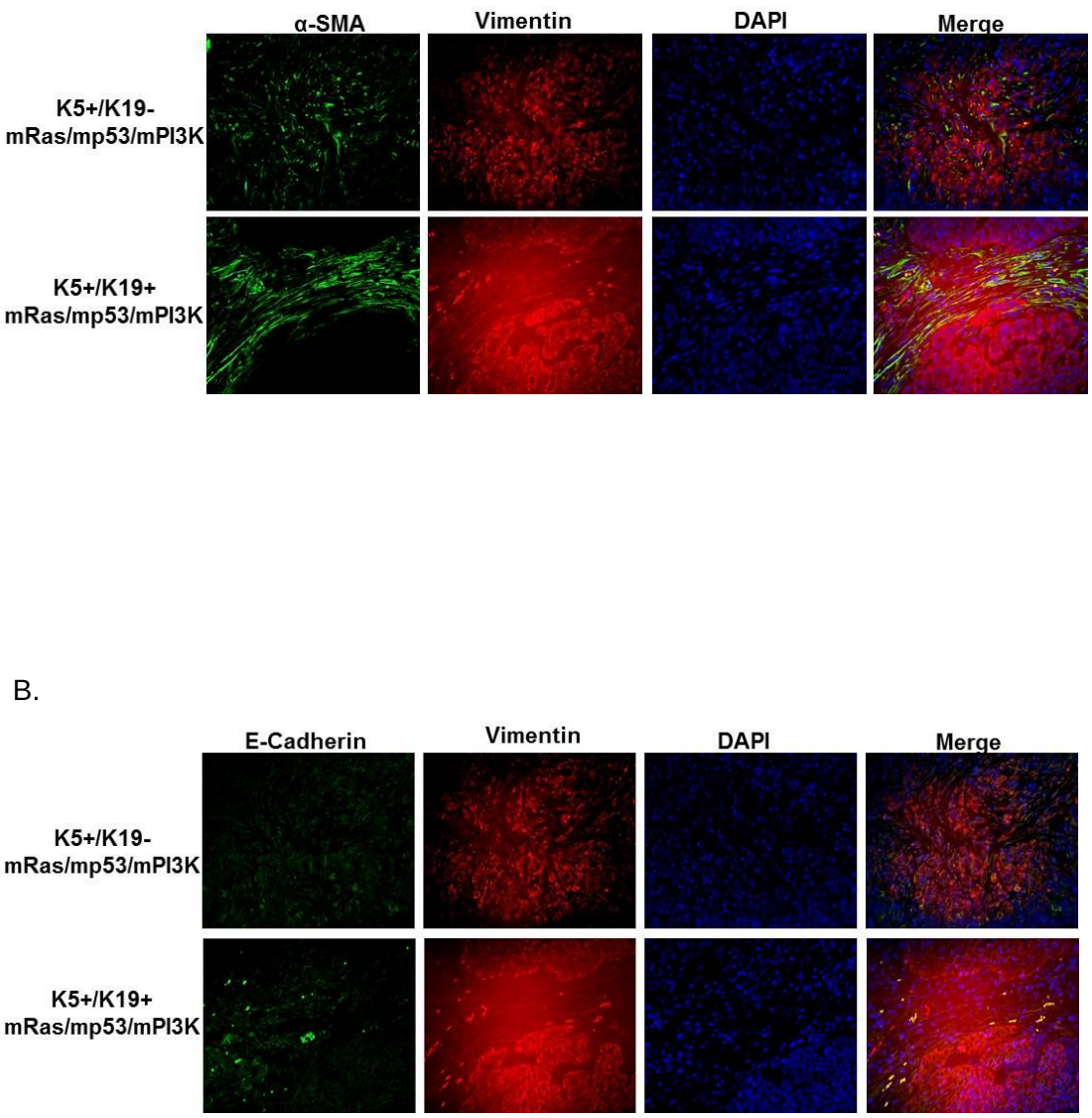

Figure 4.7: mRas/mp53/mPI3K transformed $K5^{+}/K19^{-}$ or $K5^{+}/K19^{+}$ cells give rise tumors with distinct EMT characteristics. A) Representative images of tumors from $K5^{+}/K19^{-}$ or$K5^{+}/K19^{+}$ cells double immunostained with anti-αSMA (green) and anti-vimentin (red) show presence of claudin-low (SMA^{+}/$vimentin^{+}$) areas within different tumors. B) Same tumor sections double immunostained with E-Cadherin (green) and vimentin (red) show presence of lowering of luminal like E-$Cadherin^{+}$ staining. DAPI (blue) shows nucleus.

Figure 4.8: mRas/mp53/mPI3K transformed K5$^+$/K19$^-$ or K5$^+$/K19$^+$ tumor derived cells maintain their EMT phenotypes.

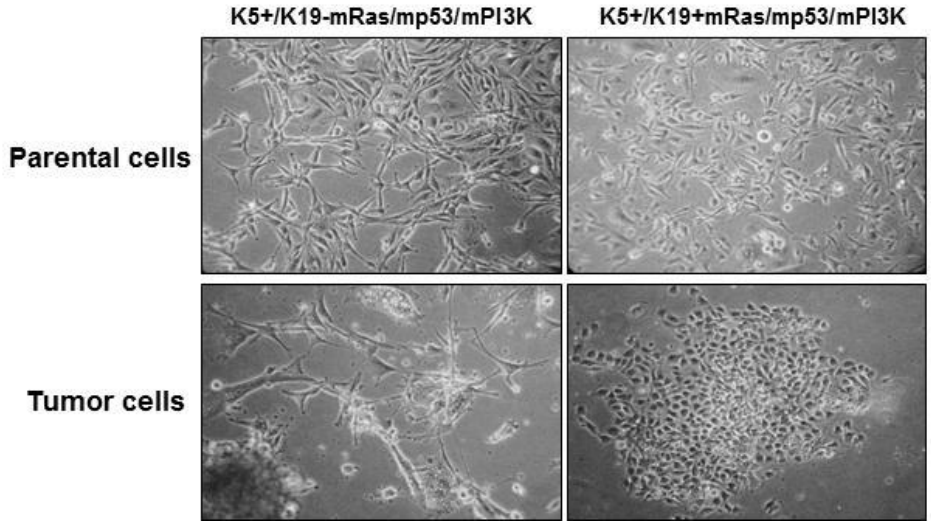

Figure 4.8: mRas/mp53/mPI3K transformed K5$^+$/K19$^-$ or K5$^+$/K19$^+$ tumor derived cells maintain their EMT phenotypes. Tumors formed by transformed K5$^+$/K19$^-$ or K5$^+$/K19$^+$ cells were excised and cultured to isolate primary tumor cells. Phase contrast images of parental transformed K5$^+$/K19$^-$ or K5$^+$/K19$^+$ cells (upper panel) and tumor derived cells (lower panel) showing differences in EMT phenotype between the K5$^+$/K19$^-$ or K5$^+$/K19$^+$ cells.

Figure 4.9: Cyto-keratin expression in tumor derived cells from mRas/mp53/mPI3K transformed K5^{+}/K19^{-} or K5^{+}/K19^{+} tumors.

A.

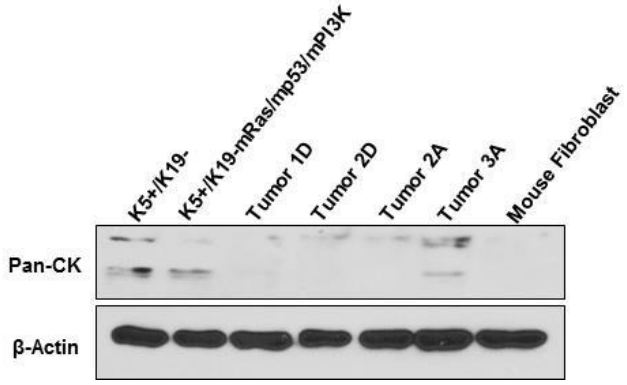

B.

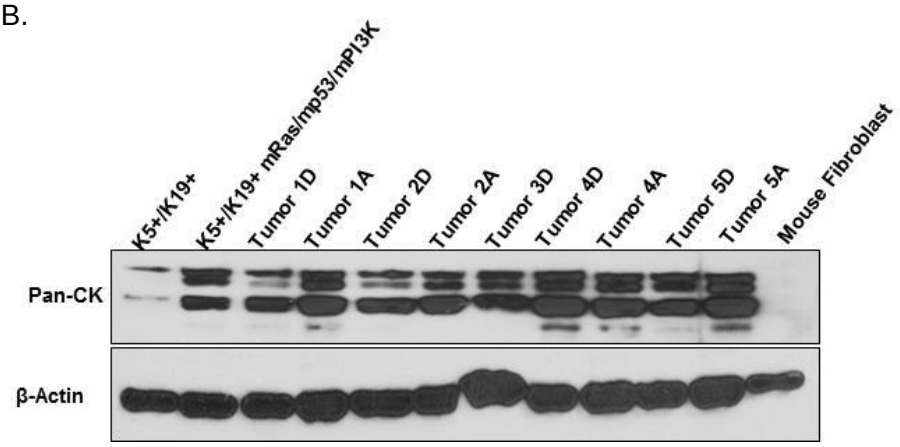

Figure 4.9: Cyto-keratin expression in tumor derived cells from mRas/mp53/mPI3K transformed K5^{+}/K19^{-} or K5^{+}/K19^{+} tumors. Transformed A) K5^{+}/K19^{-} or B) K5^{+}/K19^{+} parental or tumor derived cell lines were analyzed by Western Blotting. β-Actin was used as loading control. A- refers to cells cultured in alpha-MEM medium and D- refers to DFCI medium.

K5+/K19- cells have a pre-existing up-regulation of EMT like gene signatures as compared to K5+/K19+ cells.

In order to understand underlying reason for phenotypic differences that occurred as a result of transformation by mRas/mp53/mPI3K over-expression, we analyzed the genes that were differentially expressed in the parental K5+/K19- or K5+/K19+ cells (Zhao et al. 2010). Table 4.1 and Table 4.2 shows list of genes that were up-regulated in K5+/K19- or K5+/K19+ cell types. Notably, K5+/K19- cells had an up-regulated expression of genes that are involved with activation of mesenchymal or desmoplastic stromal reaction in tumors. THBS2 was the most highly expressed gene in K5+/K19- cells. It has been shown to be involved in activation of fibroblasts in tumors (Del Pozo Martin et al.,2015; Kim et al. 2010). Collagen proteins- COL5A1 and COL5A2 that were found to be highly expressed in K5+/K19- cells, are also associated with EMT like phenotypes in tumors (Grigoriadis et al., 2006; Kiemer et al., 2001; Kim et al. 2010). However, we did not find any highly expressed transcription factor that could be responsible for inducing mesenchymal state in K5+/K19- cells or correlate with this high expression of EMT markers in the cells. Overall, these differences in the gene expression of EMT markers THBS2, COL5A1 or COL5A2 between K5+/K19- and K5+/K19+ cells, could be the likely reason for development or increased susceptibility of EMT from K5+/K19- than K5+/K19+ cells. In addition to comparing the gene expression changes with K5+/K19+, we also assessed the fold change with respect to K5-/K19- cells. K5-/K19- are myoepithelial progenitor cells that were generated previously from K5+/K19- or K5+/K19+ cells (Zhao et al. 2010) and have a phenotypically EMT like morphology *in-vitro*. We observed that, overall K5+/K19- cells had a closer expression correlation with the phenotypically EMT like myoepithelial progenitor cells than

K5+/K19+, suggesting that these cells have an existent gene expression profile that correspond more to the EMT phenotype.

Table 4.1: List of genes differentially up-regulated in K5+/K19- cells.

Gene symbol	K5+19-/K5+19+	K5+19-/K5-19-
THBS2	28.55945	1.309682
COL5A2	65.37363	0.195327
NELL2	12.81322	35.77253
KCNJ15	15.92035	1.12689
LCP1	31.44195	15.92979
ZNF20 /// ZNF625	12.01684	0.816946
COL5A1	63.10417	0.327495
PDE4DIP	24.15854	0.462634
TSPAN18	16.61856	2.178378
ALKBH4	15.31068	0.937574

Table 4.2: List of genes differentially up-regulated in K5+/K19+ cells.

Gene symbol	K5+19+/K5+19-	K5+19+/K5-19-
KRT19	5207.431818	17625.15385
TFPI	401.9534884	1.915124654
CFI	19.96238245	0.103948679
CDH2	96.13114754	0.181789999
CYYR1	19.14937759	209.7727273
EPDR1	278.6875	85.75
NME5	58.73214286	3.594535519
ZNF558	12.42105263	5.410934744
DNAJA4	69.70454545	92.93939394
KRT33A	45.58928571	69

4.4 DISCUSSION

Heterogeneity in BC is widely prevalent and is responsible for failure of therapeutic response in patients. Several studies have focused on understanding the etiology of BC heterogeneity. Owing to several variable such as the microenvironment changes, accumulation of mutations, loss of differentiation, it becomes difficult to understand the underlying factors that initiate or possibly mediate progression of the disease. Using defined cellular precursors and by introducing different oncogenes we and others have observed that heterogeneity or subtypes in breast tumors is likely to be caused as an effect of both the nature of affected cell type as well as the oncogene(s)/tumor-suppresor altered in the cell (Bhagirath et al., 2015; Johnson et al., 2014; Keller et al., 2012; Melchor et al. 2014). In the present study, we introduced mutant PI3K oncogene, that is widely mutated in luminal tumors, in addition to mutant Ras and mutant p53 in K5+/K19- or K5+/K19+ cells and we assessed the effect of the combination in driving pathogenesis from the two isogenic cell lines. The oncogene combination mRas/mp53/mPI3K was potent in driving both *in-vitro* transformation (Figure 4.1) and *in-vivo* tumor formation (Figure 4.6) as was expected based on earlier studies (Oda et al., 2008; Wang et al. 2013). As previously shown in Chapter 2, we observed differences in phenotypes of the tumors formed from mRas/mp53/mPI3K transformed K5+/K19- or K5+/K19+ cells, with transformed K5+/K19- giving rise to EMT like metaplastic carcinomas as compared to those from transformed K5+/K19+ cells (Figure 4.6, 4.7) and they maintained their *in-vitro* oncogene induced EMT like phenotype both in tumors as well as tumor derived cell lines (Figure 4.9). Additionally, we observed that mRas/mp53/mPI3K oncogene combination had a differential effect in driving EMT in K5+/K19- or K5+/K19+ cells.

These results are different from our previous observation with oncogene combinations mRas/mp53/wtErbB2 or mRas/mp53/wtEGFR, where introduction of either of the two combinations did not induced any EMT morphology *in-vitro* in culture. Both, K5+/K19- or K5+/K19+ cells retained their epithelial phenotypes *in-vitro* upon over-expression of these oncogenes combination. However, we did observed generation of EMT like metaplastic tumors from mRas/mp53/wtErbB2 transformed K5+/K19- cells. These results thereby suggest that mutant PI3K is more potent in inducing EMT than either ErbB2 or EGFR. In lieu of these observations, more recently it has been shown that mutant PI3K activates multipotency in different cell-types i.e. the luminal and basal cell lineages and generates heterogeneity of tumors based on the type of cell affected (Van Keymeulen et al. 2015). To understand the reason for variation in K5+/K19- and k19+ cells, we analyzed the genes that are differentially regulated in the parental K5+/K19- and K5+/K19+ cells.

We identified that, overall K5+/K19- cells have an up-regulated gene signatures that correspond to EMT like phenotype as compared to K5+/K19+ cells. THBS2, was the most highly expressed gene in K5+/K19- and has been shown to be an important mediator of desmoplastic or stromal reaction in tumors. The secreted protein activates the myofibroblasts and facilitates in development of niches that favor metastasis and likely cause metaplastic phenotypes in tumors (Del Pozo Martin et al. 2015) . THBS2, COL5A1 and COL5A2, all of which were found to be highly expressed in K5+/K19- cells, form the metastasis activating or mesenchymal state inducing genes signature as shown previously (Kiemer et al., 2001; Kim et al. 2010). Thus up-regulation of such mesenchymal marker proteins in K5+/K19- cellular precursors, suggest that the intrinsic susceptibilities of K5+/K19- towards EMT phenotype could be governed by the existent gene expression within the parental cell type. It is however not necessary that induction

of EMT itself governs the progression of disease. Our previous study and work from others, has shown that mere up-regulation of EMT gene signatures does not correlate with metastatic disease (unpublished work, Ocana et al.,2012; Soundararajan et al. 2015). EMT is important for migration of cells however, success of metastatic colonization relies on reversion of this phenotype (Del Pozo Martin et al. 2015) the capacity of which may vary from one cell to another. We observed that although transformed K5+/K19- had a higher tendency to undergo EMT, their ability to form metastatic tumors was lesser than transformed K5+/K19+ cells. Cellular precursor that are K19+, overall show a higher transformation as well as metastatic abilities (Bhagirath et al. 2015). This susceptibly of K19+ cells might be entirely governed by the nature of genes that is expressed by the cell type and may be further affected by the oncogene expressed by these cells that make metastasis faster or late (Bhagirath et al. 2015). Further investigation in to the gene expression changes in a K19+ cellular precursor, would warrant a better understanding of role of these cells in metastasis and provide for likely management of metastatic disease by therapeutically targeting these cell types.

Our findings also highlight an important observation that, K19- cellular precursor as we know from literature do not form the major proportion of BC as compared to K19+ cells. These cells may have a lesser likelihood of getting transformed *in-vivo* and in event of transformation, these cells may have a lesser flexibility in modulating their EMT phenotypes as opposed to K19+ cells. Therefore, these cell types overall have lesser susceptibility for tumor or metastasis formation. In conclusion we observed that the intrinsic susceptibilities of different cell types govern the nature and characteristics of tumors resulting from them.

CHAPTER 5

Summary and Conclusions

Breast cancer is heterogeneous disease and is divided in to various subtypes. Gene expression analysis has allowed classification of breast tumors in following subtype: Luminal-like, ErbB2 over-expressing, basal-like, claudin-low (Prat et al., 2010; Sorlie et al., 2001). These and more recent analysis have emphasized the importance of oncogenic alterations with breast cancer pathogenesis (TCGA, 2012; Banerji et al., 2012; Sorlie et al., 2001; Stephens et al. 2012). Particularly, each subtype is associated with certain gene changes such as TP53 mutation that is commonly found in all subtypes (Sorlie et al., 2001). Likewise, luminal subtype is characterized by presence of PI3KCA mutations, ErbB2 over-expression in ErbB2 subtype and EGFR over-expression is observed in basal like BC. Furthermore, these subtypes also have characteristic gene signatures that correspond to that of the cell lineages within the mammary gland i.e. the luminal or basal cells (Perou et al., 2000). Cell of origin in which the initiating oncogenic transformation occurs plays an important role in determining of breast subtype formation (Ince et al., 2007; Keller et al., 2012).

In this thesis, my major focus was to identify and understand the contributions of both the cell type as well as oncogene(s) in determining BC pathogenesis. I utilized immortalized stem/progenitor cell lines designated as K5+/K19- and K5+/K19+ cells (Zhao et al. 2010) as cellular models to study BC development. These cellular precursors were derived from same normal reduction mammoplasty sample and therefore provided isogenic cell lines to study development of disease from two different cell type from same individual. We over-expressed oncogenes specific to different subtype including : mp53, mRas, mPI3K, wtErbB2 or wtEGFR ectopically in K5+/K19- and K5+/K19+ cells. Combination of triple oncogene(s)/tumor-suppressor – mRas/mp53/wtErbB2 or mRas/mp53/wtEGFR were efficient in completely transforming these immortalized normal K5+/K19- and K5+/K19+ cells (Bhagirath et al. 2015) as

shown by different *in-vitro* assay as well as led to generation of primary and metastatic tumors from the transformed cell lines.

Xenograft tumors formed by these cells were histologically heterogeneous, with variable proportions of luminal, basal-like and claudin-low type components depending on the cell types and oncogene combinations. Various tumor associated characteristics such as onset or incidence of primary and metastatic tumors were found to be determined by both the cell type and oncogenes combination that it expresses. Notably, K5+/K19- cells transformed with mRas/mp53/wtEGFR combination had a significantly longer latency for primary tumor development than all other cell lines, but were observed to have more lung metastasis incidence than same cells (K5+/K19-) expressing mRas/mp53/wtErbB2. K5+/K19+ cells with either oncogene combination i.e. mRas/mp53/wtErbB2 or mRas/mp53/wtEGFR overall exhibit shorter primary tumor latency, and possess a higher metastatic potential than K5+/K19- cells, suggesting that these K19+ progenitors are more susceptible to oncogenesis and metastasis (Bhagirath et al. 2015).

In order to understand the differences in the tumor characteristics for different cell type/oncogene combination, I further performed microarray analysis of the primary and metastatic tumors from each combination. K5+/K19- derived primary tumors were observed to have overall higher expression of EMT markers and transcription factors than K5+/K19+ derived tumors. Particularly, K5+/K19- expressing mRas/mp53/wtErbB2 have even higher expression of EMT markers than same cells expressing mRas/mp53/wtEGFR, suggesting a probable effect of oncogene ErbB2 in mediating more EMT than EGFR in K5+/K19- cells. We further observed an up-regulated expression of patient derived metastasis related gene signatures (Minn et al., 2005) in primary from K5+/K19+ expressing mRas/mp53/wtEGFR combination. Likewise, the

metastatic tumors from the same combination had a lower EMT gene expression and more epithelial like phenotype. These results are in concordance with the known literature on markers for metastatic disease and further explained lower metastasis latency and higher incidence observed for this combination. Additionally, the results from microarray analysis also suggested that expression of EMT markers does not necessarily suggest higher metastasis from these primary tumors. Analysis of gene expression from metastatic tumors showed up-regulation of amino acid transporter SLC6A14. SLC6A14 is involved in amino acid metabolism and its higher expression at metastatic sites suggest an important role of this molecule in driving colonization of disseminated primary tumors cells.

We lastly tested the role of oncogene combination mRas/mp53/mPI3K in driving tumorigenesis from K5+/K19- and K5+/K19+ cells. As observed previously for mRas/mp53/wtErbB2 or mRas/mp53/wtEGFR, oncogene combination mRas/mp53/mPI3K also completely transformed K5+/K19- and K5+/K19+ cells and allowed tumor formation from either cell types. Importantly, PI3K oncogene shows differential effect in mediating EMT phenotype in K5+/K19- and K5+/K19+ cells. K5+/K19- cells show complete EMT morphology upon over-expression, while K5+/K19+ cells have a mixed epithelial and EMT morphology. PI3K induced EMT morphology led to loss of ability to form polarized acini in matrigel and show an up-regulated $CD44^{High}$, $CD24^{Low}$ cell population as compared to K5+/K19+ cells. Tumors from either cell type expressing mRas/mp53/mPI3K were also distinct from each other, with K19- forming spindle like metaplastic carcinomas, while those from K19+ cells were mixture of metaplastic carcinomas and adenocarcinomas. Importantly, when we isolated and analyzed tumor cell lines from either combination we observed that these cells possess differential CK expression thereby suggesting, that transformation of K19- cells with

PI3K oncogene conferred EMT phenotype that is maintained by these cells. Together these results suggested that cell types K5+/K19- or K5+/K19+ cells have different susceptibility to undergo EMT upon oncogenic transformation. Analysis of gene expression inherent in the parental cell lines showed a higher expression of EMT related markers in K19- cells as compared to K19+ cells, thereby providing some explanation for increased susceptibility of these cells to form EMT like tumors.

Taken together, we observed that different cell types derived from same specimen possess distinct abilities to form primary or metastatic tumors and that depends both on the intrinsic nature of these cells as well the oncogene that transformed the cells. Given the clinical relevance of K19 expression in breast tumors and CTCs (Janni et al.,2016; Kabir et al. 2014) and there increased ability to show metastasis in our tumor models, future direction would be to analyze pathways associated with differentially expressed genes present in K19 positive primary or metastatic tumors. Besides, understanding the contribution of K19 expression itself and its role in driving increased tumor or metastasis would be important to identify gene targets that would allow therapeutic intervention of advanced breast cancer disease.

CONCLUSIONS

- Over-expression of oncogene combination mRas/mp53/mPI3K, mRas/mp53/wtErbB2 or mRas/mp53/wtEGFR leads to complete *in-vitro* transformation of immortalized stem/progenitor cell lines K5+/K19- and K5+/K19+ cells.
- mRas/mp53/wtErbB2 or mRas/mp53/wtEGFR transformed K5+/K19- and K5+/K19+ cells form heterogeneous tumors in mice that distinct possess luminal-like, basal-like and claudin-low component.
- Tumor characteristics such as latency and incidence of primary tumor depend both on the nature of cell type as well as the transforming oncogene.
- Primary tumors derived from transformed K5+/K19- cells overall possess higher EMT gene expression than those from K5+/K19+ cells.
- K5+/K19+ mRas/mp53/wtEGFR combination have up-regulated metastasis gene signature explaining the increased susceptibility of these cell/oncogene combination in driving early metastasis.
- K5+/K19- or K5+/K19+ cells show distinct EMT phenotypes upon oncogenic transformation by mRas/mp53/mPI3K combination.
- K5+/K19- cells have increased susceptibility to undergo EMT upon transformation than K5+/K19+ cells.

CHAPTER 6

APPENDIX

Role of matrix derived mechanical stiffness in driving tumor progression

6.1 INTRODUCTION

Breast cancer is a heterogeneous disease. Molecular profiling of patient tumors has led to identification of different subtypes of breast cancers which exhibit significantly different survival outcomes (Prat et al., 2010; Sorlie et al., 2001). Thus, understanding the biology and defining the origin of various subtypes of breast cancer is a significant area of research. Major part of my thesis has been focused on investigating the contribution of cell types and genetic alterations in determining breast tumor pathogenesis (described in chapter 2-5). In addition to this, I also examined the role of matrix derived mechanical stiffness in regulating breast tumor subtype and progression. A major fraction of human mammary gland is composed of the stromal tissue that includes ECM proteins, fibroblast and other stromal cells. The ECM provides both biochemical as well as mechanical context to the cells of mammary gland (Gjorevski and Nelson 2011). It has been long known in literature that density of the mammary gland is a strong independent risk factor for development of breast cancer. Correlative studies have shown that women with 75% or even denser breast tissue are at an increased risk of developing breast cancer than those with less dense tissue (Boyd et al., 2007; Martin and Boyd, 2008). High MD is associated with increased deposition of stromal collagen and other ECM proteins, thereby suggesting that the microenvironment in these mammary glands is altered and it is expected to be mechanically stiffer than those with low MD (Alowami et al., 2003; Guo et al., 2001). Furthermore, ECM gene signatures are also shown to determine the clinical outcomes for breast cancer patients (Bergamaschi et al., 2008). Besides ECM proteins, tumor microenvironment consists of several stromal cells that secrete growth factors and other paracrine signals in order to maintain the tumorigenicity of cells (Lu et al. 2012). Importance of matrix stiffness in driving pro-tumorigenic behavior was recently found to be associated with cancer associated fibroblasts (CAFs), where activation of mechano-regulated transcriptional factor YAP

occurs in response to stiffer matrix, which further promotes a feed forward loop that sustains matrix stiffness and subsequent activation of CAFs (Calvo et al. 2013). In addition matrix stiffness is also shown to promote *in-vitro*, malignant phenotypes (Chaudhuri et al., 2014; Paszek et al., 2005; Provenzano et al., 2009). Matrix derived mechanical forces in dense mammary glands therefore play an important role in driving tumor progression.

Vast literature supports the notion that stem cell behavior is regulated by their interaction with the niche that is composed of cells as well as the ECM. ECM is a biochemical as well as mechanical modulator of cells; while significant research is directed at biochemical cues from niche ECM, little is known about how mechanical properties of ECM modulate CSCs, despite a known clinical correlation of increased breast stiffness with cancer risk (Bertrand et al., 2013; Boyd et al., 2007). Previous studies suggest that matrix stiffness can determine and direct generation of different lineages from an uncommitted mesenchymal stem cell (Boyd et al., 2007). It is therefore possible that the stiffer microenvironment of the breast tumor tissue can drive pathogenesis of a particular subtype. Consistent with this notion, high MD (i.e. stiffer breast tissue) is a strong risk factor for development of breast cancer and high stiffness correlates with development of aggressive and invasive type of breast tumors in younger women (<50 years)(Bertrand et al. 2013)

Increased matrix stiffness has also been shown to promote invasive and proliferative behavior of cells *in vitro* (Chaudhuri et al., 2014; Paszek et al., 2005; Provenzano et al., 2009). Together these findings suggest that matrix generated mechanical forces in association with other ECM components may regulate the pathogenesis of breast cancer towards more aggressive basal-like subtype. This subtype of breast cancer comprise of 15% of all breast tumors and presents significantly poor survival of patients in comparison with other subtypes. Given the following

association of increased stiffness with disease pathogenesis, we sought to examine the role of extracellular mechanical forces to drive breast cancer progression and tumor subtype by utilizing artificially generated substrates of varying mechanical stiffness in collaboration with Dr. Sangjin Ryu, Assistant Professor, Dept. of Mechanical and Materials Engineering, UNL. We observed that high mechanical stiffness from the matrix promotes EMT in cancer cells and it regulates the differentiation potential of transformed stem/progenitor cells.

6.2 MATERIALS AND METHODS

Controlled polyacrylamide gel substrates of varying elastic moduli or stiffness

PA gel substrates of different elastic strength were prepared according to the published protocols (Lakins et al., 2012; Tse and Engler 2010). Briefly acrylamide and bis-acrylamide are allowed to polymerize in different proportions and cross-linked on a glass coverslip. Upon polymerization elastic strength of each gel substrate was quantified using AFM. Softer gels with elastic moduli <0.4kPa will have stiffness values closer to physiologically normal mammary gland while the rigid polyacrylamide gels having elastic moduli >4kPa will be considered as stiffer and would represent a tumor like condition for the cells (Paszek et al., 2005). In order to allow attachment of cells to these gel substrates were functionalized with a very thin layer of ECM proteins present as mixture (Matrigel from BD-Bioscience) or individually (Collagen, Fibronectin, Laminin) (Lakins et al. 2012). Briefly, glass coverslip with gel substrates were treated with bi-functional cross-linker Sulpho SANPAH that was linked to acrylamide in a UV crosslinker at 594nm wavelength, followed by washing with NaOH and HEPES buffer. These were then incubated overnight at 4^{o}C in matrigel solution prepared in NaOH and HEPES buffer. After 24hrs coverslips were treated with glycine solution for 1hr at room temperature, followed by washing in PBS. These were then equilibrated with α-MEM and DMEM (1:1) medium at 37^{o}C till cells were plated on the gels (Lakins et al. 2012).

Cell lines and retroviral/lentiviral infection

Mutant p53^{R249S} (mp53) in pLENTI-6 (purchased from Addgene) along with Invitrogen packaging vector (ViraPowerTM Lentiviral Packaging MIX) were transfected

into 293FT packaging cells. Lentiviral supernatants were collected after overnight incubation in fresh DMEM media. TSA54 packaging cells were transfected with retroviral constructs, mutant H-Ras ^{Q61L} (mRas) in pBABE-hygro or wild type EGFR (wtEGFR) in pMSCV-puro vector, together with PIK plasmid for packaging, and viral supernatants were collected (as mentioned above for lentiviral). $K5^{+}/K19^{+}$ stem/progenitor cell lines were infected with viral supernatants to generate cell lines with different gene combinations followed by their selection in DFCI-1 medium (Band and Sager, 1989) containing hygromycin (15ul/ml) (for mutant H-Ras), blasticidine (15ul/ml) (for mutant p53), puromycin (0.5ul/ml) (for wild type EGFR). Breast cancer cell lines MCF-7, T47D, MDA-MB231 and MDA-MB468 were cultures in α-MEM growth medium as described previously (Zhao et al., 2008).

Antibodies

The following antibodies were used for western blotting and immunofluorescence: specific mouse anti- human α-smooth muscle actin (SMA) (sc-32251) was from Santa Cruz Biotechnology. Mouse anti-human MUC1 (550486) and rat anti-human CD49f (555734) were from BD Bioscience. Mouse monoclonal anti-human E-Cadherin (E4.6) antibody.

Immunoflourescence

Transformed stem or breast cancer cells were cultured for 14 days on gel substrates of different stiffness, following which they were fixed with freshly prepared 10% paraformaldehyde for 10mins. Protocol for immunofluorescence as described (Debnath et al., 2003). Briefly formalin fixed cells were washed with 0.1M glycine for

30mins, followed by blocking with 10% goat serum for 1 hr. These were then stained with rabbit anti-CD49f, and mouse anti-MUC1 antibodies. Goat anti-rat alexa 594 and goat anti-mouse alexa 488 conjugated secondary antibodies (Invitrogen) were used for staining. The sections were mounted with anti-fade mounting media. Images were taken with fluorescence microscope (Zeiss axioplan 2 imaging microscope).

6.3 RESULTS

Growth of different breast cancer cell lines on gel substrates of varying mechanical stiffness

Mechanical stiffness from the ECM has been shown to promote malignant phenotypes of epithelial cells (Chaudhuri et al., 2014; Paszek et al., 2005; Provenzano et al., 2009). To standardize cancer cells culture on PA gel substrates of varying mechanical strength, we assessed growth of different breast cancer cell lines including MCF-7, T47D (representative of Luminal subtype), MDA-MB 468 (Basal-like) and MDA-MB231 (claudin-low) (neve,) on PA gel substrates coated with matrigel and having a range of stiffness values from 0.2 or 0.4kPa (Low), 1 or 2.55 kPa (Intermediate), 4.0 kPa, 10.6 kPa and 40.4 kPa (High) (Tse and Engler 2010). The proliferation of these cells varied with the mechanical stiffness of the gel. Lower stiffness condition (0.4 kPa) promotes formation of growth arrested acini in MCF-7 and T47D cells and rounded morphology for MDA-MB468, MDA-MB231 cells (Figure 6.1). At higher mechanical stiffness all the breast cancer cells showed higher proliferation (Figure 6). Besides increased proliferation, cells tend to spread more on to the gel surface at higher stiffness and show an EMT like morphology (Figure 6.1). These results are in agreement with the previous findings where human mammary epithelial cells (hMECs) also showed a similar increase in proliferation at higher mechanical stiffness (Provenzano et al., 2009).

Figure 6.1: *In-vitro* culture of different breast cancer cells on PA gel of varying stiffness.

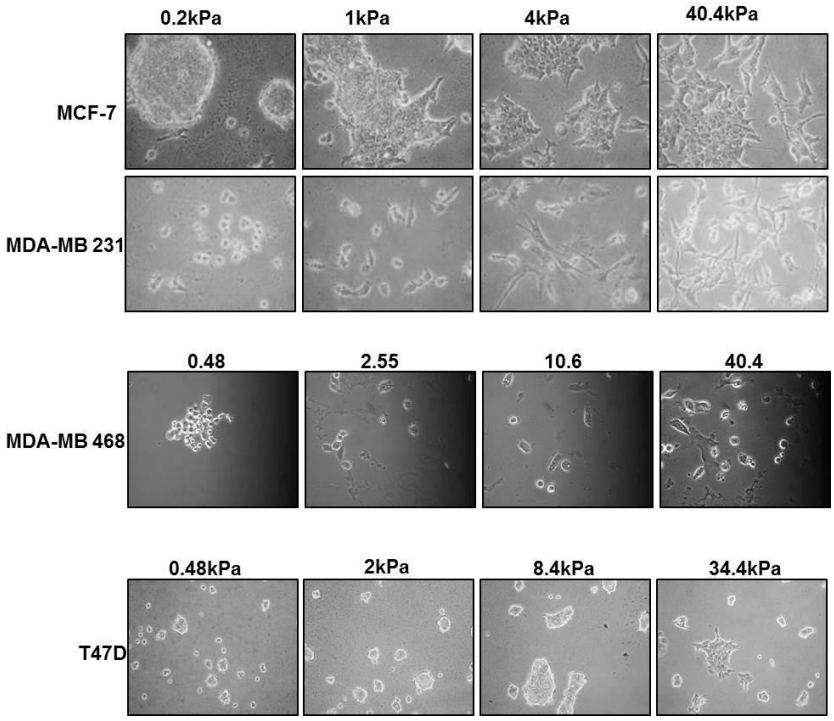

Figure 6.1: *In-vitro* culture of different breast cancer cells on PA gel of varying stiffness. Representative images of MCF-7, MDA-MB231, MD-MB468 and T47D breast cancer cells that were grown on- low (0.2kPa, 0.4kPa), intermediate (1kPa, 2.55kPa) and high (4.0kPa, 8.4kPa, 10.6kPa, 34.4kPa or 40.4kPa) mechanical stiffness. Cell images taken at magnification 20X show variation in cell growth at different stiffness.

Matrix derived mechanical stiffness drives EMT like phenotype in cultured breast cancer cells

We further confirmed if the breast cancer lines besides showing phenotypic EMT at high mechanical stiffness also undergo changes in the expression of EMT markers. Analyses of E-Cadherin expression in MCF-7 cells cultured at different (0.2, 1, 4 and 40kPa) stiffness by immunofluorescence, showed an overall decrease in expression of E-Cadherin at higher mechanical stiffness thereby suggesting a role of stiffness in modulating expression of EMT markers (Figure 6.2). We further verified these results by assessing protein expression of EMT markers by western blotting. We observed down-regulation of E-Cadherin levels at higher stiffness (40kPa) in MCF-7 cells (Figure 6.3A, 6.3C). Accordingly, an increase in expression of α-SMA was observed in both MCF-7 and MDA-MB231 cells with increase in mechanical stiffness (Figure 6.3A, 6.3B and 6.3D). Together these results suggest that increasing mechanical stiffness induces EMT in cancer cell lines.

Figure 6.2: High mechanical stiffness promotes EMT in breast cancer cells.

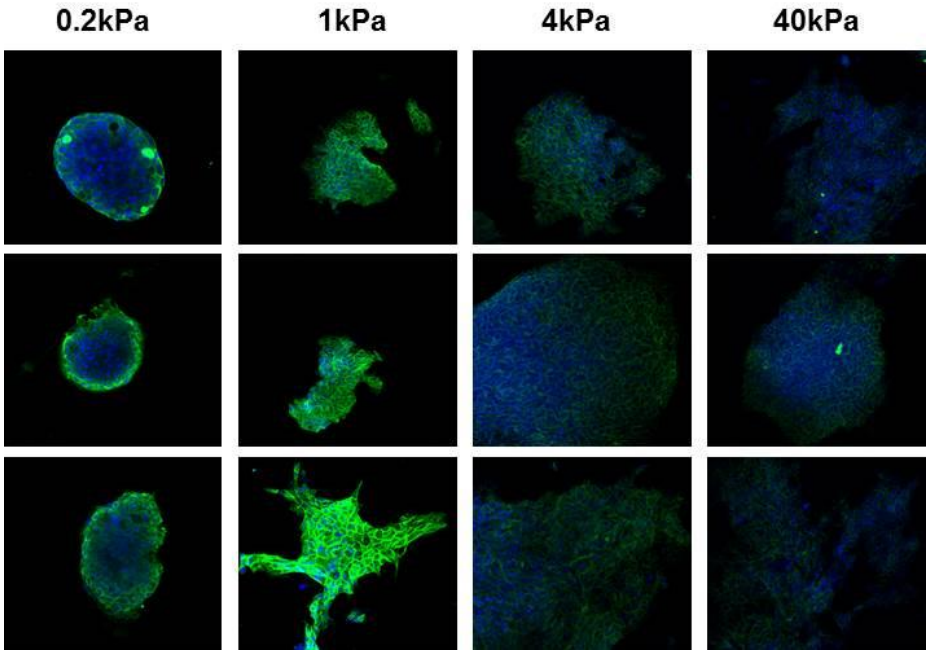

Figure 6.2: High mechanical stiffness promotes EMT in breast cancer cells.

MCF7 cells growing on different stiffness were fixed after 12 days in culture and immunostained with anti-E-Cadherin antibody. DAPI (Blue) shows the nucleus. Images taken at magnification 20X show a gradual decrease in E-Cadherin expression with increasing stiffness.

Figure 6.3: High mechanical stiffness promotes EMT in breast cancer cells.

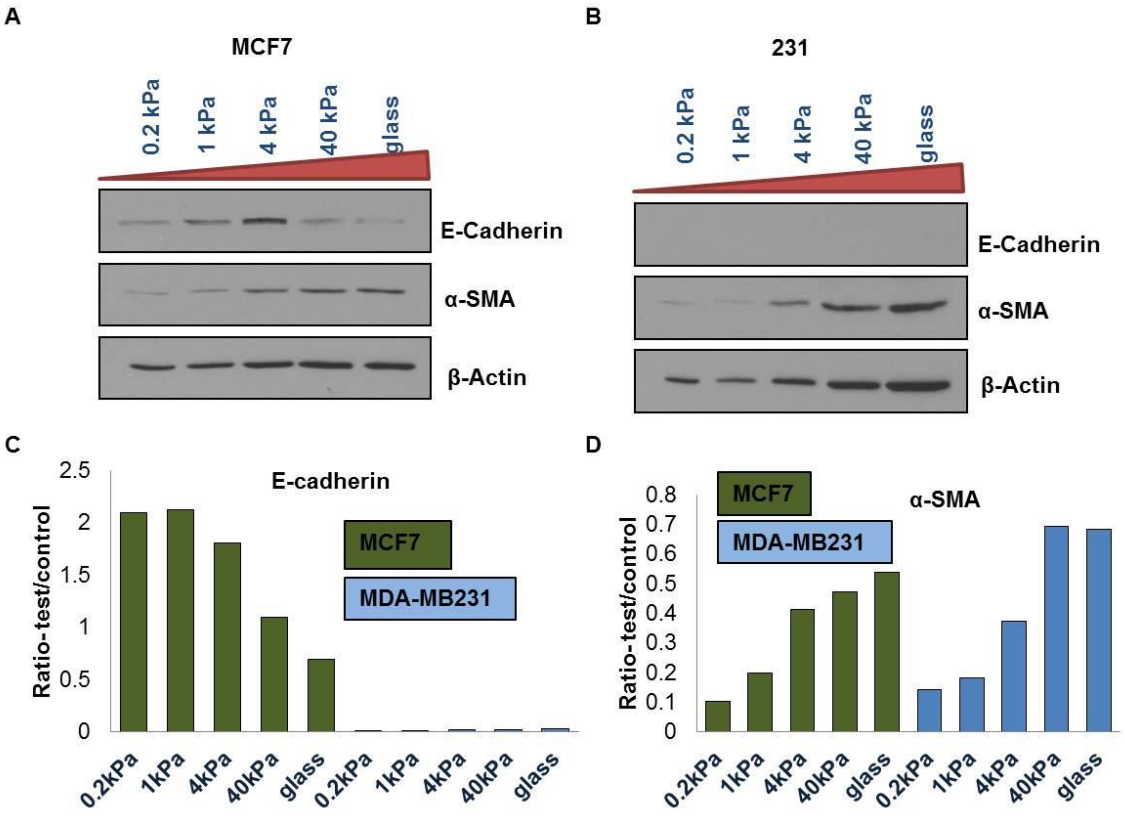

Figure 6.3: High mechanical stiffness promotes EMT in breast cancer cells.

A), B) Western blotting showing expression of EMT markers: E-Cadherin and α-SMA in A) MCF-7 cells and B) MDA-MB231 cells cultured at stiffness- 0.2kPa, 1kPa, 4kPa, 40kPa and glass (cells on coverslip). β-actin was used as loading control for western blotting. C), D) Quantitative representation of E-Cadherin and α-SMA expression in MCF-7 and MDA-MB231 cells as assessed from western blotting experiment.

High mechanical stiffness from matrix promotes self-renewal of transformed stem/progenitor cells

We further tested the effect of varying stiffness in regulating stem/progenitor cell line K5+/K19+ transformed by oncogene combination mRas/mp53/wtEGFR. It has been recently shown, that human mammary progenitor exhibit increased differentiation in to either luminal or myoepithelial lineages when cultured under low or high stiffness conditions respectively (Lui et al. 2012). Therefore, we tested the effect of high and low matrix stiffness in controlling differentiation from transformed stem/progenitor cells. As expected from our previous observation, transformed K5+/K19+ cells exhibit differences in cell growth at low and high stiffness, showing formation of growth arrested acini structure at low stiffness and an overall higher cell proliferation at high stiffness (Figure 6.4A). In addition, when we stained these cells with MUC1 (luminal differentiation marker) and CD49f (stem cell marker), we observed that transformed K5+/K19+ cells show a higher MUC1 differentiation at lower stiffness (0.48kPa and 2.55kPa) (Figure 6.4B), whereas the cells at higher stiffness showed a low MUC1 expression, suggesting a decreased differentiation of transformed progenitor at high stiffness (10.55kPa and 40kPa) (Figure 6.4B).

Figure 6.4: High mechanical stiffness promotes self-renewal of transformed stem/progenitor cells.

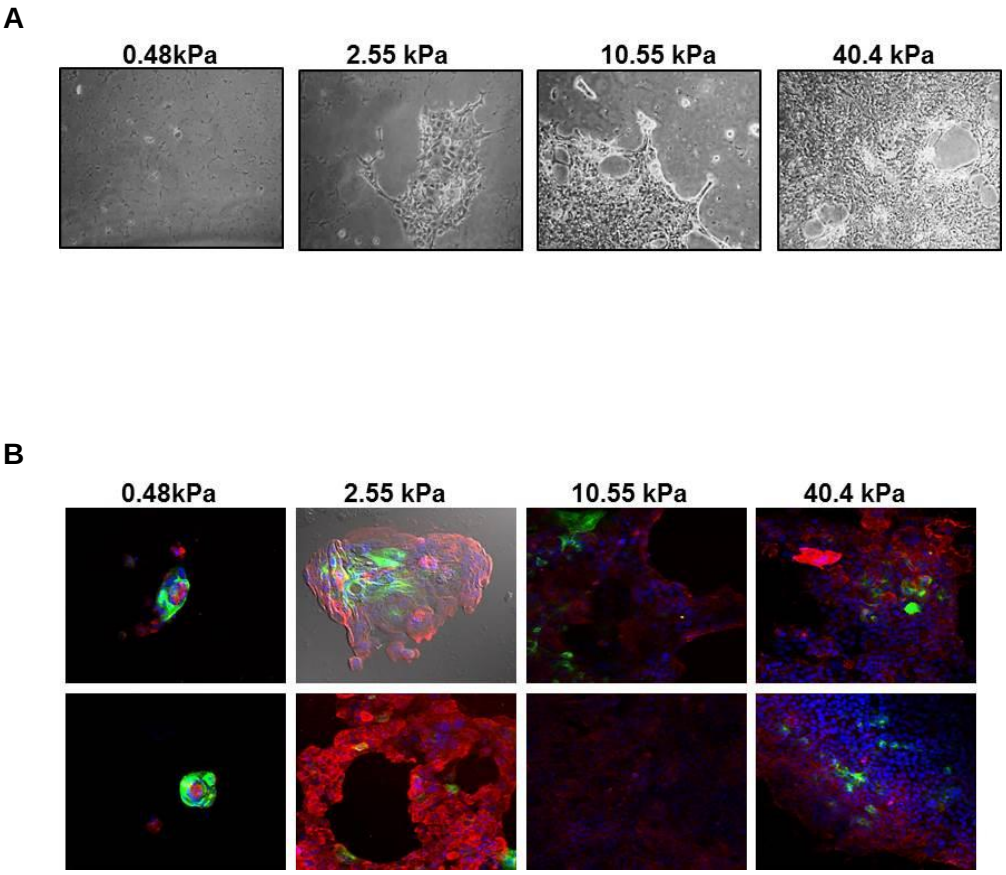

Figure 6.4: High mechanical stiffness promotes self-renewal of transformed stem/progenitor cells. A) Representative images of mRas/mp53/wtEGFR transformed K5+/K19+ cells that were grown on- low (0.48kPa, 2.55kPa), and high (4.0kPa, 8.4kPa, 10.55kPa or 40.4kPa) mechanical stiffness. Cell images taken at magnification 20X show variation in cell growth at different stiffness. B) Immunoflourscence staining of transformed stem/progenitor with antibodies anti-MUC1 (green) and anti-CD49f (red) cultured at different stiffness. Representative images taken at magnification 20X are shown.

6.4 DISCUSSION

Tumor progression is characterized by several changes in ECM and stromal compartment of tumor including increased expression of many matrix protein- collagens, laminin etc, infiltration of fibroblast and immune cells (Butcher et al., 2009). Together these changes facilitate dissemination of tumor cells from the primary site in to the blood vessels. Increased matrix stiffness in the primary tumor site promotes breast tumorigenesis (Levental et al., 2009; Provenzano et al., 2008). High stiffness has been shown to enhance malignant phenotypes from hMECS (Chaudhuri et al., 2014; Paszek et al., 2005; Provenzano et al., 2009) and also contributes towards activation of signaling pathways that promote proliferation (Provenzano et al., 2009). In accordance to these finding we also observed an increased proliferation of breast cancer cell lines and transformed stem/progenitor cells at high mechanical stiffness (Figure 6.1, 6.4A). We further observed that cells also acquired an EMT like morphology at high stiffness. Upon analysis, we observed changes in expression of EMT makers (Figure 6.3) at higher stiffness. Our results are concordance with the recent study done by Wei et al. where they also showed a similar effect of high mechanical stiffness in inducing EMT in transformed cells. Together these results emphasize a tumor promoting behavior of ECM derived stiffness, whereby matrix stiffness contributes to progression of tumor by facilitating changes such as EMT that would allow tumors cells to disseminate from their primary site.

Other studies have shown that mechanical stiffness from the substrate can control the differentiation of a normal mesenchymal stem cell (Engler et al., 2006). These functions of stiffness extend to stem cells derived from tissues of different origin such as neural and muscle stem cells (Gilbert et al., 2010; Keung et al. 2011). Matrix stiffness can regulate both self-renewal and differentiation of the muscle stem cell (Gilbert et al. 2010). It was recently shown that human mammary progenitor exhibit

increased differentiation in to either luminal or myoepithelial lineages when cultured under low or high stiffness conditions respectively (Lui et al. 2012). Taken together these findings strongly support stem cell regulator function of the stiffness. Furthermore mechanical stiffness has been also shown to affect retinoic acid induced differentiation in neuroblastoma cells. High matrix stiffness in the presence of retinoic acid promotes differentiation of neural cancer cells and leads to reduction of oncogenic transcription factor N-Myc (Lam et al. 2010). Altogether these studies suggest that ECM stiffness have the ability to regulate differentiation under both normal and transformed conditions and can therefore also regulate tumor phenotype. We observed a reduction in the differentiation ability of transformed stem/progenitor as seen by decreased MUC1 expression at high mechanical stiffness (Figure 6.4B). Tumor microenvironment undergoes changes in the stiffness of matrix as the disease progresses (Butcher et al., 2009; Lu et al. 2012). Moreover, it has also been observed in patient tumors that different subtypes have variable stiffness with aggressive tumors having higher stiffness than other subtype (Chang et al. 2013). Basal subtype of BC is characterized by presence of stem cell like gene signature, which suggests a stem cell origin of these tumors.

Given these results and our observation, it is likely that higher stiffness regulates the CSCs in basal like tumors towards a less differentiated phenotype and together with induction of EMT in cells high mechanical stiffness might contribute towards the aggressive behavior of these tumors. Further assessment of effect of mechanical forces on CSCs in terms of their functional properties in-vivo with respect to tumor subtype formation would allow better understanding on etiology of basal like breast tumors and would be useful in devising targeted therapies to treat this aggressive subtype of BC.

REFERENCES

Comprehensive molecular portraits of human breast tumours. (2012) Nature *490*, 61-70.

Al-Hajj, M., Wicha, M.S., Benito-Hernandez, A., Morrison, S.J., and Clarke, M.F. (2003). Prospective identification of tumorigenic breast cancer cells. (2003) Proc Natl Acad Sci U S A *100*, 3983-3988.

Alcaraz, J., Xu, R., Mori, H., Nelson, C.M., Mroue, R., Spencer, V.A., Brownfield, D., Radisky, D.C., Bustamante, C., and Bissell, M.J. (2008). Laminin and biomimetic extracellular elasticity enhance functional differentiation in mammary epithelia. EMBO J *27*, 2829-2838.

Allinen, M., Beroukhim, R., Cai, L., Brennan, C., Lahti-Domenici, J., Huang, H., Porter, D., Hu, M., Chin, L., Richardson, A.*, et al.* (2004). Molecular characterization of the tumor microenvironment in breast cancer. Cancer Cell *6*, 17-32.

Alowami, S., Troup, S., Al-Haddad, S., Kirkpatrick, I., and Watson, P.H. (2003). Mammographic density is related to stroma and stromal proteoglycan expression. Breast Cancer Res *5*, R129-135.

Babu, E., Bhutia, Y.D., Ramachandran, S., Gnanaprakasam, J.P., Prasad, P.D., Thangaraju, M., and Ganapathy, V. (2015) Deletion of the amino acid transporter Slc6a14 suppresses tumour growth in spontaneous mouse models of breast cancer. Biochem J *469*, 17-23.

Band, V. (2003). In vitro models of early neoplastic transformation of human mammary epithelial cells. Methods Mol Biol *223*, 237-248.

Band, V., and Sager, R. (1989). Distinctive traits of normal and tumor-derived human mammary epithelial cells expressed in a medium that supports long-term growth of both cell types. Proc Natl Acad Sci U S A *86*, 1249-1253.

Band, V., Zajchowski, D., Kulesa, V., and Sager, R. (1990). Human papilloma virus DNAs immortalize normal human mammary epithelial cells and reduce their growth factor requirements. Proc Natl Acad Sci U S A *87*, 463-467.

Banerji, S., Cibulskis, K., Rangel-Escareno, C., Brown, K.K., Carter, S.L., Frederick, A.M., Lawrence, M.S., Sivachenko, A.Y., Sougnez, C., Zou, L.*, et al.* (2012) Sequence analysis of mutations and translocations across breast cancer subtypes. Nature *486*, 405-409.

Bartek, J., Taylor-Papadimitriou, J., Miller, N., and Millis, R. (1985). Patterns of expression of keratin 19 as detected with monoclonal antibodies in human breast tissues and tumours. Int J Cancer *36*, 299-306.

Bergamaschi, A., Tagliabue, E., Sorlie, T., Naume, B., Triulzi, T., Orlandi, R., Russnes, H.G., Nesland, J.M., Tammi, R., Auvinen, P.*, et al.* (2008). Extracellular matrix signature identifies breast cancer subgroups with different clinical outcome. J Pathol *214*, 357-367.

Bertrand, K.A., Tamimi, R.M., Scott, C.G., Jensen, M.R., Pankratz, V.S., Visscher, D., Norman, A., Couch, F., Shepherd, J., Fan, B.*, et al.* (2013) Mammographic density and risk of breast cancer by age and tumor characteristics. Breast Cancer Res *15*, R104.

Bhagirath, D., Zhao, X., West, W.W., Qiu, F., Band, H., and Band, V. (2015) Cell type of origin as well as genetic alterations contribute to breast cancer phenotypes. Oncotarget *6*, 9018-9030.

Bidard, F.C., Mathiot, C., Degeorges, A., Etienne-Grimaldi, M.C., Delva, R., Pivot, X., Veyret, C., Bergougnoux, L., de Cremoux, P., Milano, G.*, et al.* (2010) Clinical value of circulating endothelial cells and circulating tumor cells in metastatic breast cancer patients treated first line with bevacizumab and chemotherapy. Ann Oncol *21*, 1765-1771.

Boyd, N.F., Guo, H., Martin, L.J., Sun, L., Stone, J., Fishell, E., Jong, R.A., Hislop, G., Chiarelli, A., Minkin, S.*, et al.* (2007). Mammographic density and the risk and detection of breast cancer. N Engl J Med *356*, 227-236.

Brandt, R., Eisenbrandt, R., Leenders, F., Zschiesche, W., Binas, B., Juergensen, C., and Theuring, F. (2000). Mammary gland specific hEGF receptor transgene expression induces neoplasia and inhibits differentiation. Oncogene *19*, 2129-2137.

Bresnick, A.R., Weber, D.J., and Zimmer, D.B. (2015) S100 proteins in cancer. Nat Rev Cancer *15*, 96-109.

Butcher, D.T., Alliston, T., and Weaver, V.M. (2009). A tense situation: forcing tumour progression. Nat Rev Cancer *9*, 108-122.

Calmon, M.F., Jeschke, J., Zhang, W., Dhir, M., Siebenkas, C., Herrera, A., Tsai, H.C., O'Hagan, H.M., Pappou, E.P., Hooker, C.M.*, et al.* (2015) Epigenetic silencing of neurofilament genes promotes an aggressive phenotype in breast cancer. Epigenetics *10*, 622-632.

Calvo, F., Ege, N., Grande-Garcia, A., Hooper, S., Jenkins, R.P., Chaudhry, S.I., Harrington, K., Williamson, P., Moeendarbary, E., Charras, G.*, et al.* (2013) Mechanotransduction and YAP-dependent matrix remodelling is required for the generation and maintenance of cancer-associated fibroblasts. Nat Cell Biol *15*, 637-646.

Cerrito, M.G., Galbaugh, T., Wang, W., Chopp, T., Salomon, D., and Cutler, M.L. (2004). Dominant negative Ras enhances lactogenic hormone-induced differentiation by blocking activation of the Raf-Mek-Erk signal transduction pathway. J Cell Physiol *201*, 244-258.

Charafe-Jauffret, E., Ginestier, C., Iovino, F., Wicinski, J., Cervera, N., Finetti, P., Hur, M.H., Diebel, M.E., Monville, F., Dutcher, J.*, et al.* (2009). Breast cancer cell lines contain functional cancer stem cells with metastatic capacity and a distinct molecular signature. Cancer Res *69*, 1302-1313.

Chang, J.M., Park, I.A., Lee, S.H., Kim, W.H., Bae, M.S., Koo, H.R., Yi, A., Kim, S.J., Cho, N., and Moon, W.K. (2013) Stiffness of tumours measured by shear-wave elastography correlated with subtypes of breast cancer. Eur Radiol *23*, 2450-2458.

Chaudhuri, O., Koshy, S.T., Branco da Cunha, C., Shin, J.W., Verbeke, C.S., Allison, K.H., and Mooney, D.J. (2014) Extracellular matrix stiffness and composition jointly regulate the induction of malignant phenotypes in mammary epithelium. Nat Mater *13*, 970-978.

Cho, R.W., Wang, X., Diehn, M., Shedden, K., Chen, G.Y., Sherlock, G., Gurney, A., Lewicki, J., and Clarke, M.F. (2008). Isolation and molecular characterization of cancer stem cells in MMTV-Wnt-1 murine breast tumors. Stem Cells *26*, 364-371.

Cicalese, A., Bonizzi, G., Pasi, C.E., Faretta, M., Ronzoni, S., Giulini, B., Brisken, C., Minucci, S., Di Fiore, P.P., and Pelicci, P.G. (2009). The tumor suppressor p53 regulates polarity of self-renewing divisions in mammary stem cells. Cell *138*, 1083-1095.

Cleary, A.S., Leonard, T.L., Gestl, S.A., and Gunther, E.J. (2014) Tumour cell heterogeneity maintained by cooperating subclones in Wnt-driven mammary cancers. Nature *508*, 113-117.

Debnath, J., Muthuswamy, S.K., and Brugge, J.S. (2003). Morphogenesis and oncogenesis of MCF-10A mammary epithelial acini grown in three-dimensional basement membrane cultures. Methods *30*, 256-268.

Dexter, D.L., Kowalski, H.M., Blazar, B.A., Fligiel, Z., Vogel, R., and Heppner, G.H. (1978). Heterogeneity of tumor cells from a single mouse mammary tumor. Cancer Res *38*, 3174-3181.

Dimri, G., Band, H., and Band, V. (2005). Mammary epithelial cell transformation: insights from cell culture and mouse models. Breast Cancer Res *7*, 171-179.

Deugnier, M.A., Faraldo, M.M., Janji, B., Rousselle, P., Thiery, J.P., and Glukhova, M.A. (2002). EGF controls the in vivo developmental potential of a mammary epithelial cell line possessing progenitor properties. J Cell Biol *159*, 453-463.

Dontu, G., Abdallah, W.M., Foley, J.M., Jackson, K.W., Clarke, M.F., Kawamura, M.J., and Wicha, M.S. (2003). In vitro propagation and transcriptional profiling of human mammary stem/progenitor cells. Genes Dev *17*, 1253-1270.

Del Pozo Martin, Y., Park, D., Ramachandran, A., Ombrato, L., Calvo, F., Chakravarty, P., Spencer-Dene, B., Derzsi, S., Hill, C.S., Sahai, E*., et al.* (2015) Mesenchymal Cancer Cell-Stroma Crosstalk Promotes Niche Activation, Epithelial Reversion, and Metastatic Colonization. Cell Rep *13*, 2456-2469.

Del Pozo Martin, Y., Park, D., Ramachandran, A., Ombrato, L., Calvo, F., Chakravarty, P., Spencer-Dene, B., Derzsi, S., Hill, C.S., Sahai, E*., et al.* (2015). Mesenchymal Cancer Cell-Stroma Crosstalk Promotes Niche Activation, Epithelial Reversion, and Metastatic Colonization. Cell Rep *13*, 2456-2469.

Elenbaas, B., Spirio, L., Koerner, F., Fleming, M.D., Zimonjic, D.B., Donaher, J.L., Popescu, N.C., Hahn, W.C., and Weinberg, R.A. (2001). Human breast cancer cells generated by oncogenic transformation of primary mammary epithelial cells. Genes Dev *15*, 50-65.

Ellis, M.J., Ding, L., Shen, D., Luo, J., Suman, V.J., Wallis, J.W., Van Tine, B.A., Hoog, J., Goiffon, R.J., Goldstein, T.C*., et al.* (2012) Whole-genome analysis informs breast cancer response to aromatase inhibition. (2012) Nature *486*, 353-360.

Engler, A.J., Sen, S., Sweeney, H.L., and Discher, D.E. (2006). Matrix elasticity directs stem cell lineage specification. Cell *126*, 677-689.

Fidler, I.J. (1978). Tumor heterogeneity and the biology of cancer invasion and metastasis. Cancer Res *38*, 2651-2660.

Georgoulias, V., Bozionelou, V., Agelaki, S., Perraki, M., Apostolaki, S., Kallergi, G., Kalbakis, K., Xyrafas, A., and Mavroudis, D. (2012) Trastuzumab decreases the incidence of clinical relapses in patients with early breast cancer presenting chemotherapy-resistant CK-19mRNA-positive circulating tumor cells: results of a randomized phase II study. Ann Oncol *23*, 1744-1750.

Ginestier, C., and Wicha, M.S. (2007). Mammary stem cell number as a determinate of breast cancer risk. Breast Cancer Res *9*, 109.

Giuliano, M., Giordano, A., Jackson, S., De Giorgi, U., Mego, M., Cohen, E.N., Gao, H., Anfossi, S., Handy, B.C., Ueno, N.T.*, et al.* (2014) Circulating tumor cells as early predictors of metastatic spread in breast cancer patients with limited metastatic dissemination. Breast Cancer Res *16*, 440.

Gilbert, P.M., Havenstrite, K.L., Magnusson, K.E., Sacco, A., Leonardi, N.A., Kraft, P., Nguyen, N.K., Thrun, S., Lutolf, M.P., and Blau, H.M. (2010) Substrate elasticity regulates skeletal muscle stem cell self-renewal in culture. Science *329*, 1078-1081.

Gudjonsson, T., Villadsen, R., Nielsen, H.L., Ronnov-Jessen, L., Bissell, M.J., and Petersen, O.W. (2002). Isolation, immortalization, and characterization of a human breast epithelial cell line with stem cell properties. Genes Dev *16*, 693-706.

Grigoriadis, A., Mackay, A., Reis-Filho, J.S., Steele, D., Iseli, C., Stevenson, B.J., Jongeneel, C.V., Valgeirsson, H., Fenwick, K., Iravani, M.*, et al.* (2006). Establishment of the epithelial-specific transcriptome of normal and malignant human breast cells based on MPSS and array expression data. Breast Cancer Res *8*, R56.

Gjorevski, N., and Nelson, C.M. (2011) Integrated morphodynamic signalling of the mammary gland. Nat Rev Mol Cell Biol *12*, 581-593.

Guo, Y.P., Martin, L.J., Hanna, W., Banerjee, D., Miller, N., Fishell, E., Khokha, R., and Boyd, N.F. (2001). Growth factors and stromal matrix proteins associated with mammographic densities. Cancer Epidemiol Biomarkers Prev *10*, 243-248.

Heppner, G.H. (1984). Tumor heterogeneity. Cancer Res *44*, 2259-2265.

Hicks, D.G., Short, S.M., Prescott, N.L., Tarr, S.M., Coleman, K.A., Yoder, B.J., Crowe, J.P., Choueiri, T.K., Dawson, A.E., Budd, G.T.*, et al.* (2006). Breast cancers with brain metastases are more likely to be estrogen receptor negative, express the basal cytokeratin CK5/6, and overexpress HER2 or EGFR. Am J Surg Pathol *30*, 1097-1104.

Hohensee, I., Lamszus, K., Riethdorf, S., Meyer-Staeckling, S., Glatzel, M., Matschke, J., Witzel, I., Westphal, M., Brandt, B., Muller, V.*, et al.* (2013)Frequent genetic alterations in EGFR- and HER2-driven pathways in breast cancer brain metastases. Am J Pathol *183*, 83-95.

Ignatiadis, M., Xenidis, N., Perraki, M., Apostolaki, S., Politaki, E., Kafousi, M., Stathopoulos, E.N., Stathopoulou, A., Lianidou, E., Chlouverakis, G.*, et al.* (2007). Different prognostic value of cytokeratin-19 mRNA positive circulating tumor cells according to estrogen receptor and HER2 status in early-stage breast cancer. J Clin Oncol *25*, 5194-5202.

Ince, T.A., Richardson, A.L., Bell, G.W., Saitoh, M., Godar, S., Karnoub, A.E., Iglehart, J.D., and Weinberg, R.A. (2007). Transformation of different human breast epithelial cell types leads to distinct tumor phenotypes. Cancer Cell *12*, 160-170.

Janes, P.W., Daly, R.J., deFazio, A., and Sutherland, R.L. (1994). Activation of the Ras signalling pathway in human breast cancer cells overexpressing erbB-2. Oncogene *9*, 3601-3608.

Janni, W.J., Rack, B., Terstappen, L.W., Pierga, J.Y., Taran, F.A., Fehm, T., Hall, C., de Groot, M.R., Bidard, F.C., Friedl, T.W*., et al.* Pooled Analysis of the Prognostic Relevance of Circulating Tumor Cells in Primary Breast Cancer. Clin Cancer Res.

Jehn, B., Costello, E., Marti, A., Keon, N., Deane, R., Li, F., Friis, R.R., Burri, P.H., Martin, F., and Jaggi, R. (1992). Overexpression of Mos, Ras, Src, and Fos inhibits mouse mammary epithelial cell differentiation. Mol Cell Biol *12*, 3890-3902.

Johnson, J.P., Kumar, P., Koulnis, M., Patel, M., and Simin, K. (2014) Crucial and novel cancer drivers in a mouse model of triple-negative breast cancer. Cancer Genomics Proteomics *11*, 115-126.

Kabir, N.N., Ronnstrand, L., and Kazi, J.U. (2014) Keratin 19 expression correlates with poor prognosis in breast cancer. Mol Biol Rep *41*, 7729-7735.

Karunakaran, S., Ramachandran, S., Coothankandaswamy, V., Elangovan, S., Babu, E., Periyasamy-Thandavan, S., Gurav, A., Gnanaprakasam, J.P., Singh, N., Schoenlein, P.V*., et al.* (2011) SLC6A14 (ATB0,+) protein, a highly concentrative and broad specific amino acid transporter, is a novel and effective drug target for treatment of estrogen receptor-positive breast cancer. J Biol Chem *286*, 31830-31838.

Keller, P.J., Arendt, L.M., Skibinski, A., Logvinenko, T., Klebba, I., Dong, S., Smith, A.E., Prat, A., Perou, C.M., Gilmore, H*., et al.* (2012) Defining the cellular precursors to human breast cancer. Proc Natl Acad Sci U S A *109*, 2772-2777.

Kendall, S.D., Linardic, C.M., Adam, S.J., and Counter, C.M. (2005). A network of genetic events sufficient to convert normal human cells to a tumorigenic state. Cancer Res *65*, 9824-9828.

Keung, A.J., de Juan-Pardo, E.M., Schaffer, D.V., and Kumar, S. (2011) Rho GTPases mediate the mechanosensitive lineage commitment of neural stem cells. Stem Cells *29*, 1886-1897.

Kiemer, A.K., Takeuchi, K., and Quinlan, M.P. (2001). Identification of genes involved in epithelial-mesenchymal transition and tumor progression. Oncogene *20*, 6679-6688.

Kim, H., Watkinson, J., Varadan, V., and Anastassiou, D. (2010). Multi-cancer computational analysis reveals invasion-associated variant of desmoplastic reaction involving INHBA, THBS2 and COL11A1. BMC Med Genomics *3*, 51.

Koren, S., and Bentires-Alj, M. Breast Tumor Heterogeneity: Source of Fitness, Hurdle for Therapy. (2015) Mol Cell *60*, 537-546.

Kramer, A., Green, J., Pollard, J., Jr., and Tugendreich, S. (2013). Causal analysis approaches in Ingenuity Pathway Analysis. Bioinformatics *30*, 523-530.

Lam, W.A., Cao, L., Umesh, V., Keung, A.J., Sen, S., and Kumar, S. (2010) Extracellular matrix rigidity modulates neuroblastoma cell differentiation and N-myc expression. Mol Cancer *9*, 35.

Lawson, D.A., Bhakta, N.R., Kessenbrock, K., Prummel, K.D., Yu, Y., Takai, K., Zhou, A., Eyob, H., Balakrishnan, S., Wang, C.Y.*, et al.* (2015) Single-cell analysis reveals a stem-cell program in human metastatic breast cancer cells. Nature *526*, 131-135.

Lakins, J.N., Chin, A.R., and Weaver, V.M. (2012) Exploring the link between human embryonic stem cell organization and fate using tension-calibrated extracellular matrix functionalized polyacrylamide gels. Methods Mol Biol *916*, 317-350.

Levental, K.R., Yu, H., Kass, L., Lakins, J.N., Egeblad, M., Erler, J.T., Fong, S.F., Csiszar, K., Giaccia, A., Weninger, W.*, et al.* (2009). Matrix crosslinking forces tumor progression by enhancing integrin signaling. Cell *139*, 891-906.

Li, M.L., Aggeler, J., Farson, D.A., Hatier, C., Hassell, J., and Bissell, M.J. (1987). Influence of a reconstituted basement membrane and its components on casein gene expression and secretion in mouse mammary epithelial cells. Proc Natl Acad Sci U S A *84*, 136-140.

Lim, E., Vaillant, F., Wu, D., Forrest, N.C., Pal, B., Hart, A.H., Asselin-Labat, M.L., Gyorki, D.E., Ward, T., Partanen, A.*, et al.* (2009). Aberrant luminal progenitors as the candidate

target population for basal tumor development in BRCA1 mutation carriers. Nat Med *15*, 907-913.

Liu, H., Patel, M.R., Prescher, J.A., Patsialou, A., Qian, D., Lin, J., Wen, S., Chang, Y.F., Bachmann, M.H., Shimono, Y.*, et al.* (2010) Cancer stem cells from human breast tumors are involved in spontaneous metastases in orthotopic mouse models. Proc Natl Acad Sci U S A *107*, 18115-18120.

Li, X.Q., Li, L., Xiao, C.H., and Feng, Y.M. (2012) NEFL mRNA expression level is a prognostic factor for early-stage breast cancer patients. PLoS One *7*, e31146.

Livak, K.J., and Schmittgen, T.D. (2001). Analysis of relative gene expression data using real-time quantitative PCR and the 2(-Delta Delta C(T)) Method. Methods *25*, 402-408.

Livasy, C.A., Karaca, G., Nanda, R., Tretiakova, M.S., Olopade, O.I., Moore, D.T., and Perou, C.M. (2006). Phenotypic evaluation of the basal-like subtype of invasive breast carcinoma. Mod Pathol *19*, 264-271.

Lu, P., Weaver, V.M., and Werb, Z. (2012) The extracellular matrix: a dynamic niche in cancer progression. J Cell Biol *196*, 395-406.

Lui, C., Lee, K., and Nelson, C.M. (2012) Matrix compliance and RhoA direct the differentiation of mammary progenitor cells. Biomech Model Mechanobiol *11*, 1241-1249.

Ma, X.J., Dahiya, S., Richardson, E., Erlander, M., and Sgroi, D.C. (2009). Gene expression profiling of the tumor microenvironment during breast cancer progression. Breast Cancer Res *11*, R7.

Mammoto, T., Mammoto, A., and Ingber, D.E. (2013) Mechanobiology and developmental control. Annu Rev Cell Dev Biol *29*, 27-61.

Marcotte, R., Sayad, A., Brown, K.R., Sanchez-Garcia, F., Reimand, J., Haider, M., Virtanen, C., Bradner, J.E., Bader, G.D., Mills, G.B.*, et al.* (2016) Functional Genomic Landscape of Human Breast Cancer Drivers, Vulnerabilities, and Resistance. Cell *164*, 293-309.

Mani, S.A., Guo, W., Liao, M.J., Eaton, E.N., Ayyanan, A., Zhou, A.Y., Brooks, M., Reinhard, F., Zhang, C.C., Shipitsin, M.*, et al.* (2008). The epithelial-mesenchymal transition generates cells with properties of stem cells. Cell *133*, 704-715.

Malanchi, I., Santamaria-Martinez, A., Susanto, E., Peng, H., Lehr, H.A., Delaloye, J.F., and Huelsken, J. (2012) Interactions between cancer stem cells and their niche govern metastatic colonization. Nature *481*, 85-89.

Martin, L.J., and Boyd, N.F. (2008). Mammographic density. Potential mechanisms of breast cancer risk associated with mammographic density: hypotheses based on epidemiological evidence. Breast Cancer Res *10*, 201.

Marusyk, A., Tabassum, D.P., Altrock, P.M., Almendro, V., Michor, F., and Polyak, K. Non-cell-autonomous driving of tumour growth supports sub-clonal heterogeneity. Nature *514*, 54-58.

McLaughlin, S.K., Olsen, S.N., Dake, B., De Raedt, T., Lim, E., Bronson, R.T., Beroukhim, R., Polyak, K., Brown, M., Kuperwasser, C.*, et al.* (2013) The RasGAP gene, RASAL2, is a tumor and metastasis suppressor. Cancer Cell *24*, 365-378.

McCracken, A.N., and Edinger, A.L. Targeting cancer metabolism at the plasma membrane by limiting amino acid access through SLC6A14. (2015) Biochem J *470*, e17-19.

Melchor, L., Molyneux, G., Mackay, A., Magnay, F.A., Atienza, M., Kendrick, H., Nava-Rodrigues, D., Lopez-Garcia, M.A., Milanezi, F., Greenow, K.*, et al.* (2014) Identification of cellular and genetic drivers of breast cancer heterogeneity in genetically engineered mouse tumour models. J Pathol *233*, 124-137.

Michor, F., and Polyak, K. (2011) The origins and implications of intratumor heterogeneity. Cancer Prev Res (Phila) *3*, 1361-1364.

Minn, A.J., Gupta, G.P., Siegel, P.M., Bos, P.D., Shu, W., Giri, D.D., Viale, A., Olshen, A.B., Gerald, W.L., and Massague, J. (2005). Genes that mediate breast cancer metastasis to lung. Nature *436*, 518-524.

Molyneux, G., Geyer, F.C., Magnay, F.A., McCarthy, A., Kendrick, H., Natrajan, R., Mackay, A., Grigoriadis, A., Tutt, A., Ashworth, A.*, et al.* (2010) BRCA1 basal-like breast cancers originate from luminal epithelial progenitors and not from basal stem cells. Cell Stem Cell *7*, 403-417.

Nair, R., Roden, D.L., Teo, W.S., McFarland, A., Junankar, S., Ye, S., Nguyen, A., Yang, J., Nikolic, I., Hui, M.*, et al.* (2014) c-Myc and Her2 cooperate to drive a stem-like phenotype with poor prognosis in breast cancer. Oncogene *33*, 3992-4002.

Ocana, O.H., Corcoles, R., Fabra, A., Moreno-Bueno, G., Acloque, H., Vega, S., Barrallo-Gimeno, A., Cano, A., and Nieto, M.A. (2012) Metastatic colonization requires the repression of the epithelial-mesenchymal transition inducer Prrx1. Cancer Cell *22*, 709-724.

Oda, K., Okada, J., Timmerman, L., Rodriguez-Viciana, P., Stokoe, D., Shoji, K., Taketani, Y., Kuramoto, H., Knight, Z.A., Shokat, K.M.*, et al.* (2008). PIK3CA cooperates with other phosphatidylinositol 3'-kinase pathway mutations to effect oncogenic transformation. Cancer Res *68*, 8127-8136.

Paszek, M.J., Zahir, N., Johnson, K.R., Lakins, J.N., Rozenberg, G.I., Gefen, A., Reinhart-King, C.A., Margulies, S.S., Dembo, M., Boettiger, D.*, et al.* (2005). Tensional homeostasis and the malignant phenotype. Cancer Cell *8*, 241-254.

Perou, C.M., Sorlie, T., Eisen, M.B., van de Rijn, M., Jeffrey, S.S., Rees, C.A., Pollack, J.R., Ross, D.T., Johnsen, H., Akslen, L.A.*, et al.* (2000). Molecular portraits of human breast tumours. Nature *406*, 747-752.

Petersen, O.W., and Polyak, K. (2010) Stem cells in the human breast. Cold Spring Harb Perspect Biol *2*, a003160.

Prat, A., Parker, J.S., Karginova, O., Fan, C., Livasy, C., Herschkowitz, J.I., He, X., and Perou, C.M. (2010) Phenotypic and molecular characterization of the claudin-low intrinsic subtype of breast cancer. Breast Cancer Res *12*, R68.

Provenzano, P.P., Inman, D.R., Eliceiri, K.W., and Keely, P.J. (2009). Matrix density-induced mechanoregulation of breast cell phenotype, signaling and gene expression through a FAK-ERK linkage. Oncogene *28*, 4326-4343.

Provenzano, P.P., Inman, D.R., Eliceiri, K.W., Knittel, J.G., Yan, L., Rueden, C.T., White, J.G., and Keely, P.J. (2008). Collagen density promotes mammary tumor initiation and progression. BMC Med *6*, 11.

Reya, T., Morrison, S.J., Clarke, M.F., and Weissman, I.L. (2001). Stem cells, cancer, and cancer stem cells. Nature *414*, 105-111.

Ro, J., North, S.M., Gallick, G.E., Hortobagyi, G.N., Gutterman, J.U., and Blick, M. (1988). Amplified and overexpressed epidermal growth factor receptor gene in uncultured primary human breast carcinoma. Cancer Res *48*, 161-164.

Sainsbury, J.R., Farndon, J.R., Needham, G.K., Malcolm, A.J., and Harris, A.L. (1987). Epidermal-growth-factor receptor status as predictor of early recurrence of and death from breast cancer. Lancet *1*, 1398-1402.

Shackleton, M., Vaillant, F., Simpson, K.J., Stingl, J., Smyth, G.K., Asselin-Labat, M.L., Wu, L., Lindeman, G.J., and Visvader, J.E. (2006). Generation of a functional mammary gland from a single stem cell. Nature *439*, 84-88.

Shah, S.P., Roth, A., Goya, R., Oloumi, A., Ha, G., Zhao, Y., Turashvili, G., Ding, J., Tse, K., Haffari, G.*, et al.* (2012) The clonal and mutational evolution spectrum of primary triple-negative breast cancers. Nature *486*, 395-399.

Schedin, P., and Keely, P.J. (2011) Mammary gland ECM remodeling, stiffness, and mechanosignaling in normal development and tumor progression. Cold Spring Harb Perspect Biol *3*, a003228.

Scheel, C., Eaton, E.N., Li, S.H., Chaffer, C.L., Reinhardt, F., Kah, K.J., Bell, G., Guo, W., Rubin, J., Richardson, A.L.*, et al.* (2011) Paracrine and autocrine signals induce and maintain mesenchymal and stem cell states in the breast. Cell *145*, 926-940.

Shipitsin, M., Campbell, L.L., Argani, P., Weremowicz, S., Bloushtain-Qimron, N., Yao, J., Nikolskaya, T., Serebryiskaya, T., Beroukhim, R., Hu, M.*, et al.* (2007). Molecular definition of breast tumor heterogeneity. Cancer Cell *11*, 259-273.

Siegel, R.L., Miller, K.D., and Jemal, A. Cancer statistics, 2016. CA Cancer J Clin *66*, 7-30.

Slamon, D.J., Clark, G.M., Wong, S.G., Levin, W.J., Ullrich, A., and McGuire, W.L. (1987). Human breast cancer: correlation of relapse and survival with amplification of the HER-2/neu oncogene. Science *235*, 177-182.

Smerage, J.B., Barlow, W.E., Hortobagyi, G.N., Winer, E.P., Leyland-Jones, B., Srkalovic, G., Tejwani, S., Schott, A.F., O'Rourke, M.A., Lew, D.L.*, et al.* (2014) Circulating tumor cells and response to chemotherapy in metastatic breast cancer: SWOG S0500. J Clin Oncol *32*, 3483-3489.

Sorlie, T., Perou, C.M., Tibshirani, R., Aas, T., Geisler, S., Johnsen, H., Hastie, T., Eisen, M.B., van de Rijn, M., Jeffrey, S.S.*, et al.* (2001). Gene expression patterns of breast carcinomas distinguish tumor subclasses with clinical implications. Proc Natl Acad Sci U S A *98*, 10869-10874.

Soundararajan, R., Paranjape, A.N., Barsan, V., Chang, J.T., and Mani, S.A. A novel embryonic plasticity gene signature that predicts metastatic competence and clinical outcome. (2015) Sci Rep *5*, 11766.

Stephens, P.J., Tarpey, P.S., Davies, H., Van Loo, P., Greenman, C., Wedge, D.C., Nik-Zainal, S., Martin, S., Varela, I., Bignell, G.R.*, et al.* (2012) The landscape of cancer genes and mutational processes in breast cancer. Nature *486*, 400-404.

Stingl, J., Eirew, P., Ricketson, I., Shackleton, M., Vaillant, F., Choi, D., Li, H.I., and Eaves, C.J. (2006). Purification and unique properties of mammary epithelial stem cells. Nature *439*, 993-997.

Thiery, J.P., Acloque, H., Huang, R.Y., and Nieto, M.A. (2009). Epithelial-mesenchymal transitions in development and disease. Cell *139*, 871-890.

Tse, J.R., and Engler, A.J. (2010) Preparation of hydrogel substrates with tunable mechanical properties. Curr Protoc Cell Biol *Chapter 10*, Unit 10 16.

Van Keymeulen, A., Lee, M.Y., Ousset, M., Brohee, S., Rorive, S., Giraddi, R.R., Wuidart, A., Bouvencourt, G., Dubois, C., Salmon, I.*, et al.* (2015) Reactivation of multipotency by oncogenic PIK3CA induces breast tumour heterogeneity. Nature *525*, 119-123.

van 't Veer, L.J., Dai, H., van de Vijver, M.J., He, Y.D., Hart, A.A., Mao, M., Peterse, H.L., van der Kooy, K., Marton, M.J., Witteveen, A.T.*, et al.* (2002). Gene expression profiling predicts clinical outcome of breast cancer. Nature *415*, 530-536.

Villadsen, R., Fridriksdottir, A.J., Ronnov-Jessen, L., Gudjonsson, T., Rank, F., LaBarge, M.A., Bissell, M.J., and Petersen, O.W. (2007). Evidence for a stem cell hierarchy in the adult human breast. J Cell Biol *177*, 87-101.

Visvader, J.E. Cells of origin in cancer. (2011) Nature *469*, 314-322.

von Lintig, F.C., Dreilinger, A.D., Varki, N.M., Wallace, A.M., Casteel, D.E., and Boss, G.R. (2000). Ras activation in human breast cancer. Breast Cancer Res Treat *62*, 51-62.
Xenidis, N., Ignatiadis, M., Apostolaki, S., Perraki, M., Kalbakis, K., Agelaki, S., Stathopoulos, E.N., Chlouverakis, G., Lianidou, E., Kakolyris, S.*, et al.* (2009). Cytokeratin-19 mRNA-positive circulating tumor cells after adjuvant chemotherapy in patients with early breast cancer. J Clin Oncol *27*, 2177-2184.

Wang, G.M., Wong, H.Y., Konishi, H., Blair, B.G., Abukhdeir, A.M., Gustin, J.P., Rosen, D.M., Denmeade, S.R., Rasheed, Z., Matsui, W.*, et al.* (2013). Single copies of mutant

KRAS and mutant PIK3CA cooperate in immortalized human epithelial cells to induce tumor formation. Cancer Res *73*, 3248-3261.

Wei, S.C., Fattet, L., Tsai, J.H., Guo, Y., Pai, V.H., Majeski, H.E., Chen, A.C., Sah, R.L., Taylor, S.S., Engler, A.J.*, et al.* (2015) Matrix stiffness drives epithelial-mesenchymal transition and tumour metastasis through a TWIST1-G3BP2 mechanotransduction pathway. Nat Cell Biol *17*, 678-688.

Wiseman, B.S., and Werb, Z. (2002). Stromal effects on mammary gland development and breast cancer. Science *296*, 1046-1049.

Wozniak, M.A., Desai, R., Solski, P.A., Der, C.J., and Keely, P.J. (2003). ROCK-generated contractility regulates breast epithelial cell differentiation in response to the physical properties of a three-dimensional collagen matrix. J Cell Biol *163*, 583-595.

Wright, K.L., Adams, J.R., Liu, J.C., Loch, A.J., Wong, R.G., Jo, C.E., Beck, L.A., Santhanam, D.R., Weiss, L., Mei, X.*, et al.* (2015) Ras Signaling Is a Key Determinant for Metastatic Dissemination and Poor Survival of Luminal Breast Cancer Patients. Cancer Res *75*, 4960-4972.

Xenidis, N., Ignatiadis, M., Apostolaki, S., Perraki, M., Kalbakis, K., Agelaki, S., Stathopoulos, E.N., Chlouverakis, G., Lianidou, E., Kakolyris, S.*, et al.* (2009). Cytokeratin-19 mRNA-positive circulating tumor cells after adjuvant chemotherapy in patients with early breast cancer. J Clin Oncol *27*, 2177-2184.

Zhang, M., Behbod, F., Atkinson, R.L., Landis, M.D., Kittrell, F., Edwards, D., Medina, D., Tsimelzon, A., Hilsenbeck, S., Green, J.E.*, et al.* (2008). Identification of tumor-initiating cells in a p53-null mouse model of breast cancer. Cancer Res *68*, 4674-4682.

Zhao, X., Malhotra, G.K., Lele, S.M., Lele, M.S., West, W.W., Eudy, J.D., Band, H., and Band, V. (2010). Telomerase-immortalized human mammary stem/progenitor cells with ability to self-renew and differentiate. Proc Natl Acad Sci U S A *107*, 14146-14151.

Zhang, M., Behbod, F., Atkinson, R.L., Landis, M.D., Kittrell, F., Edwards, D., Medina, D., Tsimelzon, A., Hilsenbeck, S., Green, J.E.*, et al.* (2008). Identification of tumor-initiating cells in a p53-null mouse model of breast cancer. Cancer Res *68*, 4674-4682.

Zhao, X., Malhotra, G.K., Band, H., and Band, V. (2011) A block in lineage differentiation of immortal human mammary stem / progenitor cells by ectopically-expressed oncogenes. J Carcinog *10*, 39.

Zhao, X., Malhotra, G.K., Band, H., and Band, V (2012). Derivation of myoepithelial progenitor cells from bipotent mammary stem/progenitor cells. PLoS One *7*, e35338.

Zhao, X., Mirza, S., Alshareeda, A., Zhang, Y., Gurumurthy, C.B., Bele, A., Kim, J.H., Mohibi, S., Goswami, M., Lele, S.M.*, et al.* (2012) Overexpression of a novel cell cycle regulator ecdysoneless in breast cancer: a marker of poor prognosis in HER2/neu-overexpressing breast cancer patients. Breast Cancer Res Treat *134*, 171-180.

Zhao, X., Goswami, M., Pokhriyal, N., Ma, H., Du, H., Yao, J., Victor, T.A., Polyak, K., Sturgis, C.D., Band, H.*, et al.* (2008). Cyclooxygenase-2 expression during immortalization and breast cancer progression. Cancer Res *68*, 467-475.